The Role of Cdc42 Rho GTPase in the Cystic Fibrosis Intestinal Epithelial Barrier

---

A Dissertation Presented to

The Faculty of the Graduate School

At the University of Missouri

In Partial Fulfillment

Of the Requirement for the Degree

Doctor of Philosophy

By

Dr. Rowena A. Woode

Dr. Lane Clarke, Dissertation Supervisor

December 2022

The undersigned, appointed by the dean of the Graduate School have examined the dissertation entitled

The Role of Cdc42 Rho GTPase in the Cystic Fibrosis Intestinal Epithelial Barrier

Presented by Rowena A. Woode, DVM

A candidate for the degree of Doctor of Philosophy

And hereby certify that, in their opinion, it is worthy of acceptance

_____

Lane Clarke, DVM, PhD

_____

Christopher Baines, PhD

_____

Salman Hyder, PhD

_____

James Amos-Landgraf, PhD

ACKNOWLEDGEMENTS

I would like to express my deepest gratitude to Dr. Lane L. Clarke, my PhD advisor, for his wonderful mentoring. He has provided me with the tools I need in order to pursue my goals as a researcher. I could not have done it without him.

I would also like to thank the members of my doctoral committee, Drs. James Amos-Landgraf, Christopher Baines, and Salman Hyder. I have been so very fortunate to have all of you as advisors. Your guidance and questions regarding my research have prompted me to think more deeply about what my contributions mean in the context of the greater body of scientific knowledge.

To all the members of the Clarke laboratory, past and present, I would not have learned half of what I know today regarding the running of a laboratory if it had not been for your help. Thank you for making seemingly daunting tasks that much easier.

It goes without saying that the love and support of my family and friends has been a huge part of why I am able to write any of this. As much as I love science and research, the most important thing I have learned over the years is that it is the people in my life that matter most.

TABLE OF CONTENTS

LIST OF TABLES

LIST OF FIGURES

LIST OF ABBREVIATIONS

APC - adenomatous polyposis coli

BAC - Bacterial artificial chromosome

BCECF, AM - 2',7'-Bis-(2-Carboxyethyl)-5-(and-6)-Carboxyfluorescein, Acetoxymethyl Ester

Ca^{2+} - Calcium

cAMP - Cyclic adenosine monophosphate, Cyclic AMP

CB – Cascade Blue

Cdc42 - Cell Division Cycle 42

CF - Cystic fibrosis

CFTR - Cystic fibrosis transmembrane conductance regulator

CK1 - casein kinase 1

Cl^- - Chloride

COPD - Chronic Obstructive Pulmonary Disease

Daam1 - Dishevelled-associated activator of morphogenesis 1

DBS – Dbl's Big Sister

DEP - Dvl, Egl-10, Pleckstrin

DIOS - Distal intestinal obstructive syndrome

DMSO - Dimethyl sulfoxide

Dvl - Disheveled

EGFP - Enhanced Green Fluorescent Protein

ELISA – enzyme-linked immunosorbent assay

FAM13A – family with sequence similarity 13 member A

FBS - Fetal Bovine Serum

FIS – forskolin-induced swelling

FITC – Fluorescein isothiocyanate

GAP - GTPase activating protein

GDI - guanine dissociation inhibitor

GEF - guanine exchange factor

GI - Gastrointestinal

GSK3 - glycogen synthase kinase 3

GST – glutathione S-transferase

H^+ - Hydrogen

HA – Human influenza hemagglutinin

HCO_3^- - Bicarbonate

IBD – inflammatory bowel disease

ISC – Intestinal stem cell

K^+ - Potassium

KBR - Kreb's bicarbonate Ringer

kD/kDa – kilodalton

Klf4 – Kruppel-like factor 4

KO - Knock-out

LEF - Lymphoid Enhancer-Binding Factor

LPS - lipopolysaccharide

MLCP – myosin light chain phosphatase

MLC –myosin light chain

MCF2L – MCF.2 Cell Line Derived Transforming Sequence Like

MDCK – Madin-Darby canine kidney cells

MW – molecular weight

Myc – myelocytomatosis oncogene

Na^+ - Sodium

NHERF-1 – Na+/H+ exchanger regulatory factor isoform 1

N-WASP - Neural Wiskott-Aldrich syndrome protein

Oct3/4 - octamer-binding transcription factor 3, 4

PAK – p21-activated kinase

PBD - p21-binding domain

PBS - Phosphate Buffered Saline

PCP - Planar Cell Polarity

PDZ - Postsynaptic density 95, Discs Large, Zona Occludens-1

PFA - Paraformaldehyde

pH_i - Intracellular pH

PP2A - Protein phosphatase 2

pwCF – people with cystic fibrosis

Rac1 - Ras-Related C3 Botulinum Toxin Substrate 1

RBD - Rho binding domain

RhoA - Ras Homolog Family Member A

ROCK - Rho-associated protein kinase

ROR – receptor tyrosine kinase-like orphan receptor

RT – room temperature

Sox2 – Sex Determining Region Y-Box 2

SIBO - small intestinal bacterial overgrowth

siRNA – small interfering RNA

TAZ - Transit amplifying zone

TES - N-tris(hydroxymethyl)-methyl-2-aminoethanesulfonic acid

TCF - T-cell factor

WT - wild-type

ZO-1 - Zona Occludens-1

ZONAB - Zona Occludens-1 nucleic acid binding protein

The Role of Cdc42 Rho GTPase in the Cystic Fibrosis Intestinal Epithelial Barrier

Dr. Rowena A. Woode

Dr. Lane Clarke, Dissertation Supervisor

ABSTRACT

Cystic fibrosis (CF) is caused by mutations in the cystic fibrosis transmembrane conductance regulator (*CFTR*) gene. People with CF and CF mouse models experience increased intestinal permeability, but the molecular mechanisms linking CFTR dysfunction with intestinal barrier dysfunction are not well understood. Previously, we demonstrated that intracellular pH (pH_i) is increased in *Cftr* KO mouse intestinal epithelium compared to wild-type (WT). Loss of Cftr-mediated Cl^- and HCO_3^- conductance increased pH_i and Dishevelled (Dvl)-mediated Wnt/β-catenin signaling and intestinal stem cell proliferation. Dvl also transduces the noncanonical Wnt/planar cell polarity (PCP) signaling pathway to activate the Rho GTPases RhoA, Rac1, and Cdc42 to regulate the cytoskeleton and tight junction remodeling during cell proliferation and migration. We hypothesized that Dvl-mediated transduction of the Wnt/PCP pathway in CF would lead to increased tight junction remodeling and paracellular permeability. In this study, we show that *Cftr* KO mouse enteroids have increased paracellular permeability *in vitro*, but not *CFTR* KO Caco-2 monolayers when compared to WT. Regardless, Cdc42 activity is increased in CF to maintain barrier function in the hyperproliferative CF intestinal epithelium.

Chapter 1: Introduction and Background

Cystic Fibrosis Overview

Cystic fibrosis (CF) is a lethal autosomal recessive genetic disease caused by mutations in the gene for the cystic fibrosis transmembrane conductance regulator (*CFTR*) protein. More than 1,700 CF-causing mutations of the *CFTR* gene have been identified as of 2017, and according to the Cystic Fibrosis Foundation 2020 Patient Registry Annual Data Report, over 31,000 people have cystic fibrosis in the United States, with a recent report published in the Proceedings of the National Academy of Sciences indicating more than 10 million Americans carry a mutated *CFTR* gene[1,2]. CFTR is a cyclic nucleotide-regulated anion channel that conducts chloride and bicarbonate ions across epithelial cell membranes, facilitating pH regulation and hydration of epithelial surfaces. CFTR dysfunction results in epithelial surface dehydration, pH dysregulation, and the accumulation of thick, viscous mucus, or mucoviscidosis, which results in the multi-system manifestations of CF[3,4].

The leading cause of death of people with CF (pwCF) is progressive lung disease and eventual respiratory failure due to insufficient mucociliary clearance, recurring microbial infections, chronic inflammation, and airway remodeling[1,5]. Over the last few decades, the life expectancy of pwCF has increased from childhood to a median predicted age of survival of 50 years for individuals born between 2016 and 2020 thanks to advances in CF therapies[1]. These advances

include physiotherapy and mucolytics to aid in airway clearance, antibiotics to treat respiratory infections, and, for more severe cases of CF, lung transplantation. In addition, recently developed CFTR modulator drugs can correct CFTR protein processing and increase anion conductance for individuals with specific CF-causing mutations[6,7]. Even though CF is mostly known as a respiratory disease, the gastrointestinal system is also severely affected by CFTR dysfunction. In fact, the GI system is one of the first body systems to be adversely affected, and much like CF respiratory disease, CF GI disease requires lifelong management[3,4,8].

Cystic Fibrosis Gastrointestinal Disease

CFTR is expressed throughout the length of the GI tract, with weak expression in the stomach and the highest expression occurring in the duodenum, with CFTR expression decreasing in the aboral direction. A gradient of CFTR expression also exists along the crypt-villus axis, with the highest expression in the proliferative crypt domain[9]. CFTR dysfunction leads to decreased fluid secretion, pH dysregulation, mucoviscidosis, and intestinal dysmotility, causing the characteristic GI manifestations of CF[4]. Mucus plugging of the pancreatic ducts blocks secretion of pancreatic enzymes and bicarbonate-rich secretions, leading to exocrine pancreatic insufficiency, maldigestion, and malabsorption[3,10]. The accumulation of inspissated mucus and dehydrated luminal contents contributes to meconium ileus (MI) in infants, and later, chronic constipation, distal intestinal obstruction syndrome (DIOS), and small intestinal

bacterial overgrowth (SIBO)[3,10]. Treatment of CF GI symptoms include oral pancreatic enzymes and acid-suppressing medications to aid digestion, and a dietary plan to provide sufficient nutritional support[1,3,10]. Chronic constipation and intestinal blockages can be relieved by use of osmotic laxatives, enemas, and mucus-thinning medications, but more serious obstructions, usually occurring in the distal ileum or proximal colon, may require surgical intervention to prevent intestinal rupture, sepsis, and death[4,11].

Other significant characteristics of the CF intestine are a chronic inflammatory phenotype, and an altered microbial composition, also known as dysbiosis. A normal, healthy intestine has a relatively small microbial population in the small intestine, with numbers increasing dramatically in the large intestine[12]. Most microbes ingested with food are killed by gastric acid, preventing them from colonizing the small intestine. However, the lack of acid-neutralizing, bicarbonate-rich pancreatic secretions means that many pwCF must take acid-blocking medications to aid digestion and treat gastroesophageal reflux disease (GERD)[1]. Another major mechanism of controlling the microbial population is intestinal peristalsis coupled with the lubricating action of gel-forming mucins secreted from goblet cells. In the CF intestine, viscous mucus adheres to the intestinal epithelium and intestinal motility is reduced, which creates an environment that promotes abnormal microbial colonization and growth[13–15]. Intestinal inflammation is present in the majority of pwCF, characterized by an increase in immune cells in the lamina propria, increased fecal calprotectin (a neutrophil marker), and the presence of structural changes

to the mucosa, including mucosal ulceration, edema, and erythema[16,17]. This chronic, low-grade intestinal inflammation may be a contributing factor to the increase in the risk of developing GI cancer experienced by pwCF[18,19]. The origins of intestinal inflammation in pwCF are still not entirely understood, and dysbiosis is thought to be a contributing factor to the inflammatory phenotype[17,20–22]. However, the CF intestine is also characterized by an increase in permeability, which also contributes to intestinal mucosal inflammation via the translocation of bacterial factors and other luminal antigens into the body.

Intestinal Permeability in Cystic Fibrosis

The intestinal mucosal barrier is comprised of a single layer of columnar epithelial cells that separates the luminal environment from the internal environment of the body. The regulation of this internal-external interface is critical for the health of the organism as it allows for the absorption of water and nutrients, while limiting the entrance of potentially harmful antigens and microorganisms. The routes of entry for luminal contents across the intestinal barrier include the transcellular route and the paracellular route (Figure 1.1)[23]. The transcellular route includes both the movement of lipophilic molecules through the cell membrane via diffusion and the specific transport of hydrophilic ions and molecules through transport proteins. The paracellular route refers to the movement of ions and solutes through the space between neighboring cells, which is regulated by tight junctions. Tight junctions, a component of the apical junctional complex, are made up of the intramembrane proteins occludin and

various claudins, as well as intracellular zonula occludens (ZO) proteins that organize and connect the intramembrane proteins to the cytoskeleton (Figure 1.1A)[24]. Tight junctions are a component of the apical junctional complex, which also includes the adherens junctions and desmosomes. Tight junction protein composition determines paracellular ion conductance, known as the “pore” pathway, and the diffusion of molecules through the paracellular space, known as the “leak” pathway (Figure 1.1B)[23,25]. Tight junction protein expression and composition can be altered by different stimuli, including mechanical stresses, growth factors, and cytokine-mediated signaling[26,27]. By the same token, tight junctions can influence epithelial cell polarization, migration, and proliferation by modulating gene transcription via sequestration of transcription factors, which are released during tight junction remodeling[24,28–30].

Increased intestinal permeability has been reported in both children and adults with CF using the analysis of urinary lactulose to mannitol ratios and serum lipopolysaccharide (LPS) concentration[31–33]. Intestinal barrier dysfunction in CF is believed to contribute to chronic intestinal inflammation through the translocation of microbes, luminal antigens, and other pro-inflammatory substances[34]. CF mouse models recapitulate human CF intestinal disease, including intestinal obstruction, dysbiosis, and increased intestinal permeability[35,36]. Further, CF mice also demonstrate abnormalities in tight junction protein expression and organization in intestinal epithelial cells[37]. Interestingly, increased intestinal permeability is characteristic of other diseases, including gastrointestinal cancer, inflammatory bowel disease (IBD; Crohn’s

disease and ulcerative colitis), and celiac disease, which are experienced at a higher frequency by pwCF compared to the general population[18,19,38–41]. The clinical significance of increased intestinal permeability in pwCF is not fully understood, but it is believed that the gut microbiota influence disease severity and progression in the hepatobiliary and respiratory systems via the translocation of microbial factors into the portal circulation[42]. In addition, pwCF with high circulating levels of LPS develop LPS/endotoxin tolerance in circulating blood monocytes, which reduces cytokine production and causes a less effective host response to pathogens[32,43]. Interestingly, increased intestinal permeability has been reported in a wide range of disease states, including chronic obstructive pulmonary disease (COPD), chronic heart failure, chronic kidney disease, Alzheimer's disease, and inflammatory bowel disease[40,41,44–47]. The relationship between these diseases and increased intestinal permeability has been termed the 'leaky gut hypothesis', in which intestinal barrier dysfunction induces chronic, low-grade inflammation in various downstream organ systems due to the translocation of luminal components into the circulation[41]. However, it is important to note that while increased intestinal permeability may be associated with these diseases, no studies have demonstrated a clear cause-and-effect relationship. Despite the lack of consensus on intestinal permeability's specific contributions to CF and other disease states, it is of increasing interest as a therapeutic target using both pharmaceutical and dietary approaches[27,48,49].

The specific molecular mechanisms by which CFTR dysfunction leads to tight junction structural abnormalities has not been fully elucidated. As noted

previously, tight junction structure and function can be influenced by inflammation, and studies have demonstrated the effects of cytokines on intestinal epithelial permeability[50–52]. Several *in vitro* studies have assessed the pore and leak pathways of paracellular permeability in CF epithelial cells to determine if paracellular permeability of CF epithelium is increased independent of inflammatory factors. A study performed by Weiser et al. measured the transepithelial electrical resistance (TER), a measure of the pore pathway, and the paracellular flux of mannitol, a measure of the leak pathway, in wild-type (WT) *CFTR* (16HBE14o-) and delF508-*CFTR* (CFBE41o−, CF) human bronchial epithelial cell lines[53]. Under basal conditions, the CF monolayers demonstrated a higher paracellular flux of mannitol and a lower TER compared to WT monolayers. Similarly, a study by Castellani et al. using the same WT and CF human bronchial epithelial cell lines found that CF cell monolayers presented disorganization of tight junction proteins, as well as an increased permeability to a fluorescently labeled dextran probe compared to WT monolayers[54]. Studies by Gróf et al. compared *in vitro* monocultures of human bronchial epithelial cell lines expressing either wild-type or delF508-*CFTR* channels with the same cells co-cultured with human vascular endothelial cells to characterize a more lung-relevant disease model[55]. Monocultures of the delF508-*CFTR* cells demonstrated the lower TER and greater paracellular flux of fluorescein dextran and albumin compared to WT monocultured cells. Interestingly, the co-culture of the delF508-*CFTR* cells with human vascular endothelial cells resulted in increased TER and decreased permeability of fluorescein dextran and albumin, highlighting the

importance of supporting cells to epithelial barrier properties. In contrast, experiments performed by Molenda et al. using the same cell lines found no difference in fluorescein dextran flux under basal conditions, but the delF508-*CFTR* monolayer TER was significantly lower compared to WT monolayers[56]. Studies using non-respiratory cells have demonstrated similar findings to those described above, with Ruan et al. showing that siRNA-mediated knockdown of *Cftr* in murine epididymal cells led to a decrease in TER and zonula occludens-1 (ZO-1) protein expression[57]. Fiorotto et al. utilized polarized monolayers of cholangiocytes isolated from WT, DeltaF508, and *Cftr*-KO mice to measure TER and transepithelial flux of fluorescein-labeled dextran, with *Cftr*-KO cholangiocyte monolayers demonstrating a decrease in TER and an increase in paracellular permeability to dextran[58]. The *Cftr*-KO cholangiocyte monolayers also had a significant disruption of tight junction protein organization, including greater cytoplasmic localization of ZO-1 and splitting of the subcortical actin ring. These studies and others highlight the importance of elucidating the relationship between CFTR and the structure and function of tight junctions.

Currently, there have been no studies exploring the paracellular permeability characteristics of CF intestinal epithelial cells *in vitro*. The development of 3-D intestinal organoid cultures has allowed researchers to study intestinal epithelium that retains the biochemical properties of the parent tissue in vitro[59,60]. Studies of intestinal organoids from the small intestine of *Cftr* KO mice and wild-type, sex- and age-matched littermates demonstrated that Cftr modulates intracellular pH (pH_i) dynamics through its anion channel function, and

Cftr dysfunction leads to a sustained increase in pH_i due to chloride and bicarbonate retention[60,61]. Dynamics of pH_i play an important role in the regulation of cell proliferation, migration, and polarization due to its effect on the activity of pH-sensitive proteins[62–67]. In intestinal epithelium, the canonical Wnt/β-catenin signaling pathway is necessary for intestinal stem cell function[68]. Binding of Wnt ligand to the Frizzled receptor causes cytoplasmic accumulation and nuclear translocation of β-catenin where it acts as a transcriptional coactivator with TCF/LEF transcription factors (Figure 1.2). This pathway depends on the Wnt signal transduction protein Dishevelled (Dvl), which interacts with the Frizzled receptor to inhibit the β-catenin destruction complex[69]. An alkaline pH_i increases the association of the polybasic DEP domain of Dvl to the negatively charged phospholipids of the inner leaflet of the plasma membrane due to a reduction in proton electrostatic interference, stabilizing its association with Frizzled[70]. Wnt/β-catenin signaling is increased in *Cftr* KO mice via pH- and charge-dependent stabilization of Dvl, leading to intestinal stem cell hyperproliferation[71]. The Dvl protein is also involved in the noncanonical Wnt/Planar Cell Polarity (PCP) pathway, which activates the Rho GTPase proteins to induce cytoskeletal changes, which lead to changes in paracellular permeability through tight junction remodeling[72,73].

The Wnt/PCP Pathway and Rho GTPases in Intestinal Barrier Function

Dvl acts as a signal transducer for the noncanonical Wnt/PCP signaling pathway, which activates the Ras homologous (Rho) GTPases, members of the

Ras superfamily of small GTPases (Figure 1.3)[74]. The most well-characterized and ubiquitously expressed Rho GTPases are RhoA, Rac1, and Cdc42, which act as key regulators of cytoskeletal dynamics and gene transcription in different cellular processes, including cell migration, adhesion, polarity, and membrane trafficking via numerous downstream targets[75]. Rho GTPases cycle between active GTP- and an inactive GDP-bound states, which are spatiotemporally regulated by guanine nucleotide exchange factors (GEFs), GTPase activating proteins (GAPs), and guanine dissociation inhibitors (GDIs)[76]. The association of the cytoskeleton with tight junction structural proteins means that Rho GTPase activity plays an important role in intestinal epithelial barrier function[72,77].

Cdc42, Rac1, and RhoA alter cytoskeleton dynamics in response to growth factors and mechanical stimuli, inducing different effects on intestinal barrier function depending upon their downstream effectors[75]. RhoA activates the serine/threonine Rho kinases (ROCK1 and ROCK2) that phosphorylate and inactivate myosin light chain phosphatase (MLCP) and phosphorylate myosin light chain (MLC) to stimulate actinomycin contractility, increasing paracellular permeability[77]. Rac1 and Cdc42 activation share effector proteins in the p21 activated kinases (PAKs 1-6) and Neural Wiskott-Aldrich syndrome protein (N-WASP), which regulates actin filament nucleation via the Arp2/3 complex[77]. Rho GTPase activity is tightly regulated, as indicated by the presence of over 60 GEFs and over 70 GAPs identified in the human genome[76]. The importance of tightly controlled Rho GTPase activity is also evidenced by the disruptive effects that occur with either hyperactivation or inhibition of Rho GTPases. For Cdc42,

intestinal-specific Cdc42 KO mice demonstrate intestinal epithelial hyperplasia, crypt enlargement, and increased epithelial permeability compared to control mice[78]. Studies of RhoA deletion in murine small intestinal epithelium resulted in a loss of epithelial polarity, reduced cell proliferation, increased apoptosis, and a reduction in the number of intestinal stem cells[79], while a conditional intestinal epithelial-specific Rac1 KO mouse found that loss of Rac1 resulted in the expansion of the crypt domain and shortening of the villus domain due to changes in cell shape rather than proliferation and migration[80]. In the case of IBD, Rho activity was increased in the colonic epithelium of Crohn's disease patients, as well as in rats with 2, 4, 6-trinitrobenzene sulfonic acid-induced colitis[81]. The increased inflammatory cytokines were associated with an increase in Rho and ROCK activity in inflamed regions. Conversely, Rac1 and Cdc42 GTPase activity was decreased in inflamed colonic mucosa in IBD patients compared to unaffected regions, with Rac1 inhibition in human intestinal organoids causing actin cytoskeleton disorganization and defects in epithelial cell shedding[82,83]. Notably, increased activity of RhoA, Rac1, and Cdc42 has been associated with colorectal cancer progression and a poorer prognosis[84–86]. These findings further indicate that Rho GTPase activity requires a balance between activation and inhibition in order to prevent pathological changes to the intestinal epithelial barrier.

The integrity of the intestinal barrier depends upon the continuous renewal of the epithelial cell layer. This turnover process requires continuous proliferation and migration of the intestinal epithelium, which involves remodeling of the

cytoskeleton and tight junction proteins[87]. Previous studies have demonstrated an increase in cell migration from the intestinal crypts caused by increased epithelial proliferation in *Cftr* KO mice[88]. The combined influences of intestinal stem cell hyperproliferation and increased Dvl-mediated Rho GTPase activity via Wnt/PCP signaling may be contributing factors to tight junction remodeling and increased paracellular permeability in the CF intestine.

Dissertation Overview

The genetic disease cystic fibrosis (CF) is caused by mutations in the cystic fibrosis transmembrane conductance regulator (*CFTR*) gene. People with CF and CF mouse models experience increased intestinal epithelial permeability, which leads to the translocation of luminal antigens into the body, adversely affecting downstream organ systems. The molecular mechanisms by which CFTR dysfunction causes intestinal barrier dysfunction are not well understood. Our previous research demonstrated that intracellular pH (pHi) is increased in *Cftr* KO mouse intestinal epithelium compared to wild-type (WT) due loss of Cftr chloride and bicarbonate conductance. The alkaline pH_i increased the plasma membrane association of the pH-sensitive Wnt transduction protein Disheveled (Dvl), increasing Wnt/β-catenin signaling and intestinal stem cell proliferation. Dvl also transduces the noncanonical Wnt/planar cell polarity (PCP) signaling pathway. Wnt/PCP signaling activates the Ras homologous (Rho) GTPases Rho, Rac, and Cdc42 to regulate cytoskeletal dynamics and tight junction remodeling during cell proliferation, migration, adhesion, and membrane trafficking. It is

hypothesized that increased pH_i will increase Dvl-mediated transduction of the Wnt/PCP pathway, leading to increased epithelial tight junction remodeling and paracellular permeability. The following chapters describe studies of the Wnt/PCP pathway in the *Cftr* KO mouse model, and in a recently developed Caco-2 *CFTR* KO human intestinal epithelial cell line generated using CRISPR-Cas9 gene editing[89].

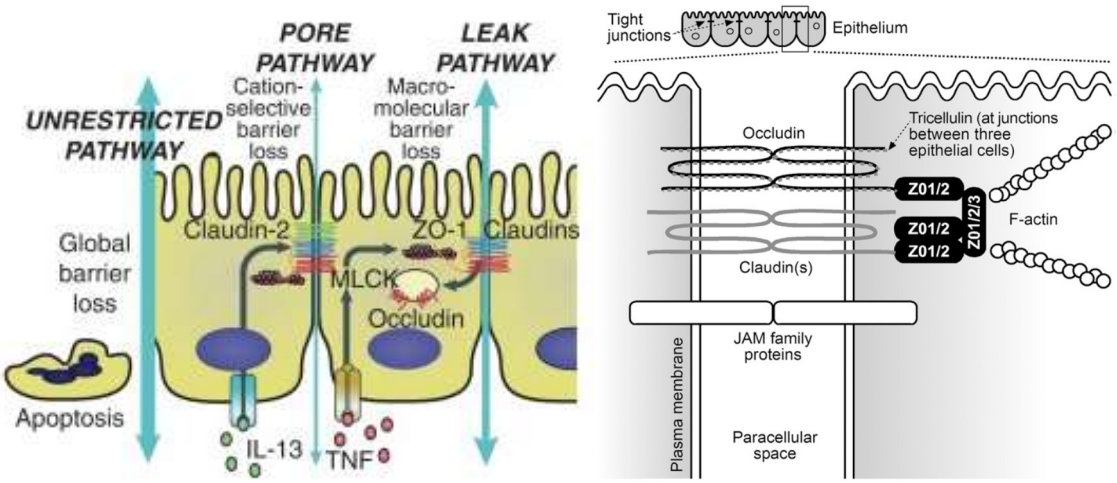

Figure 1.1. A.) A diagram illustrating different permeability pathways of the intestinal epithelial barrier in health and disease. The pore pathway is determined by the composition of different pore-forming transmembrane proteins (e.g., claudin-2) and refers to the ionic conductance of the epithelial layer. The leak pathway is regulated by other tight junction transmembrane proteins, such as occludin endocytosis, respectively. The unrestricted pathway is a tight junction-independent pathway of permeability that occurs at sites of epithelial injury. Figure modified from Buckley and Turner[23]. B.) Schematic of tight junction structure. Tight junction proteins include the transmembrane proteins occludin, claudins, and junctional adhesion molecules (JAMs) that regulate passage of ions and solutes through the paracellular space. Intracellular zonula occludens proteins act as scaffolding proteins to connect the transmembrane proteins of the tight junctions to the actomyosin ring. Figure modified from Ulluwishewa et al[25].

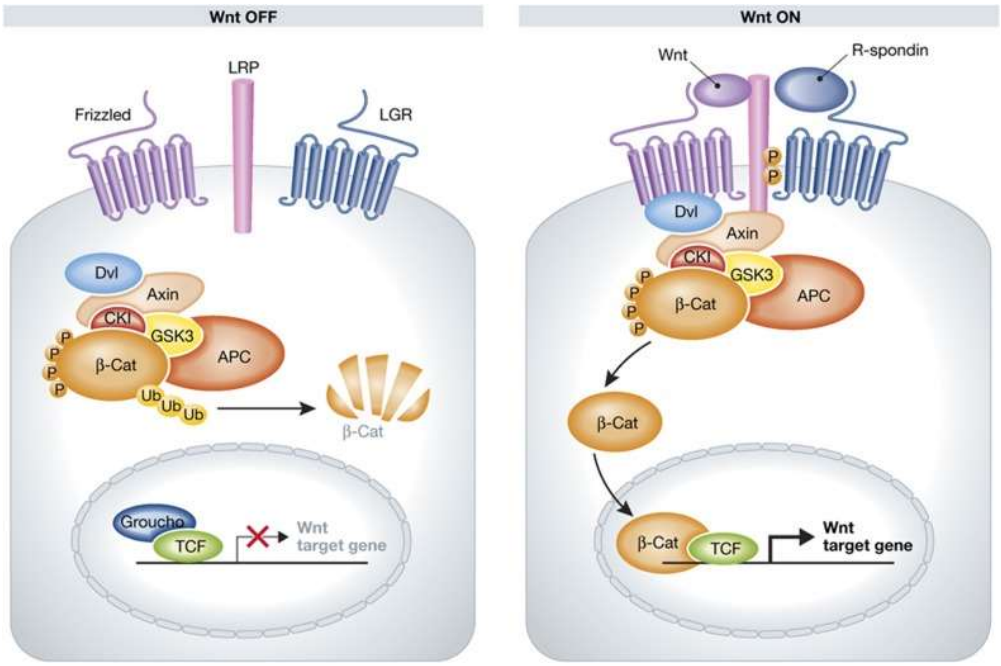

Figure 1.2. Diagram of the canonical Wnt/β-catenin signaling pathway. In the absence of Wnt ligand (left, Wnt OFF), cytoplasmic β-catenin is ubiquitinated and degraded by proteosomes via the action of a destruction complex. The β-catenin destruction complex includes the proteins Axin, adenomatosis polyposis coli (APC), protein phosphatase 2A (PP2A, not shown), glycogen synthase kinase 3 (GSK3), and casein kinase 1α (CK1α). In the presence of Wnt ligand (right, Wnt ON), the activity of the β-catenin destruction complex is disrupted by Dishevelled (Dvl)-mediated recruitment to the plasma membrane, preventing degradation of β-catenin. β-catenin accumulates in the cytoplasm and is able to translocate to the nucleus to act as a transcriptional coactivator of transcription factors that belong to the TCF/LEF family. Figure modified from Schuijers and Clevers[90].

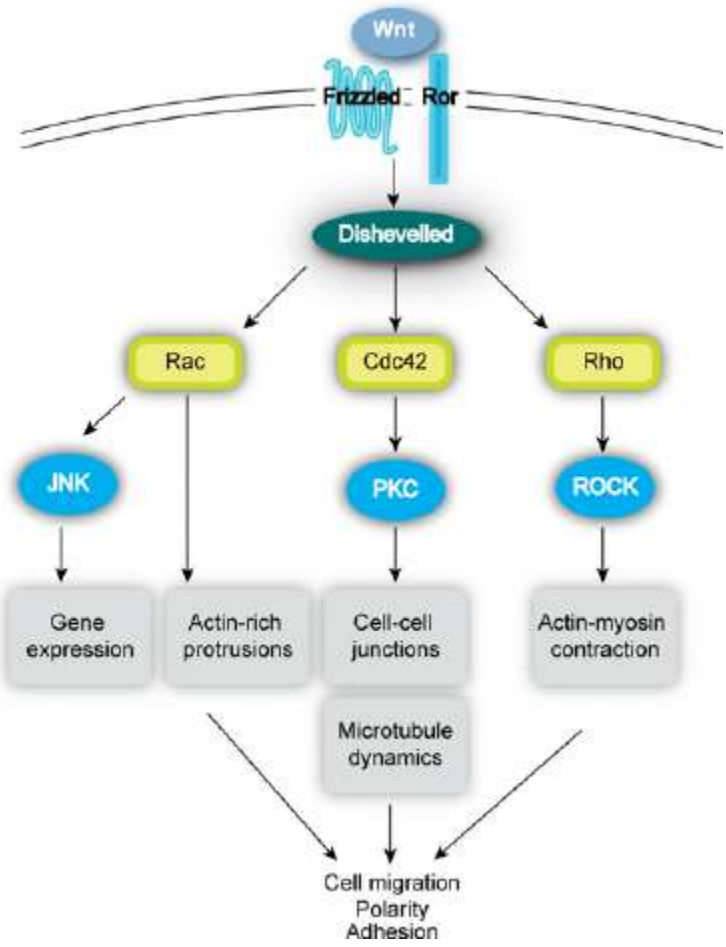

Figure 1.3. Diagram of the noncanonical Wnt/Planar Cell Polarity (PCP) pathway. Like the canonical Wnt/β-catenin signaling pathway, the Wnt/PCP pathway activates the Dishevelled (Dvl) signal transduction protein. Wnt/PCP signaling occurs when Wnt ligand binds to the Frizzled receptor and its co-receptor Ror. The assembly of Dvl-effector complexes (e.g., Dvl-Daam1, Dishevelled associated activator of morphogenesis 1) recruit guanine nucleotide exchange factors (GEFs) to promote Rho GTPase activation, initiating pathways to regulate cytoskeleton dynamics. Figure modified from Schlessinger et al.[91]

Chapter 2: Cell-Autonomous Cdc42 Rho GTPase Activity Maintains Epithelial Barrier Function in the Cystic Fibrosis Intestine

Abstract

Increased intestinal paracellular permeability is a manifestation of cystic fibrosis (CF) intestinal disease in people with CF (pwCF) and in *Cftr*-null mice. Increased paracellular permeability has been found in CF airway epithelium cultured in the absence of inflammatory factors, suggesting an inherent defect in CF epithelial barrier function. We hypothesized that the alkaline intracellular pH (pH_i) of CF intestinal epithelium would facilitate increased Dishevelled (Dvl)-mediated Wnt planar cell polarity (PCP) signaling, increasing Rho GTPase activity (RhoA, Rac1, and Cdc42), tight junction remodeling, and paracellular permeability. *Ex vivo* measurement of paracellular permeability in murine enteroids revealed increased leak pathway permeability in *Cftr* KO compared to WT. Tight junctions in *Cftr* KO crypt epithelium showed increased localization of the Rho GTPase Cdc42. This correlated with accumulation of Dvl2 at the apical membrane of *Cftr* KO enteroid crypts. Tight junction accumulation of Cdc42 did not result from increased Cdc42 expression *in vivo* or *in vitro*. Using a *CFTR* KO Caco-2 model, which recapitulates the sustained alkaline pH_i, increased Wnt/β-catenin signaling, and increased proliferation rate of the *Cftr* KO mouse epithelium, we found that only Cdc4242 activity was increased relative to WT cells. The increase in paracellular permeability and Cdc42 tight junction localization was normalized in the *Cftr* KO small intestine by inhibiting Wnt

signaling. However, inhibition of Cdc42 activity resulted in significant disruption of *Cftr* KO epithelial barrier function. Unlike *Cftr* KO, WT enteroid permeability characteristics were not significantly affected by increased proliferation rate, Cdc42 inhibition, or Wnt inhibition. We conclude that increased leak permeability in CF intestinal epithelium is not simply a result of enhanced proliferation, but may include changes in noncanonical Wnt signaling secondary to pH_i dysregulation.

Introduction

Cystic fibrosis (CF) is a lethal autosomal recessive genetic disease caused by mutations in the gene for the cystic fibrosis transmembrane conductance regulator (*CFTR*) protein. The gastrointestinal system is one of the earliest affected body systems in CF, and requires life-long management[3]. The CFTR anion channel is responsible for chloride and bicarbonate ion conductance in epithelial cells, and is expressed throughout the length of the GI tract[9]. Therefore, CFTR dysfunction leads to decreased fluid secretion, pH dysregulation, and mucoviscidosis in the gastrointestinal system[4]. The accumulation of adherent mucus, reduced intestinal motility, and microbial dysbiosis[13–15] contribute to the chronic inflammatory phenotype that characterizes the CF intestinal environment[16,17]. Together, these factors likely contribute to the increase in intestinal permeability that has been reported in people with CF (pwCF)[31–33] and in CF mouse models[35,36]. Decreased intestinal barrier function negatively affects the long term health of pwCF via the

translocation of microbial components into the circulation, adversely affecting the hepatobiliary and respiratory systems[8,32,42].

The intestinal barrier is made up of a single layer of cells that separates the internal and external environments, allowing for the absorption of water and nutrients while restricting the passage of potentially harmful luminal contents. The space between adjacent cells is regulated by the tight junctions, which restrict the paracellular movements of ions and solutes through the paracellular space. Although tight junction structure and function can be disrupted by inflammatory signaling[50–52], several studies have demonstrated tight junction defects in CF cells cultured in the absence of these factors, suggesting a cell autonomous characteristic. Several studies in CF airway epithelium have found abnormalities in the 'leak' pathway of permeability[54,56,92], which refers to the paracellular flux of larger molecules, while others have found abnormalities in the 'pore' pathway of permeability, or the conductance of specific ions through the paracellular space[56,57]. The specific molecular mechanisms by which CFTR dysfunction leads to tight junction abnormalities is not yet clear, but loss of CFTR function in intestinal epithelium causes dysregulation of intracellular pH (pH_i)[60,61], which is responsible for regulating numerous cellular processes, including tight junction remodeling[62–67].

In previous studies, we demonstrated that the sustained alkaline pH_i of *Cftr* KO intestinal epithelium increased the plasma membrane electrochemical association of the pH-sensitive Wnt transduction protein Dishevelled (Dvl). This led to increased Wnt/β-catenin signaling and intestinal stem cell (ISC)

hyperproliferation *in vivo* and *in vitro*. Dvl also acts as a key signal transducer for the noncanonical Wnt/planar cell polarity (PCP) signaling pathway, which activates the Ras homologous (Rho) GTPases RhoA, Rac1, and Cdc42 to regulate cytoskeletal dynamics and tight junction remodeling during cell proliferation, migration, adhesion, and membrane trafficking[77,93]. Rho GTPases alter cytoskeleton dynamics in response to growth factors and mechanical stimuli, inducing different effects on intestinal barrier function depending upon their downstream effectors[75]. The cycling of Rho GTPases between active (GTP-bound) and inactive (GDP-bound) states is tightly controlled in normal, healthy cells[76], and dysregulation of activity is associated with several gastrointestinal disease states, including inflammatory bowel disease (IBD)[81–83] and colorectal cancer[84–86].

Currently, there are no studies exploring the paracellular permeability characteristics of CF intestinal epithelial cells *in vitro*. In the present study, we evaluate the noncanonical Wnt/PCP pathway in the *Cftr* KO mouse model, and in a recently developed Caco-2 *CFTR* KO human intestinal epithelial cell line generated using CRISPR-Cas9 gene editing[94]. It is hypothesized that increased pH_i will facilitate Dvl-mediated transduction of the Wnt/PCP pathway, leading to increased epithelial tight junction remodeling and paracellular permeability via increased Rho GTPase activity.

Materials and Methods

Mice. Mice with gene targeted disruptions of the murine homolog of *Cftr* [abcc7, *Cftr* knock-out (KO)] and sex-matched wild-type (WT, +/+ or +/-) littermates or siblings were used. Mice were outbred to Black Swiss mice (Charles River Laboratories) at generational intervals and resultant F1 heterozygotes were crossed to generate F2 offspring for experimentation. The *Cftr* KO mouse line was crossed with both *Dvl2* KO/*Dvl2*-EGFP BAC transgenic mice[95] (a kind gift of Dr. Anthony Wynshaw-Boris, University of California San Diego, La Jolla, California, United States of America, Department of Pediatrics and Institute for Human Genetics, University of California San Francisco School of Medicine, San Francisco, California, United States of America) and Gt(ROSA)26Sortm4(ACTB-tdTomato,-EGFP)Luo/J (*Rosa*$^{mT/mG,}$ The Jackson Laboratory) mice to generate WT and *Cftr* KO/*Dvl2* KO/*Dvl2*-EGFP/*Rosa*$^{mT/mG}$ expressing mice for evaluation of Dvl2 apical membrane localization experiments. Genotypes were identified by PCR analysis of tail-snip DNA as previously described for *Cftr* KO mice[96], *Dvl2* KO and *Dvl2*-EGFP expression[97], and *Rosa*$^{mT/mG}$ (The Jackson Laboratory). Copy number for the *Dvl2*-EGFP transgene was verified by TaqMan® GFP copy number assay (ThermoFisher Scientific). Only mice expressing 2 copies of the *Dvl2*-EGFP transgene were used for experimental analysis. All mice were maintained ad libitum on standard laboratory chow (Formulab 5008, Rodent Chow; Ralston Purina) and distilled water containing Colyte® (Schwartz Pharma) laxative to prevent intestinal obstruction in the *Cftr* KO mice. Mice were housed individually in a temperature- and light-controlled room (22-26°C; 12-hour light:

12-hour dark cycle) in the Association for Assessment and Accreditation of Laboratory Animal Care- accredited animal facility at the Dalton Cardiovascular Research Center, University of Missouri. Mouse experiments were performed in accordance with guidelines outlined in “Guide for the Care and Use of Laboratory Animals” prepared by the National Academy of Sciences and published by the National Institutes of Health and with approval from the University of Missouri IACUC.

Enteroid culture. Crypts from mouse proximal jejunum were used to culture three-dimensional intestinal organoids (enteroids) in Matrigel™ (Corning), as described in detail in previous studies[60]. Cultures were overlaid with growth medium containing Ham’s F-12 medium with 5% FBS, 50μg/mL gentamicin, 125ng/mL R-spondin1, 25ng/mL noggin and 12.5ng/mL epidermal growth factor. Growth medium was changed every 3-4 days and enteroids were passaged every 7-10 days using Cell Recovery Solution (BD Sciences). Passages 1-3 were used for experimentation.

Caco-2 culture. Six Caco-2 cell lines, three WT with sham-CRISPR/Cas9 gene editing and three *CFTR* KO by CRISPR/Cas9 gene editing, were kind gifts of Dr. Mitchell Drumm, Case Western Reserve University. Caco-2 cells were maintained in Minimum Essential Medium (Gibco) with 10% FBS, 1% glutamine, and 1% penicillin-streptomycin (100 IU/mL penicillin, 100 IU/mL streptomycin). Cells were maintained at 37°C in an atmosphere of 95% air: 5% CO_2. Medium was replaced every 3 to 4 days, and cells were passaged via trypsinization using

TrypLE Express (Gibco) upon reaching 70-80% confluency. All experiments were performed using Caco-2 cells from passages 5 to 30.

Immunoblotting. Fresh crypts: mice were euthanized by CO_2 asphyxiation followed by cervical dislocation. A laparotomy was used for removal of the proximal jejunum. The intestine was flushed with ice-cold PBS and crypt epithelium collected using an EDTA technique, as described previously[60], and suspended in ice-cold PBS containing Halt Protease inhibitor (ThermoFisher Scientific) and lysed at 4°C by supersonication. Enteroids: cells were removed from Matrigel using Cell Recovery Solution (Corning), suspended in ice-cold PBS with Halt protease inhibitor (Life Technologies), and lysed at 4°C by supersonication. Caco-2 Cells: Cells were grown to approximately 60% confluence and lysed with RIPA buffer containing HALT protease inhibitor cocktail (ThermoFisher Scientific). Protein from all lysates was quantified via Coomassie (Bradford) protein assay (Bio-Rad). Total protein lysate was loaded onto 4-20% SDS-polyacrylamide gels for electrophoresis and transferred to a PVDF or nitrocellulose membrane for immunoblotting. Primary antibodies for immunoblotting were rabbit anti-Cdc42 (Abcam Cat# ab64533, RRID:AB_1310067, 1ug/mL) and mouse anti-active beta-catenin (Millipore Cat# 05-665, RRID:AB_309887, 1:1000). Secondary antibodies were goat anti-rabbit horseradish peroxidase (Cell Signaling Technology Cat# 7074, RRID:AB_2099233, 1:1000) and m-IgGκ BP-HRP antibody (Santa Cruz Biotechnology Cat# sc-516102, RRID:AB_2687626, 1:5000). Densitometry was performed using Image Lab Software (version 5.2.1; Bio-Rad).

Quantitative real-time PCR. Fresh crypt epithelium from the proximal jejunum of *Cftr* KO and WT mice was collected and stored in RNAlater (Invitrogen) at -20°C until processing. Total RNA extraction was performed using a RNeasy Plus Mini Kit, with reverse transcription performed using SuperScript III 1st Strand (Invitrogen) to generate cDNA according to the manufacturer's instructions. The cDNA was mixed with TaqMan Gene Expression Master Mix (Applied Biosystems), according to the manufacturer's instructions and loaded onto customized 96-well mini-array plates containing TaqMan assays for the genes of interest (Table 2.1). A Mastercycler EP RealPlex thermocycler (Eppendorf) was used for quantitative PCR, with the cDNA from *Cftr* KO and WT crypts run simultaneously on one plate. For *Cftr* KO and WT enteroids (passages 1-3, 7 days old), cells were removed from Matrigel® using Cell Recovery Solution (Corning), washed with ice-cold PBS, and stored in RNAlater solution at -20°C until processing. Total RNA extraction and reverse transcription were performed as above. The cDNA was mixed with TaqMan Gene Expression Master Mix (Applied Biosystems) and gene-specific TaqMan assays according to the manufacturer's instructions and loaded onto a blank MicroAmp Optical 96-well reaction plate (Applied Biosystems). The threshold cycle (Ct) of Cdc42 (Assay ID Mm01194005_g1) and claudin 2 (Assay ID Mm00516703_s1) was subtracted from the geometric mean Ct of three housekeeping genes (β-glucuronidase, Assay ID Mm00446953_m1, hypoxanthine guanine phosphoribosyl transferase 1, Assay ID Mm00446968_m1, and mitochondrial ribosomal protein L19, Assay

ID Mm00452754_m1) to yield ΔCt. The mRNA expression of *Cftr* KO relative to WT enteroids was calculated using the ΔΔCt method[98].

Table 2.1. Gene name, symbol, and Applied Biosystems assay ID for customized 96-well TaqMan® mini-array

Gene Name(s)	Gene Symbol(s)	Assay ID
18S ribosomal RNA*	*18s rRNA*	Hs99999901_s1
actin, beta†	*Actb*	Mm00607939_s1
glucuronidase, beta‡	*Gusb*	Mm00446953_m1
hypoxanthine guanine phosphoribosyl transferase‡	*Hprt*	Mm00446968_m1
mitochondrial ribosomal protein L19‡	*Mrpl19*	Mm00452754_m1
F11 receptor	*F11r*	Mm00554113_m1
junction adhesion molecule 2	*Jam2*	Mm00470197_m1
junction adhesion molecule 3	*Jam3*	Mm00499214_m1
claudin 1	*Cldn1*	Mm00516701_m1
claudin 2	*Cldn2*	Mm00516703_s1
claudin 3	*Cldn3*	Mm00515499_s1
claudin 4	*Cldn4*	Mm00515514_s1
claudin 5	*Cldn5*	Mm00727012_s1
claudin 6	*Cldn6*	Mm00490040_s1
claudin 7	*Cldn7*	Mm00516817_m1
claudin 8	*Cldn8*	Mm00516972_s1
claudin 9	*Cldn9*	Mm00517434_s1
claudin 12	*Cldn12*	Mm01316510_m1
claudin 13	*Cldn13*	Mm00491038_s1
claudin 15	*Cldn15*	Mm00517635_m1
claudin 17	*Cldn17*	Mm00626967_s1
occludin	*Ocln*	Mm00500912_m1
crumbs family member 3	*Crb3*	Mm00724087_m1
tight junction protein 1	*Tjp1*	Mm00493699_m1
tight junction protein 2	*Tjp2*	Mm00495620_m1
tight junction protein 3	*Tjp3*	Mm01148877_m1
Y box protein 3	*Ybx3*	Mm00516166_m1
par-6 family cell polarity regulator alpha	*Pard6a*	Mm00480004_m1

par-6 family cell polarity regulator beta	*Pard6b*	Mm00480520_m1
par-3 family cell polarity regulator	*Pard3*	Mm00473929_m1
T cell lymphoma invasion and metastasis 1	*Tiam1*	Mm00437079_m1
lethal giant larvae homolog 2 (Drosophila)	*Llgl2*	Mm00520730_m1
scribbled homolog (Drosophila)	*Scrib*	Mm00506424_m1
Wiskott-Aldrich syndrome-like (human)	*Wasl*	Mm01136990_m1
MAP/microtubule affinity regulating kinase 2	*Mark2*	Mm01220150_g1
cell division cycle 42	*Cdc42*	Mm01194005_g1
RAS-related C3 botulinum substrate 1	*Rac1*	Mm01201653_mH
ras homolog gene family, member A	*Rhoa*	Mm00834507_g1
IQ motif containing GTPase activating protein 1	*Iqgap1*	Mm01313746_m1
protein kinase C, zeta	*Prkcz*	Mm00776345_g1
poliovirus receptor-related 1	*Pvrl1*	Mm00445392_m1
poliovirus receptor-related 2	*Pvrl2*	Mm00436144_m1
poliovirus receptor-related 3	*Pvrl3*	Mm01342993_m1
poliovirus receptor-related 4	*Pvrl4*	Mm01295284_m1
cadherin 1	*Cdh1*	Mm01247357_m1
dishevelled, dsh homolog 1 (Drosophila)	*Dvl1*	Mm00438592_m1
dishevelled 2, dsh homolog (Drosophila)	*Dvl2*	Mm00432899_m1
X-linked inhibitor of apoptosis	*Xiap*	Mm01311594_mH

*Manufacturing control; †no reverse transcriptase control; ‡ housekeeping gene.

Dvl2 Localization: Enteroids grown from *Cftr* KO and WT/*Dvl2*-EGFP mice were grown on glass bottom culture dishes (Fluorodish, World Precision Instruments) and maintained at 37°C and gassed with 95% air: 5% CO_2 in a culture dish incubator (Warner Instruments). Images were acquired using an Olympus

FV1000 confocal microscope. Dvl-EGFP intensity was measured from the dTomato apical membrane to 5μm into the cell interior. Dvl2-EGFP intensity was normalized to the peak Dvl2-EGFP intensity of the supranuclear region of interest to attain apical membrane Dvl2-EGFP intensity values for WT and *Cftr* KO.

Enteroid Paracellular Permeability. After 7 days in primary culture, enteroids were passed through a 28-gauge needle in Advanced DMEM/F-12 (Thermo Fisher Scientific) plus 0.3 U/mL dispase (BD Biosciences) and 10μM anoikis inhibitor Y-27632 (Tocris Bioscience) to attain a suspension of single cells and enteroid fragments. Cells were pelleted by centrifugation at 200 x g for 30 seconds and washed twice with ice-cold PBS before being resuspended in PBS and mixed 1:2.5 vol/vol with Matrigel™ (Corning) and plated on glass bottom culture dishes (World Precision Instruments). Enteroids 2-3 days post-plating were mounted in a temperature- and atmosphere-controlled microincubator chamber (Warner Instruments) on an Olympus FV1000 confocal microscope for imaging. *ENDO-IWR1 experiments*: enteroids were treated with either 10μM ENDO-IWR1 (Tocris) or 1:1000 DMSO (vehicle) for 24 hours prior to imaging. Following treatment, enteroids were exposed to 1mg/mL FITC-Dextran (ThermoFisher Scientific, 3kD MW) in Kreb's bicarbonate Ringer (KBR) solution containing 10mM glucose, 5 mM N-tris(hydroxymethyl)-methyl-2aminoethanesulfonic acid (TES) buffer gassed with 95% O_2: 5% CO_2 (pH 7.4, 37°C). Images were taken every 5 minutes to assess the entry of the dye into the enteroid lumen. *ML141 experiments*: enteroids were treated with either 10μM ML141 (Millipore-Sigma) or 1:1000 DMSO for 30min prior to imaging. Following

treatment, enteroids were exposed to 1mg/mL Cascade Blue-Dextran (ThermoFisher Scientific, 3kD MW) and 0.5mg/mL FITC-Dextran (ThermoFisher Scientific, 500kD MW) in Kreb's bicarbonate Ringer (KBR) solution containing 10mM glucose, 5 mM N-tris(hydroxymethyl)-methyl-2aminoethanesulfonic acid (TES) buffer gassed with 95% O_2: 5% CO_2 (pH 7.4, 37°C). Images were taken every 5 minutes to assess the entry of the dye into the enteroid lumen. Image processing was performed using Slidebook 5.0 software (3i, Denver, CO).

Immunofluorescence. Freshly isolated crypts or enteroids were fixed in 4% paraformaldehyde (PFA) and stored at 4°C until processing. Fixed enteroids and Matrigel™ were scraped from the culture plates, transferred to 1.5mL microcentrifuge tubes, centrifuged at 200 x g for 1min and washed 3x with 1X PBS to remove Matrigel™ and fixative solution. Samples were permeabilized for 1 hour using 0.5%Triton X-100 (Sigma-Aldrich) in PBS and blocked for 30min with constant agitation in fish skin gelatin buffer [10mM Tris, 5mM EDTA, 0.15M NaCl, 0.25% fish skin gelatin (Sigma-Aldrich), 0.05% Tween20]. Samples were incubated overnight at 4°C with rabbit anti-Cdc42 antibody (Abcam Cat# ab64533, RRID:AB_1310067, 5ug/mL) diluted in fish skin gelatin buffer, washed 3x in fish skin gelatin buffer, and incubated with Alexa Fluor 405 goat anti-rabbit secondary antibody (Invitrogen, Molecular Probes Cat# A-31556, RRID:AB_221605, 1:500) for 4-5 hours with constant agitation at room temperature. Samples were washed three times for 10min in fish skin gelatin buffer. Samples were then resuspended in SlowFade® gold antifade mounting medium (ThermoFisher Scientific) and sealed under No. 1 glass coverslips on

microscope slides (ThermoFisher Scientific). Fresh crypts and enteroids were imaged using an Olympus FV1000 confocal microscope.

Proliferation Assay*:* WT and *CFTR* KO Caco-2 cells were plated at 10,000 live cells/well in triplicate on a 96 well optical bottom plate with 100µL of medium made with phenol red-free MEM (Gibco). Cells were collected at 0 and 72 hours. At collection, culture medium was aspirated from the wells and cells were lysed and stored at -80^{o}C until analysis. DNA concentration was attained using the CyQUANT™ Proliferation Assay (Invitrogen) according to the manufacturer's instructions. Fluorescence values were attained using a Modulus™ II Microplate Multimode Reader (Turner BioSystems) and converted to DNA concentrations using a standard curve.

Intracellular pH via BCECF-AM microfluorimetry*:* WT Caco-2 cells were used to perform pH_i calibration using BCECF, AM ratiometric dye (Invitrogen). 495nm-to-440nm ratios were converted to pH_i using the K^+/nigericin technique[99]. Cells loaded with BCECF, AM dye were perfused with pH 8.0, 7.5, 7.0, 6.5 and 6.0 calibration solutions (135mM KCl, 2mM K_2HPO_4, 20mM HEPES, 1.2mM $CaCl_2$, 0.8mM $MgSO_4$) containing 10µM nigericin. Cells were imaged using a SensiCam digital camera (COOKE, Auburn Hills, MI) on an upright microscope (model BX50WI, Olympus) using a 40x water-immersion objective. Image processing was performed using Slidebook 5.0 software (3i, Denver, CO). For steady-state pH_i measurements, Caco-2 cells were cultured on tissue culture treated 35mm dishes for 3-4 days. Cells were loaded with BCECF-AM (Invitrogen, 16 uM) in culture medium at 37°C for 40 min. BCECF-AM loaded cells were imaged on the

stage of an upright microscope (model BX50WI, Olympus) using a x40 water-immersion objective and perfused with [Tris(hydroxymethyl)methyl]-2-aminoethanesulfonic acid (TES) buffered ringers (TBR), which was gassed with 100% O_2 (pH 7.4, 37°C). pH_i was measured using dual excitation (440 nm and 495 nm) and imaged at 535-nm emission, which was collected using a SensiCam digital camera (COOKE, Auburn Hills, MI) and Slidebook 5.0 software (3i, Denver, CO). Data were acquired from single cells (n = 10 per experiment). The 495 nm-to-440 nm ratios were converted to pH_i using the standard curve generated using the K^+/nigericin technique.

Lateral Crypt Bud Counting. After 7 days in primary culture, enteroids were passed through a 28-gauge needle in Advanced DMEM/F-12 (Thermo Fisher Scientific) plus 0.3 U/mL dispase (BD Biosciences) and 10μM anoikis inhibitor Y-27632 (Tocris Bioscience). Enteroid fragments were pelleted by centrifugation at 200 x g for 30 seconds and washed twice with ice-cold PBS before being resuspended in PBS and mixed 1:2.5 vol/vol with Matrigel™ (Corning, Tewksbury, MA). Enteroid fragments were then plated onto glass bottom dishes (Fluorodish, World Precision Instruments, 35mm diameter, 10mm well) in Matrigel™ for lateral crypt bud counting and were overlaid with 200μL growth medium/well. The anoikis inhibitor Y-27632 was maintained in the growth medium for 2 days following passage, and medium was changed at days 2 and 4 post-passage. Lateral crypt bud formation was determined for WT and *Cftr* KO enteroids under two growth conditions: 1.) 7 days in FRENS medium (Ham's F-12 medium containing 20% FBS, 50μg/mL gentamicin, 500ng/mL R-spondin1,

100ng/mL noggin and 50ng/mL epidermal growth factor, after Sato et al.), or 2.) 7 days in 25% FRENS medium (Ham's F-12 medium with 5% FBS, 50µg/mL gentamicin, 125ng/mL R-spondin1, 25ng/mL noggin, and 12.5ng/mL epidermal growth factor). Lateral crypt buds were counted for ten enteroids per mouse on day 7 using an Olympus FV1000 confocal microscope. A 1µm slice of the midsection (greatest diameter) of each enteroid was attained to perform lateral crypt bud counts.

GTPase activity assay. Rho GTPase activity was determined using the RhoA/Rac1/Cdc42 Activation Assay Combo Biochem Kit™ (Cat. # BK030, Cytoskeleton, USA) according to the manufacturer's instructions. Briefly, WT and *CFTR* KO Caco-2 Cells were grown to approximately 60% confluency for each assay. Then, the growth medium was aspirated, and the cells were washed once with ice-cold PBS before lysing. Clarified lysates were snap frozen in liquid nitrogen and stored at -80°C while a small aliquot of each lysate was used for protein concentration determination using a Coomassie (Bradford) Protein Assay (Bio-Rad). Equivalent protein amounts of lysate were incubated with Rhotekin-RBD (RhoA) or PAK-PBD (Rac1/Cdc42) beads for 1 hour at 4°C on a rocker. The beads were pelleted by centrifugation at 4000 x g at 4°C for 1 minute. The beads were washed once with wash buffer, pelleted by centrifugation at 4°C at 4000 x g for 3 minutes, and the supernatant removed. Beads were resuspended in 20 µL of 2x Laemmli sample buffer (Bio-Rad) and boiled for 2 minutes. The pulldown samples were analyzed by Western blot using a 1:500 dilution of anti-RhoA, 1:500 anti-Rac1 or 1:250 anti-Cdc42 antibody provided by the kit. Active

RhoA, Rac1, or Cdc42 was calculated by taking GTP-bound Rho GTPase over the total Rho GTPase present in each sample determined via Western blot.

Materials. The axin stabilizer ENDO-IWR1 was purchased from Tocris (Cat. No. 3532). The Cdc42 inhibitor ML141 was purchased from Millipore-Sigma (Cat. No. 217708). Other supplies and reagents were purchased from ThermoFisher Scientific.

Statistics. Cumulative data are reported as the mean ± SE. Data between two groups were compared using a two-tailed unpaired Student's t-test or, if not normally distributed with equal variances, by Mann-Whitney Rank Sum test. Data from enteroid permeability assays were compared using a one-way repeated measures ANOVA with a Bonferroni test. Dvl2-EGFP data was analyzed using a one-way ANOVA with Holm-Sidak multiple comparisons test. A probability value of $p < 0.05$ was considered statistically significant.

Results

Increased "leak" permeability in Cftr KO enteroids.

As compared to WT, *Cftr* KO mice show increased proliferation and crypt cell migration in the small intestine *in vivo*[88]. Hyperproliferation of the *Cftr* KO small intestinal epithelium is sustained in primary cultured enteroids, indicating an epithelial-autonomous phenotype that was found to be dependent on increased Wnt/β-catenin signaling[71]. We asked whether increased proliferation and associated tight junction remodeling in the *Cftr* KO small intestine contributes

to the reduced barrier function that has been described in both pwCF and *Cftr* KO mouse models[33,35,100,101]. Previous studies of *Cftr* KO intestine in Ussing chambers do not report an increase in paracelluar ion conductance[102], an indicator of “pore” permeability, but few studies have evaluated the “leak” permeability to larger molecular weight molecules in the *Cftr* KO intestine[23]. To assess “leak” permeability in enteroids, 2–3-day old primary enteroids were incubated in Cascade blue®-labeled 3 kD dextran (CB 3kD dex, 1mg/mL) in the culture medium under a 95% CO_2: 5% O_2 atmosphere at 37°C. As shown in figure 2.1A, the labeled dye enters a WT enteroid rapidly for ~30 min followed by slower rate over the next 2.5 hr. A comparison of the dye entry into the lumen of 2-3 enteroids from a WT and *Cftr* KO sex-matched littermate mouse pair showed a more rapid increase in the luminal intensity in the *Cftr* KO enteroids as compared to that of the WT enteroids. A tight junction-impermeant FITC-labeled 500 kD dextran was included in the culture medium to ensure integrity of the enteroid sphere (0.5mg/mL). As shown in figure 2.1B, the CB 3 kD dex did not immediately reach a steady intensity in the bath, but required approximately 15 min likely due to slower diffusion in the Matrigel® matrix encasing the 3D enteroids. For quantitative estimates, dye intensity in the lumen of the enteroids and in the enteroid bath were measured at 5 min intervals after the bath dye intensity had reached a steady level (dotted lines). The ratio of the lumen dye intensity in the enteroid lumen and in the bath (inside to outside ratio, I/O ratio) were used to assess the “leak” pathway. As shown in figure 2.1C, the I/O ratio of the *Cftr* KO enteroids was consistently increased during the 15 – 30 min period in

evidence of an increased “leak” pathway of the intestinal barrier in the *Cftr* KO enteroids relative to WT.

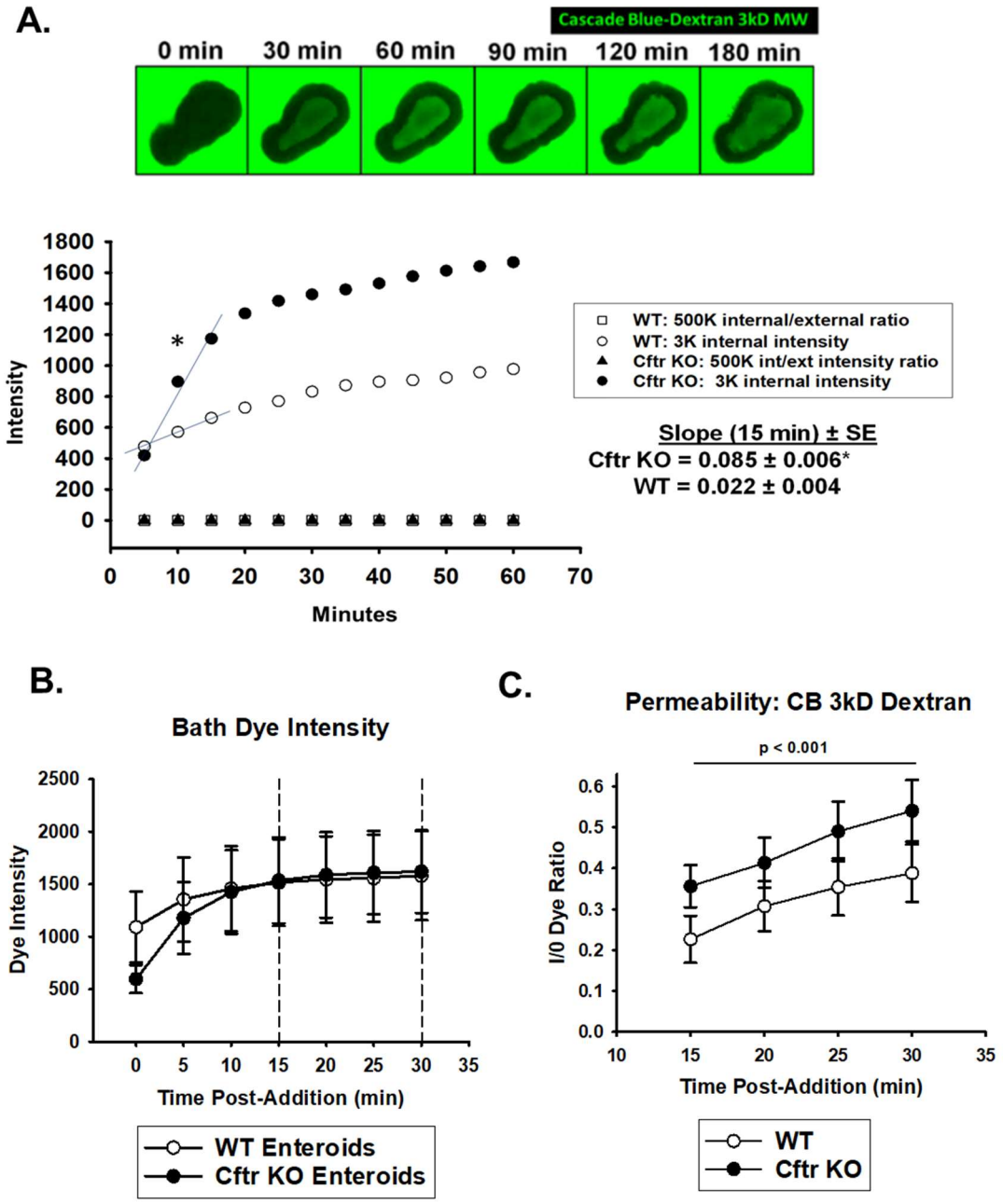

Figure 2.1. A. Top: Sequential live cell confocal microscopic images showing luminal appearance of Cascade Blue-Dextran 3kD MW (green) over time after addition of dye to the external bath. Bottom: Enteroids excluded 500kD MW

FITC-Dextran in WT (open square) and *Cftr* KO (filled triangle) as evidence of intact tight junctions. Internal Cascade Blue 3kD MW dextran entry over time as a function of the external concentration in WT (open circles) and *Cftr* KO (filled circles). Slope of *Cftr* KO 3kD dye entry was significantly different from WT. *p<0.0002 vs. WT. n = 3-6 enteroids from 3 sex-matched *Cftr* KO-WT pairs, slopes compared using Student's t-test. B. The external fluorescence intensity of Cascade Blue 3kD dextran over time, with the intensity reaching a steady state starting at 15 minutes after addition to the medium. C. Cumulative data of WT (open circles) and *Cftr* KO (filled circles) enteroids from n = 3 WT/*Cftr* KO pairs (3 female pairs). Values are represented as the intensity of luminal CB 3kD dextran over time as a function of the external concentration. *p<0.001 using one-way repeated measures ANOVA. Data represented as mean values ± SE.

The tight junctional complex in the rapidly proliferating Cftr KO crypt epithelium exhibits an overt localization of the Rho GTPase Cdc42.

Studies of knockout mice have shown that the small Rho GTPase Cdc42 is critical for coordinating proliferation, polarity and migration of the small intestinal epithelium[78]. Based on increased proliferation in *Cftr* KO intestinal organoids (enteroids), Cdc42 localization within the crypt epithelium of WT and *Cftr* KO enteroids was assessed by immunofluorescence. WT and *Cftr* KO mice were crossbred to *Rosa*$^{mT/mG}$ mice to identify the plasma membrane of the epithelial cells. Intracellular Cdc42 was apparent in both WT and *Cftr* KO crypts as shown in figure 2.2A. Remarkably, Cdc42 was overtly accumulated in the region of the tight junctions in the *Cftr* KO crypt, whereas tight junction immunolocalization was rarely evident in the WT crypts. To determine whether this phenomenon occurs *in vivo*, crypts from WT and *Cftr* KO mice were freshly isolated and prepared for immunofluorescence. As shown in figure 2.2B, labeled Cdc42 was diffusely localized to the upper transit-amplifying zone (TAZ) of the WT crypts, but appeared more densely accumulated throughout a considerable length of the crypt (from crypt base to TAZ) in the *Cftr* KO crypts. In confocal slices to provide an *en face* view at the apical membrane of the fresh crypt epithleum, there is a startling increase of Cdc42 located at the apical aspect of the cells in the TAZ (figure 2.2B, inset) of the *Cftr* KO crypts where it surrounded the apical membrane of epithelial cells in a ‘chicken-wire’ appearance.

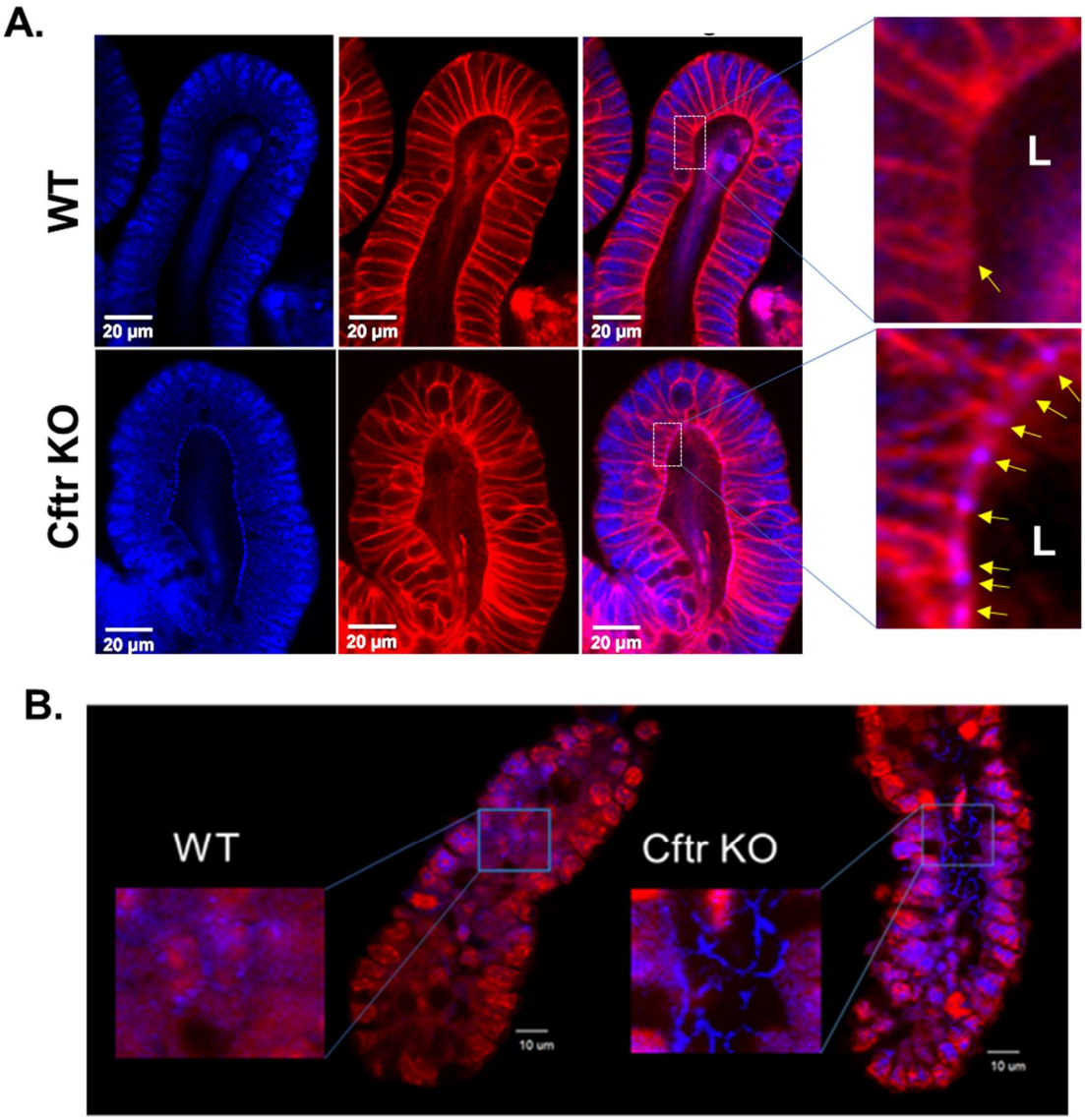

Figure 2.2. Increased Cdc42 tight junction localization and paracellular permeability in *Cftr* KO intestinal epithelium. A. Cdc42 (cyan) increased at tight junctions in *Cftr* KO/*Rosa*$^{mT/mG}$ vs. WT/*Rosa*$^{mT/mG}$ enteroids. Yellow arrows, Cdc42 at tight junctions. B. Nuclei (red) and Cdc42 (cyan); inset, magnification of Cdc42 tight junction localization in the transit-amplifying zone (TAZ) of freshly isolated small intestinal crypt epithelium.

Evidence of increased noncanonical Wnt signaling at the apical membrane of Cftr KO crypt epithelium of the small intestine.

A sustained alkaline pH_i in crypt-base columnar cells of the *Cftr* KO small intestine facilitates increased Wnt/β-catenin signaling and stem cell proliferation by enhancing electrochemical membrane localization of the Wnt transducer Dvl2[70]. Dvl transduction is also a component of noncanonical Wnt signaling for directed cell motility (e.g., planar cell polarity pathway), in which Dvl-effector complexes activate the small GTPases of the Rho family in the intestine (RhoA, Rac1, and Cdc42)[93]. Since the upper crypt epithelium (e.g., the TAZ) also demonstrates an alkaline pH_i in the *Cftr* KO intestine[103], we asked whether Dvl is localized to the apical membrane throughout the *Cftr* KO crypt epithelium. As in previous studies[71], membrane localization of Dvl2 was assessed by measuring the intensity of EGFP-Dvl2 as a function of linear distance (in pixels) from the red fluorescent apical membrane in the crypt epithelium of live enteroids from *Cftr* KO and WT sex-matched littermate mice crossed into *Dvl2* KO mice with BAC EGFP-*Dvl2* rescue and *Rosa*$^{mT/mG}$ mice. As shown in figure 2.3A and 2.3B, EGFP-Dvl2 intensity at the apical plasma membrane was significantly increased in crypt-base columnar cells (intestinal stem cells, ISCs), but was more highly localized at the apical membrane in transit-amplifying population in the *Cftr* KO crypts, as compared to WT. Increased EGFP-Dvl2 membrane association in the TAZ where Wnt/β-catenin signaling plays a minor role in cell proliferation[104] is consistent with an increased role for noncanonical Wnt signaling and cell migration in the *Cftr* KO crypt epithelium.

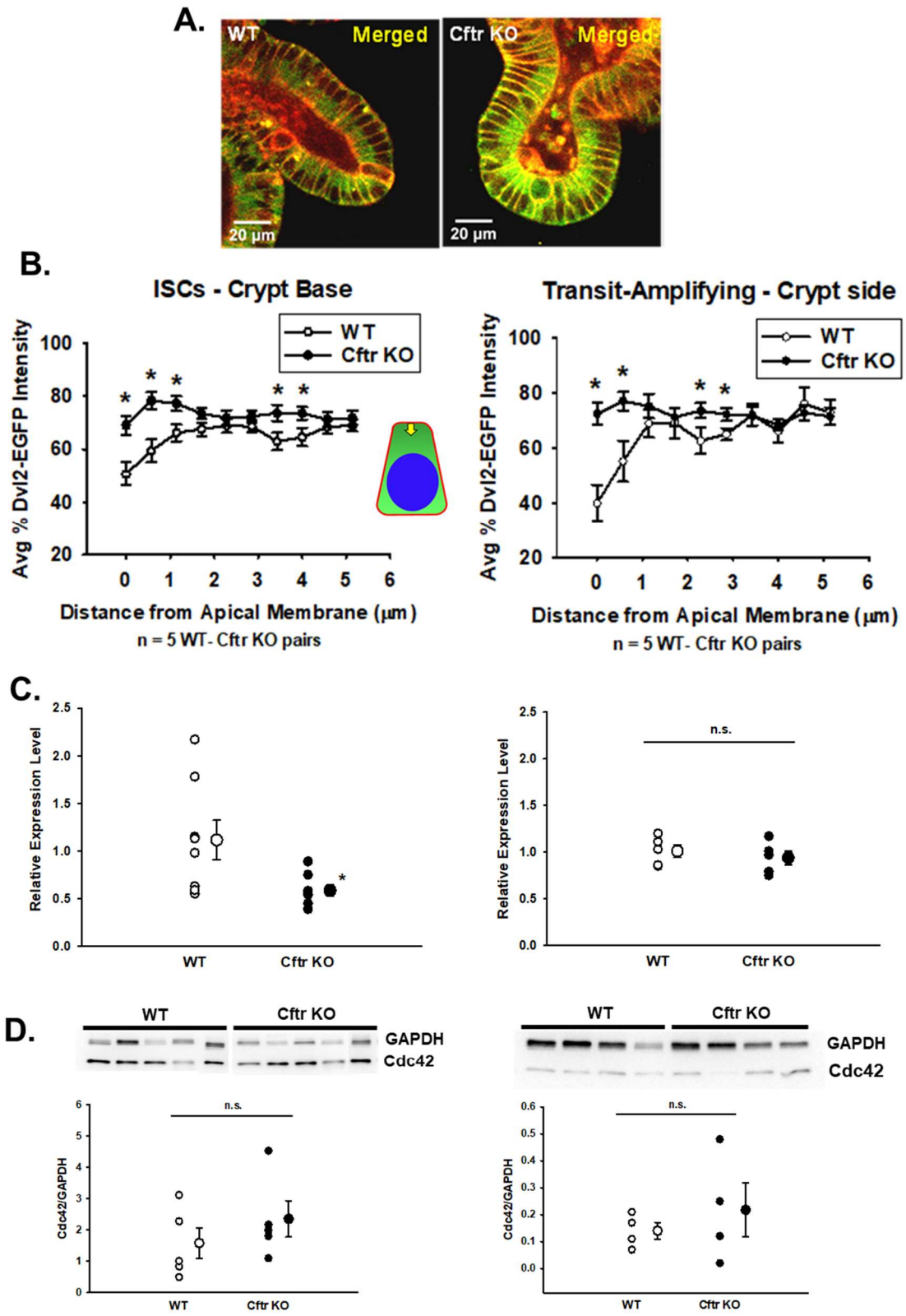
A.
WT
Merged
Cftr KO
Merged
20 µm
20 µm
B.
ISCs - Crypt Base
Transit-Amplifying - Crypt side
WT
Cftr KO
Avg % Dvl2-EGFP Intensity
Distance from Apical Membrane (µm)
n = 5 WT- Cftr KO pairs
C.
Relative Expression Level
n.s.
WT
Cftr KO
D.
GAPDH
Cdc42
Cdc42/GAPDH

Figure 2.3. Dvl2-EGFP apical membrane localization in crypt base columnar cells (CBCs) and transit-amplifying cells in WT and *Cftr* KO enteroids. A. Merged (yellow) images of Dvl2-EGFP (green) and membrane-localized tdTomato (red) images of WT and *Cftr* KO enteroids. B. Dvl2-EGFP intensity profile starting at the apical membrane (inset, point 0). *p<0.05 vs. WT, n = 15 crypts from 5 WT/*Cftr* KO sex-matched littermates. Inset, measurement of Dvl2-EGFP intensity within 1 mm of the apical membrane. * p<0.05 vs WT using one-way ANOVA. Data shown as mean values ± SE. C. Quantitative Real Time PCR mRNA expression levels of *Cdc42* in WT and *Cftr* KO in freshly isolated crypt epithelium (left) and early passage enteroids (right). Left: *Cdc42* mRNA relative expression in *Cftr* KO (filled circles) vs WT (open circles), n = 8 WT/*Cftr* KO pairs (4 females, 4 males). *p<0.05 using Welch's t-test. Right: *Cdc42* mRNA relative expression level in early passage enteroids from 5 WT/*Cftr* KO pairs (2 females, 3 males). n.s. = not significant using Student's t-test. Data shown as individual mouse values (small circles) and mean values ± SE (large circles). D. Western blot and densitometry analysis of Cdc42 in WT and *Cftr* KO fresh crypts (left) and early-passage enteroids (right). n = 5 WT-*Cftr* KO mouse pairs (fresh crypts), p = 0.341; n = 4 WT-*Cftr* KO mouse pairs (enteroids), p = 0.485, densitometric values compared using Student's t-test. Data shown as individual mouse values (small circles) and mean values ± SE (large circles).

Protein expression of Cdc42 is not increased in freshly isolated crypts or enteroids of the Cftr KO small intestine.

To evaluate whether the increased Cdc42 immunolocalization in the *Cftr* KO crypts was due to increased expression, we measured *Cdc42* mRNA and protein expression in freshly isolated crypt epithelium and in early passage enteroids in *Cftr* KO and WT mice. In addition, we evaluated *RhoA*, *Rac1*, and several other tight junction and polarity-associated genes for differences in mRNA expression in WT and *Cftr* KO fresh crypts (Table 2.1). In specimens from the *Cftr* KO small intestine, *Cdc42* mRNA expression in freshly isolated crypt epithelium was significantly decreased but was unchanged in early passage enteroids (figure 2.3C, table 2.2), as compared to WT. As shown in figure 2.3D, Cdc42 protein expression was not significantly different in either freshly isolated crypt epithelium or in early passage enteroids. We also noted that claudin-2 mRNA expression was significantly increased in *Cftr* KO crypt epithelium, but not significantly different in early-passage enteroids (table 2.2). Claudin-2 is a tight junction transmembrane protein that forms a paracellular channel for the passage of small cations (i.e., Na^+, K^+) and water, and is frequently upregulated in IBD, celiac disease, and intestinal dysbiosis, where it contributes to diarrhea by promoting the flux of ions and water into the GI lumen[105].

Freshly Isolated Crypt Epithelium					
Gene	**WT Relative Expression Level**	**WT ± SE**	**Cftr KO Relative Expression Level**	**Cftr KO ± SE**	**p-value**
F11r+	1.03	0.46	1.03	0.70	0.964
Jam2	2.04	0.93	5.73	3.45	0.319
Jam3	1.17	0.27	8.64	5.60	0.204
Cldn1	1.05	0.12	0.99	0.54	0.645
Cldn2*	1.06	0.13	1.75	0.21	0.015
Cldn3	1.23	0.15	0.81	0.55	0.175
Cldn4	1.12	0.20	2.00	1.03	0.413
Cldn5	1.63	0.49	2.62	0.92	0.381
Cldn6	1.22	0.24	1.39	0.47	0.757
Cldn7	1.04	0.11	1.18	0.25	0.614
Cldn8	1.10	0.18	0.68	0.16	0.101
Cldn9	1.14	0.20	1.67	0.43	0.281
Cldn12	1.05	0.11	0.87	0.17	0.408
Cldn13	1.70	0.76	2.05	0.69	0.738
Cldn15	1.13	0.20	0.81	0.21	0.290
Cldn17	1.73	0.46	2.46	0.70	0.395
Ocln	1.18	0.25	1.62	0.32	0.610
Crb3+	1.09	0.23	1.34	0.41	0.613
Tjp1	1.01	0.07	0.79	0.12	0.127
Tjp2	1.04	0.11	1.12	0.14	0.609
Tjp3	1.01	0.06	1.12	0.20	0.618
Ybx3+	1.02	0.08	1.19	0.16	0.372
Pard6a	1.91	0.53	2.03	0.59	0.956
Pard6b	1.67	0.43	0.62	0.10	0.125
Pard3	1.54	0.76	0.61	0.04	0.246
Tiam1	1.04	0.12	0.99	0.12	0.737
Llgl2+	1.05	0.13	1.14	0.31	0.799
Scrib+	1.00	0.04	0.85	0.06	0.061
Wasl+	1.02	0.09	1.24	0.39	0.587
Mark2+	1.02	0.09	0.94	0.09	0.541
Cdc42*	1.12	0.21	0.59	0.06	0.028
Rac1	1.03	0.10	0.94	0.07	0.467
Rhoa	1.03	0.17	0.86	0.09	0.235
Iqgap1	1.07	0.05	1.04	0.07	0.755
Prkcz	1.05	0.12	1.58	0.60	0.402
Pvrl1+	1.22	0.32	2.98	1.51	0.279
Pvrl2	1.10	0.16	1.03	0.19	0.788
Pvrl3+	1.02	0.09	0.83	0.22	0.442
Pvrl4+	1.05	0.15	1.17	0.15	0.600
Cdh1	1.52	0.36	1.44	0.43	0.926
Dvl1+	1.06	0.14	0.83	0.24	0.429
Dvl2+	1.15	0.21	1.28	0.41	0.775
Xiap+	1.06	0.17	1.52	0.27	0.174
Early Passage Enteroids					
Cdc42	1.03	0.07	0.98	0.09	0.015
Cldn2	1.11	0.24	1.04	0.23	0.028

Table 2.2. Tight junction and noncanonical Wnt signaling pathway-associated gene expression results in WT and *Cftr* KO freshly isolated crypt epithelium and early passage enteroids. Freshly isolated crypt epithelium: *p<0.05 using Student's t-test; n = 8 WT/*Cftr* KO pairs (4 male, 4 female pairs), +n = 6 WT/*Cftr* KO mouse pairs (3 male, 3 female pairs). Early passage enteroids: n = 5 WT/*Cftr* KO pairs (3 male, 2 female pairs).

Increased active (GTP-bound) Cdc42 in a CFTR KO human Caco-2 model.

Rho GTPases, such as Cdc42, cycle between a GTP-bound (active) and GDP-bound (inactive) state[24]. Pulldown assays utilizing Rhotekin-RBD and GST-PAK1-PBD agarose beads allow for the determination of GTP-bound Rho GTPases in biological samples. Due to the necessity for rapid collection of lysates to measure the labile GTP-bound state of Rho GTPases, the length of time required to collect fresh crypts from mouse small intestine or enteroids from Matrigel® was not conducive for adaptation of the pulldown assay. To overcome this obstacle, we utilized human Caco-2 cell lines in which *CFTR* was knocked out by CRISPR/Cas9 gene editing[94]. To validate the utility of our strategy, studies of pH_i, Wnt/β-catenin signaling, and cell proliferation were first performed to determine whether the *CFTR* KO Caco-2 cells recapitulated our findings in the *Cftr* KO mouse intestine. As shown in figure 2.4A-C, when compared to sham-CRISPR/Cas9 gene-edited Caco-2 cell lines (WT), the *CFTR* KO Caco-2 cells had a sustained alkaline pH_i, increased Wnt/β-catenin signaling as indicated by immunoblots for “active” (non-phosphorylated at Ser37 and Thr41[106]) β-catenin, and a higher rate of proliferation.

Rho pull-down assays in *CFTR* KO and WT Caco-2 extracts were used to compare the activity of the three primary Rho GTPases in the noncanonical Wnt/PCP pathway (RhoA, Rac1, and Cdc42)[77]. As shown in figure 4D, active Cdc42 was significantly greater in *CFTR* KO Caco-2 cells versus WT, an increase that was not associated with an overall increase in Cdc42 protein (figure

2.4E). In contrast, RhoA and Rac1 activity were not significantly different between *CFTR* KO and WT Caco-2 cells (figure 2.4F and 2.4G).

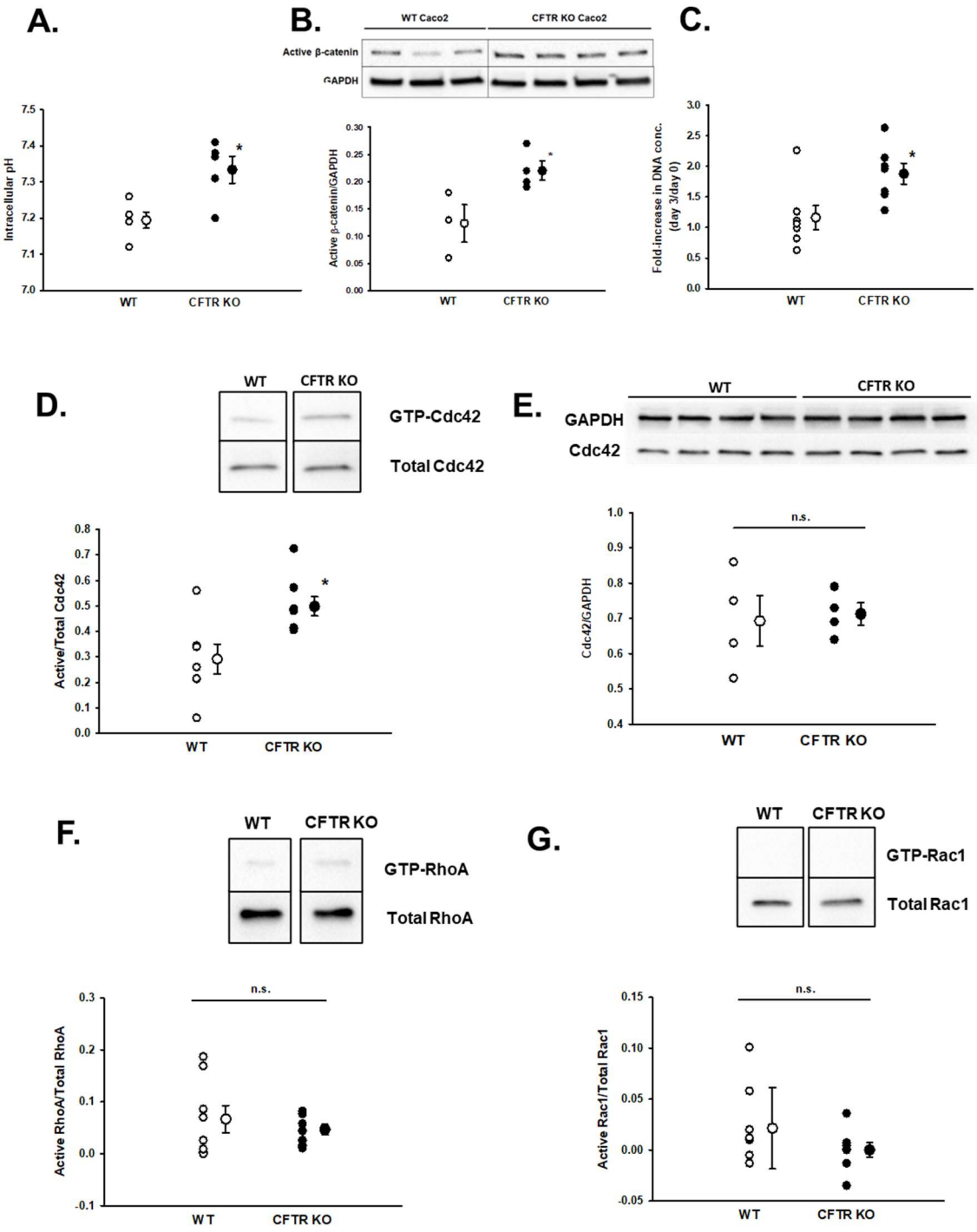

Figure 2.4. *CFTR* KO Caco-2 human intestinal epithelial cells recapitulate characteristics of *Cftr* KO murine intestinal epithelium and demonstrate increased Cdc42 Rho GTPase activity. A. Caco-2 pH_i as measured using the ratiometric,

cell-permeant pH-sensitive dye BCECF, AM while cells were perfused with TES-buffered Ringer's solution gassed with 100% O_2 (pH 7.4, 37°C). n = 5, 10 cells measured per experiment, *p = 0.0123 using Student's t-test. B. Densitometric analysis (bottom) and bands (top) of active β-catenin protein in WT vs *CFTR* KO Caco-2 cells; n = 3 WT, 4 *CFTR* KO, *p = 0.018 using Student's t-test. C. Fluorescence-based measurement of DNA content in Caco-2 cells comparing fold-increase in DNA on day 3 vs. day 0; n = 7, *p = 0.009 using Student's t-test. D. GST-PAK1-PBD agarose bead pulldown assay measurement of GTP-bound (active) Cdc42 in *CFTR* KO and WT Caco2 intestinal epithelial cells (n= 4) *p = 0.0106, using Student's t-test. E. Densitometric analysis (bottom) and Western blot image (top) of Cdc42 protein in WT and *CFTR* KO Caco-2 lysates (n = 4), n.s. = not significant using Student's t-test. F, G. Rhotekin-RBD (RhoA) and GST-PAK1-PBD (Rac1) agarose beads determination of GTP-bound RhoA (F) and Rac1 (G) in Caco-2 lysates (n = 4), n.s. = not significant using Student's t-test. Data in all graphs shown as individual values (small circles) and mean values ± SE (large circles).

Increased paracellular permeability and Cdc42 tight junction localization is normalized in the Cftr KO small intestine by inhibiting Wnt signaling

Given the interplay between tight junction remodeling and crypt proliferation[24], we asked if increased 'leak' permeability and Cdc42 immunolocalization at the tight junctions could be altered by inhibiting rapid proliferation in the *Cftr* KO crypt epithelium. *Cftr* KO and WT enteroid permeability to CB 3kD dex was measured after treatment with the Axin stabilizer ENDO-IWR1 for 24hr to inhibit Wnt/β-catenin signaling. Interestingly, as shown in figure 2.5A (left), treatment with ENDO-IWR1 significantly decreased the permeability of WT enteroids. ENDO-IWR1 treatment of *Cftr* KO enteroids, however, resulted in an even greater decrease in permeability (figure 2.5A, right). To evaluate Cdc42 immunolocalization to the tight junctional complex, WT and *Cftr* KO immunolocalization studies were performed after vehicle (DMSO) treatment and ENDO-IWR1 treatment for 24 hrs. Intense immunolocalization of Cdc42 at the tight junctional complex was noted in the *Cftr* KO versus WT during vehicle treatment (figure 2.5B, top). However, following ENDO-IWR1 treatment, a noticeable redistribution of Cdc42 away from the tight junctions was noted in both WT and *Cftr* KO crypts. These findings suggest intestinal epithelial hyperproliferation is a contributing factor to increased paracellular permeability in the CF intestine.

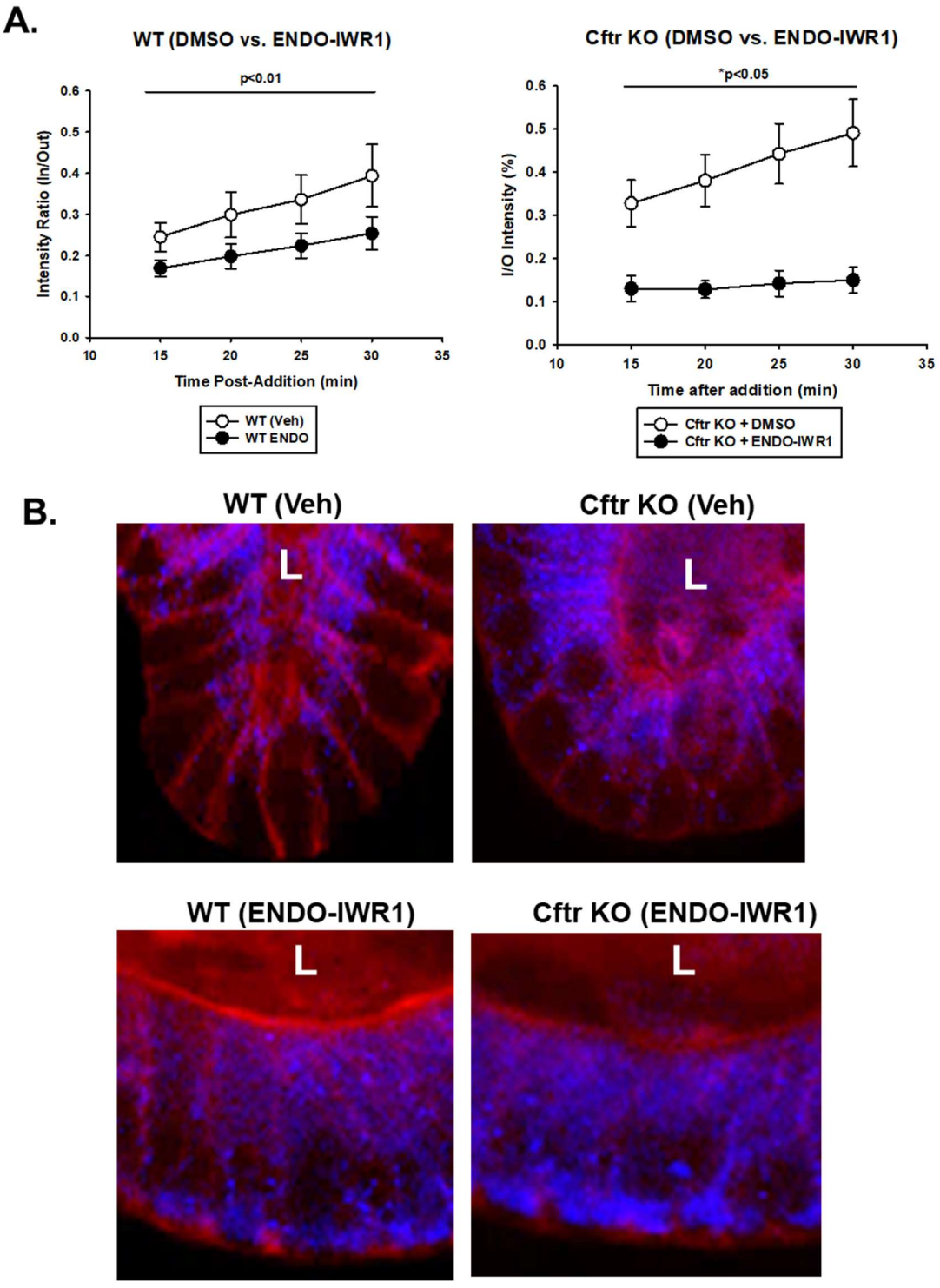

Figure 2.5. Paracellular permeability in *Cftr* KO enteroids is altered by inhibiting Wnt signaling. A. Cumulative data of vehicle (DMSO) and treated (ENDO-IWR1)

enteroids from n = 3 WT/*Cftr* KO pairs (3 female pairs). Values are represented as the intensity of luminal FITC 3kD dextran over time as a function of the external concentration in WT and *Cftr* KO. Left: vehicle- (open circles) and ENDO-IWR1-treated (filled circles) WT enteroids, *p<0.01 using one-way repeated measures ANOVA; right: vehicle- (open circles) and ENDO-IWR1-treated (filled circles) *Cftr* KO enteroids. *p <0.05 using one way repeated-measures ANOVA. B. Tight junction accumulation of the noncanonical Wnt signaling effector Cdc42 is reversed with ENDO-IWR1 treatment in *Cftr* KO/*Rosa*$^{mT/mG}$ and WT/*Rosa*$^{mT/mG}$ enteroids. L = Lumen, cyan = Cdc42, red = tdtomato-labeled membrane. Images representative of n = 6 WT/*Cftr* KO sex-matched littermate pairs (4 female, 2 male WT/*Cftr* KO pairs).

Disruption of Cdc42 activity induces more severe consequences to the paracellular permeability in the Cftr KO crypt epithelium.

Cdc42 is a key regulator of tight junctions and actin cytoskeleton remodeling[78,107]. The immunofluorescence studies and Rho GTPase activity assays suggest an important role for Cdc42 in maintaining the integrity of the rapidly-proliferating *Cftr* KO crypt epithelium. To assess its contribution to the intestinal barrier, early passage enteroids were treated with the Cdc42 inhibitor ML141 for 30 minutes prior to the addition of 3kD Cascade Blue dextran and FITC 500 kD dextran (which is typically tight junction-impermeant). As shown in figure 2.6A, acute inhibition of Cdc42 in WT enteroids had no significant effect on the luminal entry of 3kD dextran in WT organoids. In contrast, there was a significant increase in the permeability of CB 3 kD dex (figure 2.6B). Interestingly, as shown in figure 2.6C (left), Cdc42 inhibition had a profound effect on the permeability of several *Cftr* KO enteroids to FITC 500 kD dex within the time frame of the study. Others were less affected, which increased the variability of the individual response. As shown in figure 2.6C (right), there was nonetheless a significant increase in mean FITC 500 kD dex permeability in the *Cftr* KO enteroids as compared to similarly treated WT enteroids. These findings suggest that increased Cdc42 activity at the *Cftr* KO tight junctions is an appropriate response to compensate for an increased proliferation rate, which is also reflected in the redistribution of Cdc42 away from tight junctions when proliferation is inhibited.

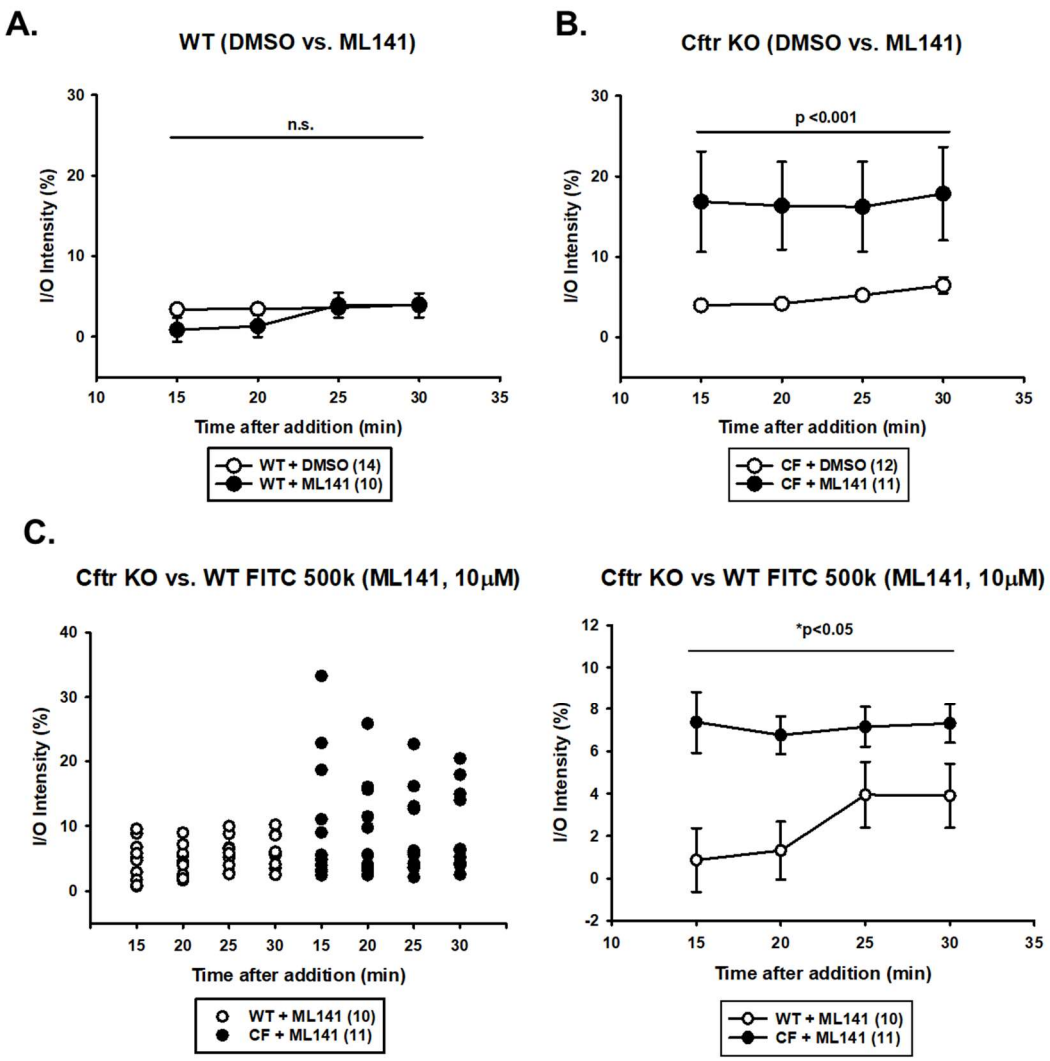

Figure 2.6. Paracellular permeability in *Cftr* KO enteroids is altered by Cdc42 inhibition. A, B. Cumulative data of vehicle-treated and ML141-treated enteroids from 5 WT/*Cftr* KO pairs (4 female, 1 male WT/*Cftr* KO pairs). Values represent luminal intensity of Cascade Blue 3kD dextran or 500kD FITC dextran over time as a function of external dye concentration in WT and *Cftr* KO. A. vehicle-treated (open circles) and ML141-treated (filled circles) WT enteroids, n.s. = not significant using one-way repeated measures ANOVA. B. vehicle-treated (open circles) and ML141 treated (filled circles) *Cftr* KO enteroids, *p<0.01 using one-

way repeated measures ANOVA. C. Individual (left) and cumulative (right) data for the luminal intensity of FITC 500kD dextran over time as a function of external dye concentration in ML141-treated WT (open circles) and *Cftr* KO (filled circles) enteroids, *p<0.05 using one way repeated-measures ANOVA. Data shown as mean values ± SE.

Paracellular permeability is not affected in WT small intestinal epithelium by increasing proliferation rate.

Crypts are the site of greatest paracellular permeability in the small intestine[108] suggesting that increased proliferation at this site may be coincident with an increase in paracellular permeability perhaps due to more rapid tight junctional remodeling. Our enteroid growth medium is reduced to 25% of the enteroid growth medium originally used by Sato et al.[59] to more closely mimic *in vivo* proliferation rates[103]. Using *de novo* crypt budding as measure of proliferation[109], WT and *Cftr* KO enteroids were compared for proliferation when provided 25% FRENS growth medium as compared to FRENS growth medium used by Sato et al[59]. As shown in figure 2.7A, *Cftr* KO enteroids proliferated at a greater rate as compared to WT when provided 25% FRENS. Proliferation in the *Cftr* KO enteroids was even greater as compared to WT when provided FRENS growth medium. Importantly, both the WT and *Cftr* KO enteroids proliferated at greater rates when provided FRENS as compared to 25% FRENS. Using this comparison in WT enteroids, CB 3kD dex permeability was compared between enteroids provided 25% FRENS versus FRENS overnight. As shown in figure 2.7B, permeability to the CB 3 kD dex was not affected by a greater rate of proliferation in the FRENS as compared to 25% FRENS. This finding suggests that increased 'leak' permeability in the *Cftr* KO crypt epithelium is not only a result of the enhanced proliferation but may be secondary to its dependence on increase Cdc42 activity, both with ties to pH_i dysregulation in the absence of Cftr.

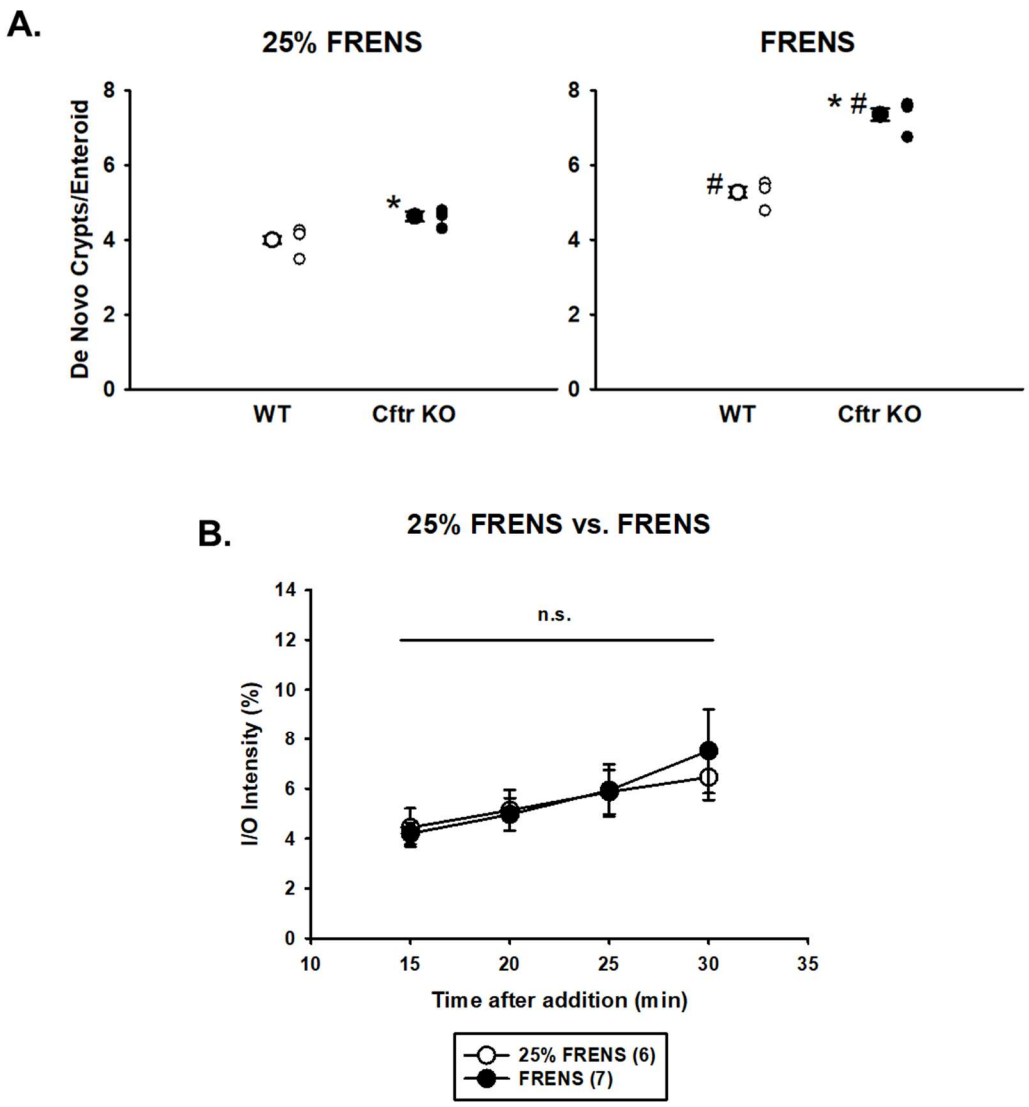

Figure 2.7. Increased proliferation rate is not associated with an increase in paracellular permeability in WT small intestinal enteroids. A. Cumulative crypt bud count data of early passage *Cftr* KO and WT organoids grown in either 25% FRENS (left) or FRENS medium (right). Left: 25% FRENS-grown enteroids. Average crypt bud count/enteroid (large circles) and averages per mouse (small circles) from n = 3 WT/*Cftr* KO pairs. *p=0.002 vs. WT 25% FRENS. Right: FRENS-grown enteroids. Average crypt bud count/enteroid (large circles) and average per mouse (small circles) from 3 WT/*Cftr* KO pairs. *p=0.001 vs. WT

FRENS, #p=0.001 vs. 25% FRENS. Comparisons of crypt bud counts made using Mann-Whitney rank sum test. Data shown as individual mouse values (small circles) and mean values ± SE (large circles). B. Cumulative intensity of luminal Cascade blue 3kD dextran over time as a function of the external concentration in WT enteroids grown in either 25% FRENS (open circles) and FRENS (filled circles) overnight, n = 6-7 organoids from 3 WT mice (1 female, 2 male). n.s. = not significant using one-way repeated measures ANOVA. Data represented as mean values ± SE.

Discussion

Increased intestinal permeability is a common manifestation of CF intestinal disease in pwCF and in *Cftr* KO mice[31–33,35,36]. In the healthy intestine, the paracellular movement of ions and solutes through the space between neighboring cells is regulated by tight junctions. Tight junction protein composition and organization determines paracellular ion conductance, known as the “pore” pathway, and the diffusion of molecules through the paracellular space, known as the “leak” pathway[23,25]. The CF intestine is characterized by chronic, low-grade inflammation and dysbiosis, which are both contributing factors to increased permeability given inflammatory signaling-mediated changes to tight junction protein organization and expression [26,27]. At the same time, disruption of the intestinal epithelial barrier contributes to intestinal inflammation through the translocation of microbes, luminal antigens, and other pro-inflammatory substances into the body, creating a vicious cycle of chronic inflammation[4,32,34]. However, increased leak pathway permeability has been found *in vitro* in delF508-CFTR human bronchial epithelial cell lines and in *Cftr* KO cholangiocyte monolayers by measuring the paracellular flux of small molecular weight probes, indicating an inherent defect in CF epithelium[26,54,92]. These studies and others have shown tight junction structural disorganization accompanied by an increase in the flux of larger molecules through the paracellular space *in vitro*, but there is still speculation as to the link between CFTR dysfunction and tight junction abnormalities. In this study, we provide new insight in the mechanism behind increased intestinal permeability in CF, linking

tight junction dysfunction with epithelial hyperproliferation. In addition, we show that enhanced Cdc42 Rho GTPase activity in CF is necessary to preserve epithelial barrier function. These studies using the *Cftr* KO mouse model and *CFTR* KO Caco-2 cells add to our understanding of the association between loss of CFTR and intestinal barrier dysfunction in the CF intestine.

Evidence of increased paracellular permeability in CF mouse intestinal epithelium was shown by an increased rate of luminal accumulation of a tight junction-permeant (3kD) dextran probe, indicating increased leak pathway permeability. Previously, we demonstrated that the absence of Cftr activity in murine crypt epithelium established an alkaline pH_i that facilitated increased Wnt/β-catenin signaling and ISC hyperproliferation via stabilization of the Wnt signal transduction protein Dvl at the apical membrane[71]. Dvl is also a key component of the noncanonical Wnt/PCP pathway, which regulates cell polarity, migration, and cell-cell junctions[74]. Imaging of *Cftr* KO and WT enteroids from mice expressing EGFP-Dvl2 showed a significant accumulation of EGFP-Dvl2 at the apical aspect of *Cftr* KO epithelial cells in the crypt buds. Notably, this accumulation was greatest in TAZ cells, which are rapidly proliferating progenitor cells migrating up the crypt-villus axis. This finding is significant as Wnt/β-catenin signaling is not a prominent contributor to transit-amplifying cell proliferation[110]. This Dvl2 transduction is positioned for increased Wnt/PCP signaling to accommodate increased crypt cell migration and tight junction remodeling in the CF intestinal crypts.

The downstream effectors of the Wnt/PCP pathway are the Rho GTPases, RhoA, Rac1, and Cdc42[77,111]. The Rho GTPases are molecular switches that cycle between an active (GTP-bound) and inactive (GDP-bound) state. Dvl-effector protein complexes in the Wnt/PCP signaling pathway activate the Rho GTPases to regulate cytoskeleton dynamics to facilitate cell migration, adhesion, polarization, membrane trafficking, and tight junction remodeling[24,91]. Using pulldown assays to assess active Rho GTPases in freshly isolated crypts and enteroids was frustrated by the time required for sample collection to preserve the labile GTP-bound state. Fortunately, our analysis was possible using a human intestinal epithelial Caco-2 cell line with *CFTR* loss-of-function mutations targeting exon 11 and 12[89]. Despite being derived from a human colon adenocarcinoma, Caco-2 cells form monolayers that have the physical and biochemical features of small intestinal enterocytes with functional CFTR[112]. Significantly, *CFTR* KO Caco-2 cells demonstrated a sustained alkaline pH_i, increased Wnt/β-catenin signaling, and an increased proliferation rate compared to WT Caco-2 cells, recapitulating our previous findings in the *Cftr* KO mouse intestine[71]. Unexpectedly, of the three primary Rho GTPases, Cdc42 was the only one significantly increased in its activity compared to WT Caco-2 cells. Imaging of Cdc42 localization in *Cftr* KO and WT freshly isolated crypts and in early passage organoids corroborated these findings by demonstrating overt accumulation of Cdc42 at the tight junctions of cells, especially in the TAZ, where the strongest Dvl apical membrane association was found. The Rho GTPase Cdc42 is critical for intestinal epithelial homeostasis as demonstrated by the

epithelial disorganization and crypt hyperplasia found in Cdc42 KO mice[78]. Further, TNFα-mediated inflammatory signaling induced *Cdc42* mRNA downregulation and intestinal barrier dysfunction in Caco-2 cells and IBD patients[83]. This is similar to our results of reduced *Cdc42* mRNA expression and increased claudin-2 expression in the freshly isolated crypt epithelium of *Cftr* KO mice, which also experience intestinal inflammation and barrier dysfunction[35,100]. Taking all of these findings into account, it is likely that Cdc42 activity is necessary for the functionality of the intestinal epithelial barrier in CF.

Maintenance of the intestinal barrier requires continuous renewal of the epithelium, which involves proliferation and migration of the intestinal epithelium and concomitant remodeling of the cytoskeleton and tight junctions[87]. Studies by Gallagher and Gottleib showed an association between increased cell migration and increased epithelial proliferation in *Cftr* KO mice, indicating a close association between the two cellular processes[88]. The important contribution of increased *Cftr* KO proliferation rate to tight junction permeability was demonstrated here by Wnt signaling inhibition via the axin stabilizer ENDO-IWR1, resulting in a dramatic decrease in paracellular permeability and a redistribution of Cdc42 away from tight junctions. Interestingly, *Cftr* KO enteroid permeability was significantly lower than WT enteroids in response to Wnt inhibition, suggesting an exaggerated response. An association between tight junction function and hyperproliferation has been noted in colorectal tumors, with increased proliferation accompanying leakier tight junctions and greater metastatic potential[113,114]. In the case of CF, hyperproliferation and tight junction

structural and functional abnormalities could be contributing factors to the increased incidence of GI cancer that pwCF experience compared to the general population[18].

Regulated Cdc42 activity is important for the assembly and maintenance of tight junction structure and function[77]. Acute inhibition of Cdc42 using the inhibitor ML141 resulted in a dramatic loss of barrier function in *Cftr* KO enteroids, increasing permeability to both 3kD and 500kD dextran probes, while WT enteroids demonstrated no significant change in barrier function. These findings are reminiscent of a study in Madin-Darby canine kidney (MDCK) cells expressing either dominant-active or dominant-negative Cdc42 mutants under the control of a tetracycline inducible repressor system[115]. MDCK cells expressing dominant-negative Cdc42 had increased paracellular flux of IgA and inulin 18 hours after doxycycline removal, with solute flux returning to control levels by 48 hours. Conversely, dominant-active Cdc42-expressing cells experienced a sustained increase in permeability. Both cell types experienced a slowing of endocytic trafficking, which is important for tight junction functionality and cell polarity maintenance[116]. Taking this into context with our own results, it is conceivable that given enough time, ML141-treated *Cftr* KO enteroids may have experienced a less profound change in paracellular permeability, and a more acute treatment with ENDO-IWR1 would have resulted in greater permeability. Regardless, our findings of increased tightening of the epithelial barrier with Wnt inhibition and increased permeability with Cdc42 inhibition indicate an exaggerated response to insults in CF epithelium. In the context of

the CF intestinal environment, this susceptibility would translate into a less effective epithelial barrier.

Our findings in WT intestinal epithelium suggests a greater adaptive capacity to challenges. To explore the effect of increased proliferation rate on WT epithelial barrier function, we measured the permeability of WT enteroids grown in FRENS medium and 25% FRENS medium. This experiment resulted in no significant change in permeability, despite FRENS medium increasing the proliferation rate of WT enteroids compared to 25% FRENS. The cell-cell junctions of epithelial layers require dynamic control of actin-driven membrane remodeling, which requires mechanisms that spatiotemporally regulate Cdc42 activity[76]. The ability of WT epithelium to adapt tight junction function to accommodate Cdc42 inhibition, decreased proliferation rate, and increased proliferation rate is likely related to its ability to modulate pH_i-sensitive mechanisms that regulate cytoskeleton dynamics and Rho GTPase activity. In normal cells, the pH_i is controlled on the scale of specific subcellular locations by ion transport proteins in response to stimuli, such as growth factor stimulation and/or metabolic rate[67]. Some Rho GTPase-activating guanine nucleotide exchange factors (GEFs), in addition to the actin-binding protein cofilin are regulated by pH_i, localizing to the more alkaline leading edge of cells to facilitate migration and remodeling of adhesions and cell-cell junctions[117,118]. In addition to pH_i regulation, CFTR also interacts with several actin-associated proteins to regulate the cytoskeleton[119]. CFTR is normally located at the apical plasma membrane in polarized epithelial cells, and the C-terminal PDZ-binding motif of

CFTR interacts with several actin cytoskeleton-associated proteins, including Na^+/H^+ exchanger regulatory factor isoform 1 (NHERF1), family with sequence similarity 13 member A (FAM13A), and zonula occludens 1 (ZO-1), which regulate the structure and function of cell-cell junctions[57,120,121]. Depending on the specific CF-causing mutation, CFTR function is disrupted by defects in protein folding, plasma membrane trafficking, plasma membrane stability, channel opening, or anion conductance[122], and mutated CFTR causes disorganization of the actin cytoskeleton and actin-associated proteins[92,120]. Therefore, the epithelial defect of *Cftr* KO epithelium may be due to a combination of pH_i dysregulation and the absence of Cftr-protein interactions.

An interesting finding in these studies was the increased Cdc42 activity in *CFTR* KO Caco-2 cells, while RhoA and Rac1 activity were not significantly different. These findings do not preclude Dvl-mediated activation of Rho GTPases, but rather it indicates other mechanisms are acting to increase Cdc42 activity in the CF intestine. For instance, adenomatous polyposis coli (APC), a component of the β-catenin destruction complex, also has Wnt-independent roles in the regulation of cell migration cell-cell junctions[123,124]. APC interacts with APC-Stimulated Guanine Nucleotide Exchange Factor (Asef), a Cdc42-specific GEF, and in colorectal cancer cells, APC-Asef-mediated Cdc42 activity promotes cell migration and increases tumor metastatic potential[125]. Another possible mechanism is via the Rho GTPase guanine nucleotide exchange factor DBS (Dbl's Big Sister), which shows catalytic activity for Cdc42[118,126]. During directed cell migration, the Golgi apparatus repositions towards the direction of migration;

this repositioning facilitates vesicular trafficking of protein and lipid components that are necessary for leading edge remodeling[127]. The Golgi membrane houses a pool of DBS protein that contributes to Cdc42 activation at the leading edge of migrating cells[128]. DBS is liberated from its membrane-bound state at more alkaline pH_i via deprotonation of histidine residues to increase Cdc42 activity[67,118]. Regardless of mechanism, Cdc42 activity appears necessary for *Cftr* KO intestinal epithelial barrier function, emphasizing the importance of discovering the mechanisms that increase its activity.

To summarize, this study provides evidence of increased leak pathway permeability in *Cftr* KO intestinal epithelium outside of the CF intestinal environment, and that hyperproliferation contributes to, but is not solely responsible for, this defect. In addition, increased Cdc42 Rho GTPase activity is a necessary response to preserve intestinal epithelial barrier function. Our findings in WT enteroids suggest the involvement of other factors in CF epithelial barrier dysfunction, such as the interaction of Cftr with actin- and tight junction-associated proteins and pH_i dysregulation. Further studies will be needed to determine the specific cause of the exaggerated responses to challenges of the *Cftr* KO epithelium. We postulate that dysregulation of pH_i dynamics plays a substantial role given the array of cellular processes with pH-dependent components[67,117,118]. Indeed, a previous study using siRNA-mediated knockdown of *CFTR* in Caco-2 cells showed that aberrantly increased production of the neutrophil chemotactic factor interleukin-8 (IL-8) was counteracted by pharmacological activation of the remaining CFTR channels, suggesting the

importance of pH_i in this response[129]. Although we did not directly show Dvl-mediated Cdc42 activation, increased Dvl apical membrane association in the TAZ suggests a role for Dvl-mediated signaling in CF. Dvl-APC association has been demonstrated at the leading edge of MDCK and HeLa cells to facilitate migration and polarity maintenance[112]. It is conceivable that Dvl-APC association may facilitate the localization of Cdc42 to tight junction complexes as a part of this process. The Caco-2 model of human CF intestinal epithelium may prove useful for the exploration of Cdc42 activation mechanisms, as well as in the CF epithelial response to different chemical and physical stimuli given its similarity to the CF mouse model. Greater knowledge of the molecular mechanisms that lead to pathological changes in CF intestinal disease may increase our understanding of the factors that contribute to the pathophysiology of barrier dysfunction in other GI-related diseases.

Chapter 3: Cdc42 Rho GTPase Activity Mediates Increased Cell Migration but not Increased Paracellular Permeability in *CFTR* Knockout Caco-2 Cells

Abstract

The Caco-2 cell line has been used extensively as an *in vitro* model of the human intestinal epithelium, including in cystic fibrosis (CF)-related research. Previously, we found that *CFTR* KO Caco-2 cells demonstrate increased intracellular pH (pH_i), Wnt/β-catenin signaling, and proliferation rate, recapitulating our findings in the *Cftr* KO mouse small intestine. *Cftr* KO intestinal organoids demonstrate increased leak permeability outside of the CF intestinal environment, suggesting an inherent defect in CF epithelial barrier function. In this study, we examine the permeability characteristics of *CFTR* KO and WT Caco-2 cells. We hypothesized that *CFTR* KO Caco-2 cells would recapitulate the increase in leak permeability found in *Cftr* KO enteroids. Interestingly, we found that the leak and pore permeability pathways were not significantly different between WT and *CFTR* KO as determined by the paracellular flux of 3kD FITC-dextran and transepithelial electrical resistance across Caco-2 cell monolayers, respectively. Measurement of *de novo* cell-cell junction formation via calcium switch assay revealed a more rapid reestablishment of the epithelial monolayer in *CFTR* KO Caco-2 cells. This finding was coupled with increased filopodia formation, Cdc42 activity, and Cdc42-dependent cell migration in *CFTR* KO Caco-2 cells. It is likely that the increased migration rate of *CFTR* KO Caco-2 cells enables the rapid reestablishment of cell-cell connections. We conclude that

while the permeability characteristics of WT and *CFTR* KO Caco-2 cells do not differ under basal conditions, this model provides an opportunity with which to study the molecular mechanisms affected by pH_i dysregulation in CF.

Introduction

Cystic fibrosis (CF) is the most common lethal genetic disease in people of Northern European descent and is caused by loss-of-function mutations in the cystic fibrosis transmembrane conductance regulator (*CFTR*) gene[130]. CF is a multisystem disease, which manifests as decreased fluid secretion, pH dysregulation, mucoviscidosis, dysbiosis, and reduced intestinal motility in the gastrointestinal system[4]. Another common manifestation of CF intestinal disease is increased intestinal permeability, which occurs in people with CF (pwCF)[31–33] and in CF mouse models[35,36]. The translocation of microbial components and other luminal contents into the portal circulation adversely effects the long-term health of pwCF by inducing inflammatory changes in the hepatobiliary and respiratory systems[8,32,42]. Even though the specific molecular mechanisms that lead to intestinal epithelial barrier dysfunction have not yet been fully elucidated, this defect has been found in CF airway, biliary, and epididymal epithelium cultured *in vitro*, indicating a cell-autonomous characteristic[54,57,58,92].

Our previous studies in the *Cftr* KO mouse revealed several abnormalities that occur as a result of intracellular pH (pH_i) dysregulation. *Cftr* KO intestinal epithelium sustains an alkaline pH_i due to loss of chloride and bicarbonate

conductance[61]. The result is increased Dishevelled (Dvl)-mediated Wnt/β-catenin signaling and epithelial hyperproliferation *in vivo* and *in vitro*. Increased proliferation rate necessitates an increase in migration rate of intestinal epithelium, which has been shown in *Cftr* KO mice[88]. Increased cell proliferation and migration require the concomitant remodeling of tight junction complexes, which regulate the passage of ions and solutes through the paracellular space[24,28]. Indeed, using an *in vitro* organoid model of small intestinal epithelium (enteroids), we found that *Cftr* KO enteroids demonstrated increased permeability to a tight junction-permeant dextran probe, which was partially a result of increased proliferation rate. *Cftr* KO cells also displayed evidence of increased Dvl-mediated Wnt/planar cell polarity (PCP) signaling, which regulates cell migration, polarity, and tight junction remodeling via the activity of the Rho GTPases RhoA, Rac1, and Cdc42[77,91]. Specifically, Cdc42 tight junction localization was increased in *Cftr* KO *in vivo* and *in vitro*, further supporting increased Wnt/PCP signaling. In order to translate these findings to a human model of CF intestinal epithelium, we utilized recently developed *CFTR* KO Caco-2 cells generated using CRISPR/Cas-9 gene editing technology[94]. We previously demonstrated that these cells recapitulate the increased pH_i, Wnt/β-catenin signaling, and proliferation rate found in *Cftr* KO intestinal epithelium.

In this study, we explore the paracellular permeability characteristics of *CFTR* KO and WT Caco-2 cells. Specifically, we examine the leak and pore pathways of permeability, or the flux of larger, uncharged molecules and ionic conductance through the paracellular space, respectively[131]. Given the

characteristics shared between the CF Caco-2 cell model and the *Cftr* KO mouse model, we hypothesize that *CFTR* KO Caco-2 monolayers will display increased paracellular permeability compared to WT Caco-2 cells due to increased proliferation and pH_i dysregulation.

Materials and Methods

Caco-2 culture. Six Caco-2 cell lines, three WT with sham-CRISPR/Cas9 gene editing and three *CFTR* KO by CRISPR/Cas9 gene editing, were kind gifts of Dr. Mitchell Drumm, Case Western Reserve University. Caco-2 cells were maintained in Minimum Essential Medium (Gibco) with 10% FBS, 1% glutamine, and 1% penicillin-streptomycin (100 IU/mL penicillin, 100 IU/mL streptomycin). Cells were maintained at 37°C in an atmosphere of 95% air: 5% CO_2. Medium was replaced every 3 to 4 days, and cells were passaged via trypsinization using TrypLE Express (Gibco) once reaching 70-80% confluency. All experiments were performed using Caco-2 cells from passages 5 to 30.

Transwell permeability assay. Caco-2 cells were passaged using TrypLE Express solution (Gibco) and seeded onto collagen-coated (3mg/mL rat tail collagen, type I, Advanced Biomatrix) 12mm polyester membrane (0.4μm pores) Transwell tissue culture inserts (Corning). Caco-2 cells were seeded on the apical surface at a density of 400,000 live cells/cm^2. The Caco-2 cells were grown in MEM (Gibco) supplemented with 10% FBS, 1% L-glutamine, and 1% penicillin-streptomycin. The medium was changed every other day of culture.

Paracellular permeability was measured for Caco-2 monolayers every week for three weeks (days 7, 14, and 21). On days 5, 12, and 19, medium was removed from the apical compartment of the Transwells to create an air-liquid interface (ALI) to promote *CFTR* expression[132]. Medium in the basal compartment was changed for each culture 24 hours prior to the assay. On the day of the assay, wells were washed once with phenol red-free MEM, and 800uL of phenol red-free MEM was added to the basal compartment. 250uL of 1mg/mL FITC-dextran (3kD MW, ThermoFisher Scientific) in phenol red-free MEM was added to the apical compartment and monolayers were protected from light and incubated for 2 hours at 37°C in an atmosphere of 95% air: 5% CO_2. After incubation, 250uL aliquots were taken from the basal compartment and transferred to a black, clear-bottom 96 well plate. A standard curve of FITC-Dextran was also added to determine the concentration of 3kD FITC dextran. FITC fluorescence intensity was determined using a Modulus™ II Microplate Multimode Reader (Turner BioSystems) using 490/520 nm excitation/emission. Flux was calculated as the amount of 3kD FITC-dextran (in ng) in the basal compartment per time unit (min) and filter area (cm^2). For the calcium switch assay, Caco-2 monolayers were grown on collagen-coated 12-well Transwell tissue culture inserts until reaching an average TER value of 1,500 $\Omega \cdot cm^2$. Monolayers were treated overnight (16h) with a calcium-free DMEM (Gibco) with 1% L-glutamine, 1% penicillin-streptomycin, and added low calcium (5uM $CaCl_2$) to promote tight junction disassembly. Transwell permeability experiments were performed as described above, and then regular MEM (Gibco) was added to allow for tight junction

formation. After 7 hours, permeability measurements were repeated. All permeability experiments were performed in triplicate Transwells.

Transepithelial resistance measurements. Confluent monolayers of Caco-2 cells were grown on collagen-coated polyester membrane Transwell culture inserts as described above. Transepithelial resistance (TER, $\Omega \cdot cm^2$) was measured using a Millicell-Electrical Resistance System (ERS) chopstick voltmeter (Millipore). For ALI experiments, TER readings were obtained for the first five days of each week before medium was removed from the apical compartment. For calcium switch experiments, TER readings were obtained immediately after overnight treatment with low calcium DMEM, and at 7 hours after regular MEM was added. All TER measurements were performed in triplicate Transwells.

Cdc42 GTPase activity assay. *CFTR* KO and WT Caco-2 cells were grown to approximately 60% confluence in culture flasks in MEM/10% FBS/1% pen-strep/1% L-glutamine medium. Activity of Cdc42 GTPase was measured using the colorimetric G-LISA assay (Cytoskeleton, Inc., Denver, CO, USA, Cat. # BK127) according to the manufacturer's instructions. All samples were performed in duplicate. Absorbance readings were performed on a Modulus™ II Microplate Multimode Reader (Turner BioSystems).

Circular wound healing assay. Caco-2 cells (400,000 live cells/cm^2) were plated in a 12-well culture plate (Corning) and grown to confluence. Cells were then serum starved overnight (medium without FBS) and wounded the following morning. Wounding was performed with a p-200 pipette tip attached to the end of an aspirator. After wounding, serum-free medium was exchanged for medium

with 0.5% FBS and 10μM ML141 (Millipore-Sigma) or 1:1000 DMSO (vehicle). Images of wounds were captured at 0 and 24 hours (40x) with an Infinity 1-3C Microscope Camera (Lumenera) on an Olmypus BH2 microscope using ImagePro Plus 6.3 software (Media Cybernetics, Bethesda, MD). Wounds were manually traced using ImageJ software (NIH, Bethesda, MD) to attain the area of the initial wound and at 24 hours post-wounding.

Caco-2 Immunofluorescence. Caco-2 cells were seeded onto poly-D-lysine no.1 coated coverslips (50 μg/mL poly-D-lysine, MP Biomedicals) at a density of 20,000 live cells/cm^2. After 24 hours, the culture medium was aspirated, cells were rinsed twice with phosphate-buffered saline (PBS) and fixed with 4% paraformaldehyde for 20 minutes at room temperature (RT). Cells were rinsed 3x with PBS and blocked/permeabilized in PBS + 1% bovine serum albumin (BSA) + 0.1% Triton® X-100 (Sigma) for 30 minutes at RT. Cells were then incubated with Acti-stain™ 488 (100nM, Cytoskeleton, Inc.) and To-Pro3 nuclear stain (1:2000 dilution, Invitrogen) in blocking/permeabilization buffer for 30 minutes at RT. Cells were rinsed 2x with PBS, washed 3x with PBS for 5 minutes each, then coverslips were mounted onto slides with ProLong Diamond Antifade mounting medium (ThermoFisher Scientific) and sealed before imaging. Images were attained using an Olympus FV1000 Confocal microscope.

Materials. L-glutamine and calcium-free DMEM was purchased from Gibco (Cat. No. 21068028). The Cdc42 inhibitor ML141 was purchased from Millipore-Sigma (Cat. No. 217708). All other materials were purchased from ThermoFisher Scientific.

Statistics. Cumulative data are reported as the mean ± SE. Data between two groups were compared using a two-tailed unpaired Student t-test or a two-tailed paired t-test. TER data were compared using a one-way repeated measures ANOVA with a Bonferroni post hoc test. A probability value of $p < 0.05$ was considered statistically significant.

Results

Leak and pore permeability does not significantly differ between WT and CFTR KO Caco-2 monolayers

Several studies have demonstrated an increase in the permeability of CF airway epithelial monolayers to small molecular weight probes[54,92], also known as the 'leak' pathway of permeability[23,25]. We asked whether *CFTR* KO Caco-2 monolayers would demonstrate the same increase in the leak pathway of permeability compared to WT Caco-2 cells. Given that Caco-2 monolayers grown on semipermeable filter supports take approximately 18-21 days to fully polarize[133–135], we measured the apical-to-basal flux of a small molecular weight (3kD MW) FITC-labeled dextran probe across Caco-2 monolayers grown on Transwell culture inserts once a week for three weeks. Surprisingly, as shown in figure 3.1A, the FITC 3kD dextran flux values did not significantly differ between WT and *CFTR* KO monolayers at any time during the experimental period, indicating no differences in leak permeability under basal conditions.

The paracellular permeability of epithelial barriers is defined by its leak permeability characteristics, as well as by its pore pathway characteristics[131]. The pore pathway refers to the ionic conductance of the paracellular space, and it is extremely size- and charge-selective[24]. Transepithelial electrical resistance (TER) is a measurement of the electrical resistance across a cell monolayer and is used as an assessment of the pore pathway[136]. Decreased TER has been noted in studies of *CFTR* KO human bronchial epithelium and also in murine epididymal epithelium with siRNA mediated *Cftr* knockdown[53,56,57]. In order to measure the pore pathway of permeability, we measured the TER of the WT and *CFTR* KO Caco-2 monolayers used to assess 3kD FITC dextran flux for the first five days of each week over a three-week period. This experiment revealed no significant difference in the development of TER for week 1 and week 3, but *CFTR* KO Caco-2 monolayer TER was significantly greater that WT for a few days during week 2, indicating a higher electrical resistance and tighter barrier in CF during that period (figure 3.1B).

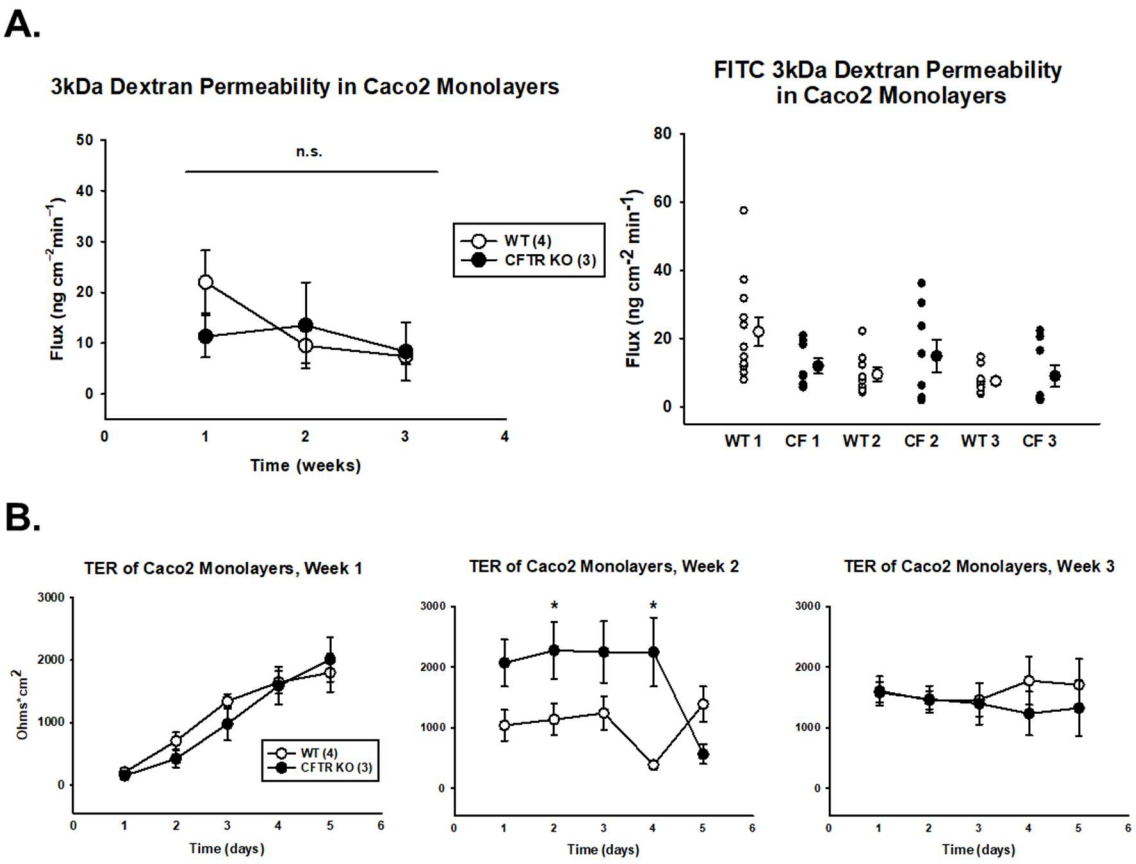

Figure 3.1. Leak and pore permeability does not differ between WT and *CFTR* KO Caco-2 monolayers. A.) Cumulative data (right) and individual values (left) of the apical-to-basal flux of 3kDa FITC-dextran after 2hrs in WT (open circles) and *CFTR* KO (filled circles), n = 4 WT, 3 *CFTR* KO independent experiments performed in triplicate, n.s. = not significant using one-way repeated measures ANOVA. Right. Data represented as mean values ± SE (large circles). Left. Data represented as mean values ± SE (large circles) and individual well flux values (small circles). B.) Cumulative data of TER in WT (open circles) and *CFTR* KO (filled circles) Caco-2 monolayers for week 1 (left), week 2 (middle), and week 3 (right) of culture. n = 4 WT, 3 *CFTR* KO independent experiments performed in

triplicate. *p<0.05 using one-way repeated measures ANOVA. Data represented as mean values ± SE.

CFTR KO Caco-2 monolayers demonstrate more rapid de novo cell-cell junction formation after calcium switch

Given that the permeability characteristics of Caco-2 monolayers did not significantly differ between WT and *CFTR* KO, we wished to determine if there was a difference in the ability of the cell monolayers to re-establish the epithelial barrier. We synchronized *de novo* junction formation in Caco-2 monolayers via calcium-switch assay, measuring TER and 3kD FITC-dextran flux at 0h and 7hrs after restoration of regular medium. Interestingly, this analysis revealed that *CFTR* KO monolayers had a significantly lower flux of 3kD FITC-dextran 7hrs after the addition of regular medium (figure 3.2, left). Conversely, the TER was not significantly different at either 0 or 7hrs after the restoration of regular calcium medium (figure 3.2, right), which supports the fact that the pore and leak pathways of permeability are independently regulated[131].

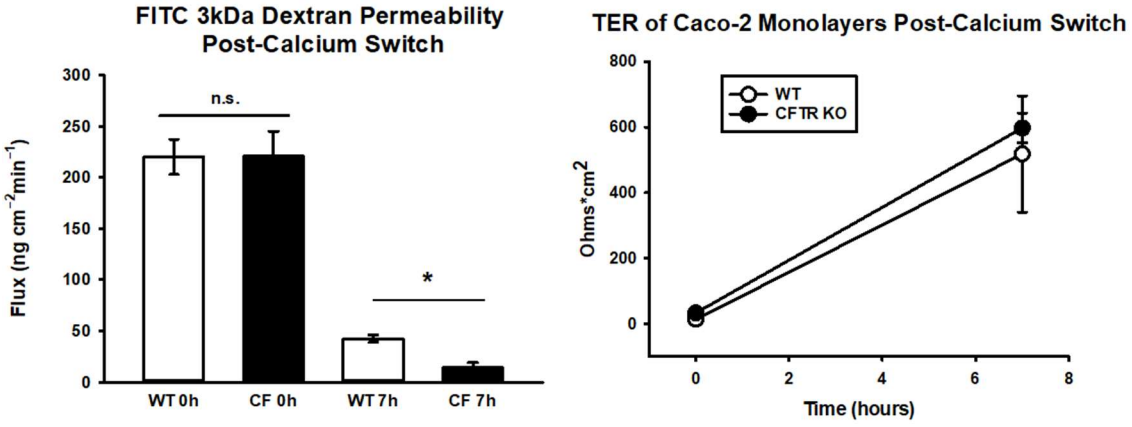

Figure 3.2. *CFTR* KO Caco-2 monolayers demonstrate an increased rate of *de novo* tight junction formation after calcium switch. Left. Apical-to-basal flux data of 3kDa FITC-dextran in WT (white) and *CFTR* KO (black) Caco-2 monolayers 0hrs and 7hrs after calcium switch. n = 3 WT and *CFTR* KO independent experiments done in triplicate; n.s. = not significant, and *p<0.01 using Student's t-test. Right. TER of WT (open circles) and *CFTR* KO (filled circles) Caco-2 monolayers for 0hrs and 7hrs after calcium switch. n = 3 WT and *CFTR* KO independent experiments performed in triplicate. Data represented as mean values ± SE.

Activity of the Rho GTPase Cdc42 and filopodia formation is increased in CFTR KO Caco-2 cells compared to WT.

The coordinated assembly and disassembly of cell adhesions and cell-cell junctions depends upon the regulation of actin cytoskeleton dynamics[137,138]. Given that the Ras homologous (Rho) family of GTPases are key regulators of the actin cytoskeleton, and the Rho GTPase Cdc42 is critical for intestinal epithelial barrier homeostasis[77,78], we investigated active (GTP-bound) Cdc42 in WT and *CFTR* KO Caco-2 cells. As shown in figure 3.3A, active Cdc42 was significantly greater in *CFTR* KO Caco-2 cells compared to WT. Cdc42 is involved in mediating cell migration, cell spreading, and filopodia formation[139,140], and increased Cdc42 activity was reflected in the morphological differences observed between *CFTR* KO and WT cells. In figure 3.3B, *CFTR* KO cells showed a flatter morphology and increased filopodia formation (white arrows) as compared to WT cells. The ability of *CFTR* KO Caco-2 cells to re-establish an epithelial barrier more rapidly after calcium-switch may be related to an increased cell spreading and migration rate to initiate junction formation and cover areas of cell loss.

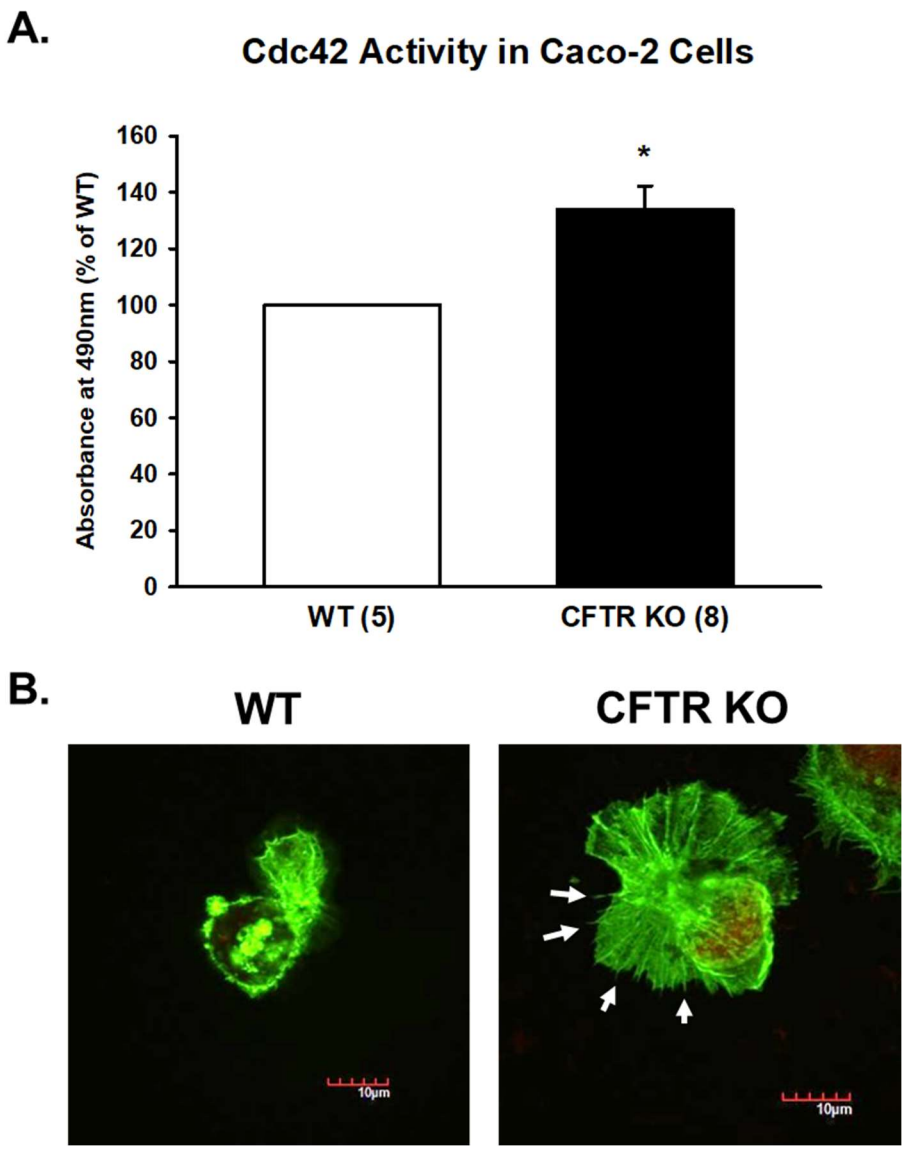

Figure 3.3. *CFTR* KO Caco-2 cells have increased Cdc42 Rho GTPase activity and filopodia formation compared to WT. A. ELISA-based assay measurement of GTP-bound (active) Cdc42 in WT (white) and *CFTR* KO (black) Caco2 cell lysates. n= 5 WT, 8 *CFTR* KO experiments run in duplicate. *p<0.05 using Student's t-test. B. Actin cytoskeleton images of WT (left) and *CFTR* KO (right) Caco-2 cells. Green = actin/phalloidin stain, red = nuclear stain. White arrows: filopodia.

Cell migration rate is increased and Cdc42 Rho GTPase-dependent in CFTR KO Caco-2 cells

Cell migration is a necessary component of epithelial restitution, which requires the coordinated movement of cells in an epithelial layer, also known as 'sheet migration'[141]. To assess the migration of Caco-2 cells, we performed a circular wound assay on serum-starved, confluent monolayers, measuring wound coverage after 24hrs (figure 3.4A). The influence of Cdc42 activity on cell migration was tested by treating wounded monolayers with the Cdc42 inhibitor ML141 or vehicle (DMSO). Initial findings show an increased rate of migration in *CFTR* KO Caco-2 cells compared to WT cells (figure 3.4B), with Cdc42 inhibition decreasing the migration rate of WT Caco-2 monolayers (figure 3.4C, left). Preliminary data of ML141-treated *CFTR* KO Caco-2 monolayers also demonstrates a decrease in migration rate of cell monolayers, indicating the importance of Cdc42 in cell migration (figure 3.4C, right).

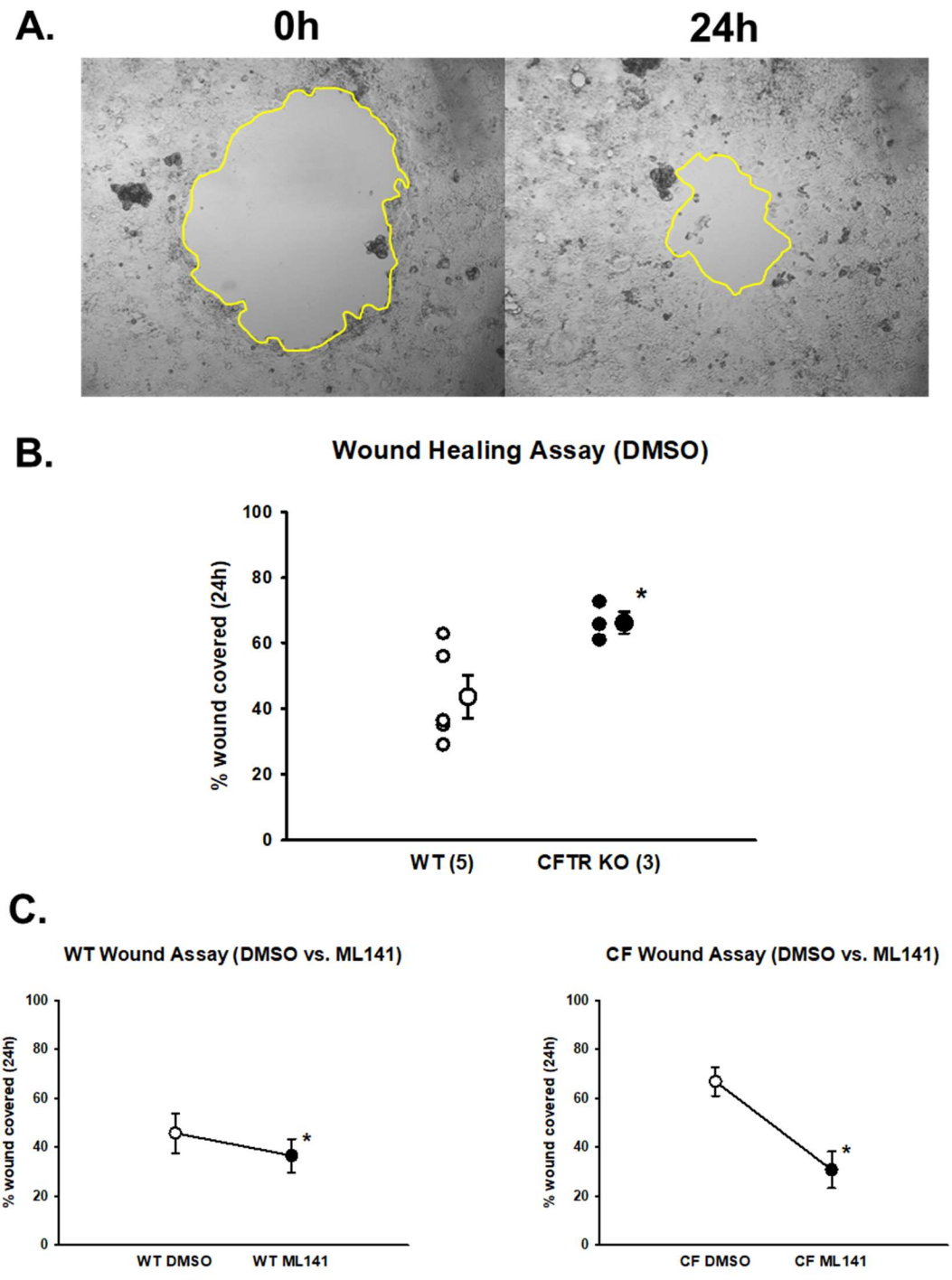

Figure 3.4. Cell migration rate is increased and Cdc42-dependent in *CFTR* KO Caco-2 cells compared to WT. A. Representative images of circular wounds in Caco-2 monolayers 0hrs (left) and 24hrs (right) after wounding. Yellow = wound

edge. B. Cumulative data of % initial wound area covered in WT (open circles) and *CFTR* KO (filled circles) Caco-2 monolayers; n = 5 WT, 3 *CFTR* KO with 2-4 wounds/monolayer. *p<0.05 using a Student's t-test. Data represented as mean values ± SE (large circles) and individual values (small circles). C. Cumulative data of % initial wound area covered for vehicle/DMSO-treated (open circles) and ML141-treated (filled circles) WT (left) and *CFTR* KO (right) Caco-2 monolayers; n = 4 DMSO and ML141-treated WT Caco-2 monolayers (left), n = 2 DMSO and ML141-treated *CFTR* KO Caco-2 monolayers (right). *p<0.05 using a paired t-test.

Discussion

The Caco-2 cell line, originally isolated from a colon carcinoma, has been used for decades as a human intestinal epithelial cell model[133,135]. Caco-2 cells develop both the morphological and biochemical characteristics of absorptive enterocytes of the small intestine when cultured after reaching confluence[133,142]. In terms of CFTR function, cyclic AMP-stimulated Cl^- current decreases as cells progress from an undifferentiated state to a differentiated state, which correlates with the expression of genes specific to absorptive enterocytes[143]. As a result, Caco-2 cells have been used as a model to study mechanisms of CFTR regulation[143]. Caco-2 cells have also been used in CF-related research to explore the roles of reduced CFTR function in intestinal epithelial cell metabolism, migration, and inflammatory signaling[129,144,145]. In many of these studies, CFTR activity is partially impaired by using either CFTR inhibitors or via shRNA- and siRNA-mediated protein knockdown. Although these studies have provided valuable information regarding the role of CFTR in regulating cellular processes, these studies do not fully represent the intestinal epithelium of pwCF. Recently, Hao et al.[94] developed Caco-2 cells with stable knockdown of *CFTR* using CRISPR/Cas9 genome editing technology to study cytokine production in CF intestinal epithelium. Unlike their sham-treated WT counterparts, *CFTR* KO Caco-2 subclones do not produce functional CFTR, providing a more representative model with which to study CF human intestinal epithelium. In this study we use these newly developed Caco-2 cells to explore the permeability characteristics of CF intestinal epithelial cells. Studies in pwCF, and in CF mouse

models have demonstrated an increase in intestinal permeability[31,35,100,146]. This defect of the intestinal epithelial barrier adversely affects the long-term health of pwCF through the translocation of microbial components into the circulation, inducing inflammatory changes in the downstream hepatobiliary and respiratory systems[8,32,42]. Interestingly, increased paracellular permeability has been found in CF epithelial cells grown *in vitro*, indicating that the barrier defect is an inherent quality of CF epithelial cell layers, and not just the result of the proinflammatory environment characteristic of the CF intestine[54,57,58,92].

The passage of ions and solutes through the paracellular space is regulated by the apical tight junction protein complexes[24]. The paracellular permeability characteristics of cell layers are divided into the leak pathway and the pore pathway of permeability, which refers to the passive diffusion of small molecules and the conductance of ions through the paracellular space, respectively[23,25]. Typically, Caco-2 cell monolayers require approximately 18-21 days to fully differentiate[133,134,143]. During that time, most cells in a monolayer differentiate in a homogenous manner, representing a model for only a single region of the crypt-villus axis[135]. The crypt domain and the villus domain vary in their permeability characteristics, with the crypt domain having the greatest paracellular permeability[108]. To determine the permeability characteristics of Caco-2 cells at different stages of differentiation, we measured TER and paracellular flux of a tight junction-permeant molecule across Caco-2 cell monolayers grown on semipermeable culture inserts over a 21-day period. Interestingly, the apical-to-basal flux of a soluble, tight junction-permeant

molecule (3kD FITC-dextran) was not significantly different between *CFTR* KO and WT Caco-2 monolayers at any point under basal growth conditions. Similarly, the measurement of TER showed no significant differences between the electrical resistance characteristics of WT and *CFTR* KO monolayers, except for a few days during week 2 when *CFTR* KO TER was significantly greater than WT. These data differ from most *in vitro* studies of CF epithelium, which demonstrate an increase in leak permeability[54,58,92], and others that show decreased TER[56,57]. The lack of difference in permeability characteristics are not dissimilar from the findings of Hao et al[94]. which found that *CFTR* KO and WT Caco-2 cells did not demonstrate a significant difference in the baseline expression of cytokines, but *CFTR* KO cells produced significantly more *CXCL8* mRNA in response to TNFα and IL1β. Therefore, in this model of human CF intestinal epithelium, the difference may lie in the response of the epithelial layer to challenges.

Epithelial cell junctions are present at points of cell-cell contact, with the composition of cell-cell junctions determining the permeability characteristics of the epithelia layer[24]. Cell-cell junctions include adherens junctions, which mediate cell-cell adhesion via the actions of nectins and cadherins, tight junctions, which regulate the passage of ions and solutes through the paracellular space, and desmosomes, which provide mechanical strength to the epithelial layer[24,147]. Adherens junction formation is essential for initiating the formation and stabilization of cell–cell connections, including tight junctions. Cadherins are Ca^{2+}-dependent, transmembrane glycoproteins found in adherens junctions with

extracellular Ca^{2+}-binding domains. Cadherins are a necessary component for the correct formation of the adherens junction, and calcium depletion results in the disassembly of cell-cell junctions[148]. The removal of calcium from cell culture medium, either through the addition of low calcium medium, or through the addition of calcium chelators, followed by subsequent addition of regular calcium-containing medium is known as a calcium switch assay. The calcium switch assay is used to investigate *de novo* tight junction formation. After calcium withdrawal, epithelial cells depolarized and attain a rounded morphology; and after calcium addition the cells reform tight junctions and reestablish polarity within a matter of hours[149]. CFTR has a role in actin cytoskeleton organization and cell-cell junction formation, with CFTR dysfunction resulting in disorganization of junctional proteins and the actin cytoskeleton[119]. Performing the calcium switch assay on Caco-2 monolayers, we expected *CFTR* KO Caco-2 cells to reestablish cell-cell junctions at a slower rate. However, our results showed a significant decrease in the paracellular flux of 3kD FITC-dextran in *CFTR* KO Caco-2 monolayers 7hrs post-calcium switch, indicating a more rapid reestablishment of the epithelial barrier compared to WT.

Calcium depletion induces the loss of cell-cell connections and cell-matrix connections, leading to the loss of some cells from the monolayer, making it necessary for cells to migrate and form cell protrusions to initiate cell-cell contacts[149,150]. These require reorganization of the actin cytoskeleton, which is regulated by the Ras homologous (Rho) family of small GTPases[77]. The most well-characterized and ubiquitous of the Rho GTPases are RhoA, Rac1, and

Cdc42[77]. Specifically, Cdc42 has an essential role in filopodia formation and directed cell migration[78,118,151,152], as well as being critical for intestinal epithelial homeostasis[78]. Analysis of active (GTP-bound) Cdc42 in *CFTR* KO and WT Caco-2 lysates revealed increased Cdc42 activity in CF. This result was reflected in the morphological differences found between *CFTR* KO and WT cells, with the *CFTR* KO Caco-2 cells demonstrating greater cell spreading and filopodia formation. These findings suggest that *CFTR* KO may have the ability to restore the epithelial barrier post-calcium switch secondary to an increased migration rate.

There have been conflicting results as to the effects of CFTR dysfunction on cell migration, with some reporting decreased cell migration in human airway and ovarian cancer cells[153,154], while others have found increased cell migration with *CFTR* knockdown in HeLa cells and human keratinocytes[155,156]. Typically, migration is measured via a wound-healing/scratch assay, which involves the mechanical disruption of a cell monolayer and determining the rate of wound closure. Assessment of migration in Caco-2 cells revealed an increased rate of migration in *CFTR* KO Caco-2 cells compared to WT. The importance of Cdc42 in cell migration was demonstrated via the effects of ML141 treatment on wound closure, which resulted in a significant decrease in migration rate for both *CFTR* KO and WT. It is important to make the distinction between what is measured in the wound healing/scratch assay versus the additional factors that characterize the wound environment *in vivo*. Scratch assays provide a measure of the migration of a cell layer, known as sheet migration. Sheet migration is a crucial

component of wound healing, which requires epithelial cells to migrate collectively to cover the wound area[141]. However, in wounded tissues, healing is influenced by many factors, including tissue oxygenation, microbial load, age, sex, nutrition status, desiccation, necrosis, and tissue tension[157]. So, while *CFTR* KO cells may demonstrate an increased migration rate and reestablish the monolayer more quickly *in vitro*, the studies of intestinal barrier dysfunction in pwCF and in CF mouse models suggests that this ability does not translate into an effective intestinal epithelial barrier. This is likely secondary to the alterations of cell-cell junctions by the proinflammatory environment of the CF intestine[4,26,27], as well as by the exaggerated inflammatory response that has been noted in CF cells[94,129].

In conclusion, our findings did not reveal any inherent differences in the permeability characteristics of *CFTR* KO and WT Caco-2 monolayers under basal growth conditions. However, our preliminary results indicate a significant increase in Cdc42-dependent cell migration in CF. Our previous characterization of *CFTR* KO Caco-2 cells revealed an increase in intracellular pH (pH_i), increased Wnt/β-catenin signaling, as well as increased proliferation rate compared to WT. These findings recapitulate previous findings in the intestinal epithelium of *Cftr* KO mice[71]. Unlike *Cftr* KO mice, *CFTR* KO Caco-2 cells did not demonstrate an increase in leak permeability *in vitro*. One interpretation of this finding is that *CFTR* KO Caco-2 cells may not be an appropriate model with which to assess CF intestinal barrier characteristics under basal conditions. Caco-2 monolayers have been used extensively as a model for predicting *in vivo*

absorption of drugs in the human intestine[133,135]. However, they have a few important limitations. First, Caco-2 cell cultures only contain one cell type, while the small intestine has multiple cell types, including stem cells, progenitor cells, goblet cells, enterocytes, Paneth cells, tuft cells, and enteroendocrine cells[158]. A study using primary jejunal organoid cultures revealed that the paracellular permeability characteristics of the epithelium varied between different cell types[159]. Second, Caco-2 cell monolayers have inherently smaller tight junctions than those found in the human intestine[160]. Third, the *CFTR* KO Caco-2 cells and their sham-treated WT counterparts were derived from several Caco-2 cell line subclones[89]. Subclones are derived from a parental line and demonstrate changes in the genomic DNA that differ from the original cells[161]. This is demonstrated in these Caco-2 cells as the different subclones possess anywhere from 2 to 4 copies of *CFTR*[89]. The variation among subclones may account for some of the variability in permeability that we found in our experiments (see figure 3.1A). Regardless of these limitations, the *CFTR* KO Caco-2 cells represent a unique opportunity to study the molecular mechanisms that contribute to intestinal barrier dysfunction in CF. Our previous findings of increased pH_i in *CFTR* KO Caco-2 cells suggests that these cells experience similar dysregulation of pH_i dynamics as that found in murine *Cftr* KO intestinal epithelium[61]. Several cellular processes rely heavily on the careful regulation of pH_i dynamics, including cell proliferation, migration, and membrane trafficking[67]. Dysregulation of pH_i dynamics in *CFTR* KO Caco-2 cells provides an opportunity to determine the cause of exaggerated responses to inflammatory stimuli in CF

intestinal cells. For example, siRNA-mediated knockdown of *CFTR* in Caco-2 cells resulted in the aberrantly increased production of interleukin-8[129], similar to the findings of Hao et al. in *CFTR* KO cells[94]. The mechanisms that promote this exaggerate response will require exploration into the possible involvement of pH-sensitive mechanisms, which may inform on our knowledge of the pathophysiology of other gastrointestinal diseases.

Chapter 4: Discussion and Future Studies

Several studies have found an increase in intestinal permeability in pwCF[31,33,146], as well as in CF mouse models *in vivo*[35,37,100]. In addition, increased paracellular permeability has been demonstrated *in vitro* in human bronchial epithelial cell lines[53,54,56], murine epididymal cell lines[57], and in primary mouse cholangiocytes[58]. Together, these findings suggest an inherent defect in epithelial barrier function as a result of CFTR dysfunction. The specific molecular mechanisms that lead to this dysfunction have yet to be fully elucidated. Regardless, intestinal epithelial barrier dysfunction is clinically relevant to pwCF given the connection between gastrointestinal (GI) health and the health of the hepatobiliary and respiratory systems, also known as the gut-liver and gut-lung axes, respectively. For example, it has been established that individuals with chronic gastrointestinal diseases, such as inflammatory bowel disease (IBD) and irritable bowel syndrome experience respiratory infections at a higher rate[162]. The same has been found in individuals with IBD being at greater risk of developing primary sclerosing cholangitis, autoimmune hepatitis, and biliary cirrhosis[163,164]. Even though no studies have demonstrated a direct relationship between increased intestinal permeability and the long-term health of pwCF, the association of increased intestinal permeability with GI and non-GI diseases has sparked interest in the causes and consequences of ‘leaky gut syndrome’, and in its potential as a therapeutic target[27,165,166].

The degree to which intestinal permeability is increased varies depending upon the specific disease process[165]. In the healthy intestine, the paracellular space is traversed by water, ions, and small organic solutes with a maximum diameter of 10-12 Å (approximately 1 nm)[131,166]. The specific permeability characteristics of the epithelial layer are determined by the composition of tight junction complexes[24], which are abnormal in CF epithelium *in vivo* and *in vitro*[54,57,100]. It is important to note that there is significant controversy over the extent to which increased intestinal permeability permits the paracellular passage of intact bacteria, microbial components (i.e., lipopolysaccharide), and dietary proteins[165,167]. Some *in vitro* studies have demonstrated that intact bacteria are able to traverse the paracellular space[168–170], while others have found that the translocation of bacteria and bacterial components into the circulation only occurs when there is substantial physical damage to the intestinal epithelium[171–173]. Regardless of the specific size permissiveness of tight junctions in the CF intestine, tight junction structural and functional abnormalities have other serious implications for the health of pwCF.

The dysregulation of tight junction structure and function is associated with chronic GI inflammation[39], carcinogenesis[174], and tumor metastasis[113]. Both chronic GI inflammation[175] and an increased risk of GI cancer are experienced by pwCF[18], with the latter occurring at a younger age than that of the general population[18,176]. The tight junction structure is made up of several transmembrane proteins that are connected to cytoplasmic scaffolding proteins and the actin cytoskeleton[177]. Tight junctions regulate cell differentiation and

proliferation through the sequestration of several cytoplasmic signaling proteins within their structure[24,178]. One example is the interaction of the tight junction scaffolding protein zonula occludens 1 (ZO-1) with the transcription factor ZO-1-Associated Nucleic Acid-Binding Protein (ZONAB)[179]. ZONAB tight junction localization is increased in cells grown to a high density with more mature tight junctions that contain higher levels of ZO-1[180]. Conversely, cells at low density with less mature tight junctions have lower levels of ZO-1 and greater ZONAB nuclear accumulation[181,182]. This modulation of the ZO-1/ZONAB pathway is similar to the findings of Ruan et al. in which *Cftr* knockdown in mouse epididymal epithelium resulted in an increase in ZONAB nuclear localization, decreased ZO-1 at tight junctions, and an increased proliferation rate[57]. We have also found that *Cftr* KO enteroids have significantly decreased ZO-1 protein compared to WT enteroids[183]. The release of ZONAB and other signaling molecules from tight junctions occurs during junctional remodeling in response to growth factor stimulation[111,178,180]. Taken together, this information suggests that CFTR plays an important role in regulating tight junction formation and cell differentiation.

The integrity of the intestinal epithelial barrier depends on the continuous proliferation and migration of epithelium from the crypt domain[184], which in turn requires concomitant remodeling of the cytoskeleton and tight junction proteins[87]. In our previous studies, we found that *Cftr* KO mouse intestinal epithelium has an alkaline pH_i relative to WT due to loss of Cftr-mediated chloride and bicarbonate conductance[103]. This resulted in increased plasma membrane association of the

pH-sensitive Wnt transduction protein Dishevelled (Dvl), increasing Wnt/β-catenin signaling and intestinal stem cell proliferation[71]. Dvl is also a key component of the noncanonical Wnt/planar cell polarity (PCP) pathway[91], which activates the Ras homologous (Rho) GTPases RhoA, Rac1, and Cdc42 to regulate cytoskeletal dynamics and tight junction remodeling during cell proliferation and migration[77]. Given the important role of the Rho GTPases in the regulation of the intestinal epithelial barrier[73], we hypothesized that Dvl-mediated transduction of noncanonical Wnt signaling would be increased in the alkaline CF intestinal epithelium, contributing to increased epithelial tight junction remodeling and paracellular permeability. In the present study we explore 1) the paracellular permeability characteristics of CF intestinal epithelium *in vitro*, 2) if intestinal epithelial hyperproliferation contributes to increased paracellular permeability, and 3) Rho GTPase activity and its role in epithelial barrier function in CF intestinal epithelium.

Cell-Autonomous Cdc42 Rho GTPase Activity Maintains Epithelial Barrier Function in the Cystic Fibrosis Intestine

Summary and Conclusions

We found increased Cdc42 tight junction localization in *Cftr* KO enteroids and increased Cdc42 Rho GTPase activity in *CFTR* KO Caco-2 cells (Chapter 2). We did not show a direct connection between increased Cdc42 activity and Dvl-mediated noncanonical Wnt signaling. However, the significant increase of Dvl

apical membrane localization throughout the TAZ in *Cftr* KO crypts suggests a role for Dvl-mediated noncanonical Wnt signaling to coordinate proliferation and migration of the progenitor cell population as Wnt/β-catenin signaling occurs mainly at the crypt base[158]. Surprisingly, our investigation of the three primary Rho GTPases RhoA, Rac1, and Cdc42 revealed that only Cdc42 was significantly increased in its activity. In addition, this activity was necessary to maintain the epithelial barrier of the hyperproliferative *Cftr* KO intestine. This was demonstrated by Cdc42 being redistributed away from tight junctions with canonical Wnt signaling inhibition, and when Cdc42 inhibitor resulted in a significant increase in paracellular permeability compared to WT. Our findings recapitulate those of Melendez et al. who found that intestinal-specific knockout of Cdc42 in mice resulted in increased epithelial permeability[78]. The specific mechanisms that drive increased Cdc42 activity will require further investigation, but given that Cdc42 is recruited and activated via pH-sensitive mechanisms, it is likely that pH_i dysregulation in CF plays a role[118]. Interestingly, WT intestinal epithelium experienced no significant change in permeability when the proliferation rate was increased, and when Cdc42 activity was inhibited. This suggests that the hyperproliferative phenotype of CF intestinal epithelium is not the primary cause of epithelial barrier dysfunction. Rather, it suggests that WT intestinal epithelium is able to adapt pH_i and pH-sensitive mechanisms that regulate cell-cell junctions to produce an appropriate response to challenges[62,67]. This lack of adaptive ability was demonstrated by *Cftr* KO epithelium, which showed a significantly greater decrease in permeability in response to Wnt

inhibition and a significant increase in permeability with Cdc42 inhibition. Overall, these findings indicate that CF intestinal epithelium experiences exaggerated responses to challenges, likely due to dysregulation of pH_i.

Cdc42 Rho GTPase Activity Mediates Increased Cell Migration but not Increased Paracellular Permeability in *CFTR* Knockout Caco-2 Cells

Summary and Conclusions

Our studies in Caco-2 cells showed that *CFTR* KO cells recapitulate the sustained alkaline pH_i, increased Wnt/β-catenin signaling, and increased proliferation rate found in *Cftr* KO mouse intestinal epithelium (Chapter 2). Given that *Cftr* KO enteroids displayed an increase in leak permeability compared to WT enteroids *in vitro*, we wished to explore the permeability characteristics of *CFTR* KO and WT Caco-2 monolayers. Unexpectedly, our analysis of the leak pathway of permeability via the apical-to-basal flux of a tight junction permeant (3kD MW) FITC-dextran probe showed no significant difference between *CFTR* KO and WT monolayers at any time during a three-week period. These results deviate from our findings in *Cftr* KO mouse enteroids, as well as from the findings of others measuring paracellular permeability in CF human bronchial epithelial cell lines[53,54] and primary mouse cholangiocytes[58]. Further, our analysis of the pore pathway of permeability via transepithelial electrical resistance (TER) measurements also showed no significant difference between *Cftr* KO and WT monolayers, except for a few days during week 2 where *CFTR* KO was

significantly higher than WT. These findings also differ from other studies showing decreased TER in CF epithelial monolayers[56,57]. Measurement of the apical-to-basal flux of 3kD FITC-dextran post-calcium switch assay indicated that *de novo* tight junction formation was significantly faster in *CFTR* KO monolayers, suggesting that *CFTR* KO Caco-2 cells were able to migrate and reestablish cell-cell connections more rapidly than WT cells. Given the involvement of the Rho GTPase Cdc42 in epithelial cell migration[78], we measured Cdc42 Rho GTPase activity in *CFTR* KO and WT Caco-2 cells. As expected, *CFTR* KO cells had significantly increased Cdc42 activity compared to WT using an ELISA-based assay, which was what we had found previously using a bead-based pulldown assay (Chapter 2). Increased Cdc42 activity facilitated an increase in migration rate of *CFTR* KO Caco-2 monolayers, which was significantly decreased in response to treatment with Cdc42 inhibitor. However, further studies will be needed to determine if the permeability characteristics of the *Cftr* KO mouse model or the *CFTR* KO Caco-2 cell line reflect the permeability characteristics of intestinal epithelium in pwCF. *In vitro* studies of pore and leak permeability in primary human intestinal epithelium would clarify the relevancy of either model for the study of intestinal barrier function. Regardless of barrier characteristics, the findings of this study suggest that *CFTR* KO Caco-2 cells are a good model to explore the cellular processes aberrantly affected by pH_i dysregulation.

Overall Conclusions and Summary of Study

In summary, the studies presented here demonstrate that Cdc42 Rho GTPase activity is increased in CF intestinal epithelium, and in *Cftr* KO mouse intestinal epithelium, Cdc42 activity is necessary for epithelial barrier function. The fact that increased proliferation and Cdc42 inhibition did not perturb the epithelial barrier in WT enteroids indicates that the barrier defect in *Cftr* KO enteroids is not a result of increased proliferation rate. Rather, it suggests that the defect lies in the response of the CF epithelium to challenges, likely exaggerated as a result of pH_i dysregulation. In addition, we found that the *CFTR* KO Caco-2 cells recapitulate the increased pH_i, Wnt/β-catenin signaling, and proliferation rate of the *Cftr* KO mouse intestinal epithelium, but that they do not reproduce the increase in paracellular permeability of this model. Although each model of the CF intestinal epithelium represents an opportunity to study the consequences of pH_i dysregulation, further studies will be needed in order to determine which model more accurately represents the intestinal epithelium in pwCF.

Potential Limitations

Intestinal organoid (enteroid) permeability assay

Our measurements of the luminal accumulation of tight junction-permeant dextran probes in WT and *Cftr* KO enteroids showed an increase in leak permeability in the *Cftr* KO intestinal epithelium. These experiments used

enteroids 2-3 days post-plating since many enteroids less than 2 days old are not fully enclosed, and enteroids older than 4 days begin to form crypt buds, making it difficult to obtain a clear image of the enteroid lumen. However, we noted that there was a noticeable difference in the diameter between *Cftr* KO and WT enteroids despite using a restricted age range (figure 4.1). This size difference is likely the result of functional Cftr in WT enteroids facilitating fluid secretion into the enteroid lumen, which is the premise behind the forskolin-induced swelling (FIS) assay[61,103]. It is conceivable that dye dilution would occur in WT enteroids with a larger volume. Our findings in *Cftr* KO and WT enteroids could be verified by measuring leak permeability of epithelium grown on semipermeable culture inserts with a fixed culture area, which has been demonstrated in both mouse and human primary intestinal epithelium[185].

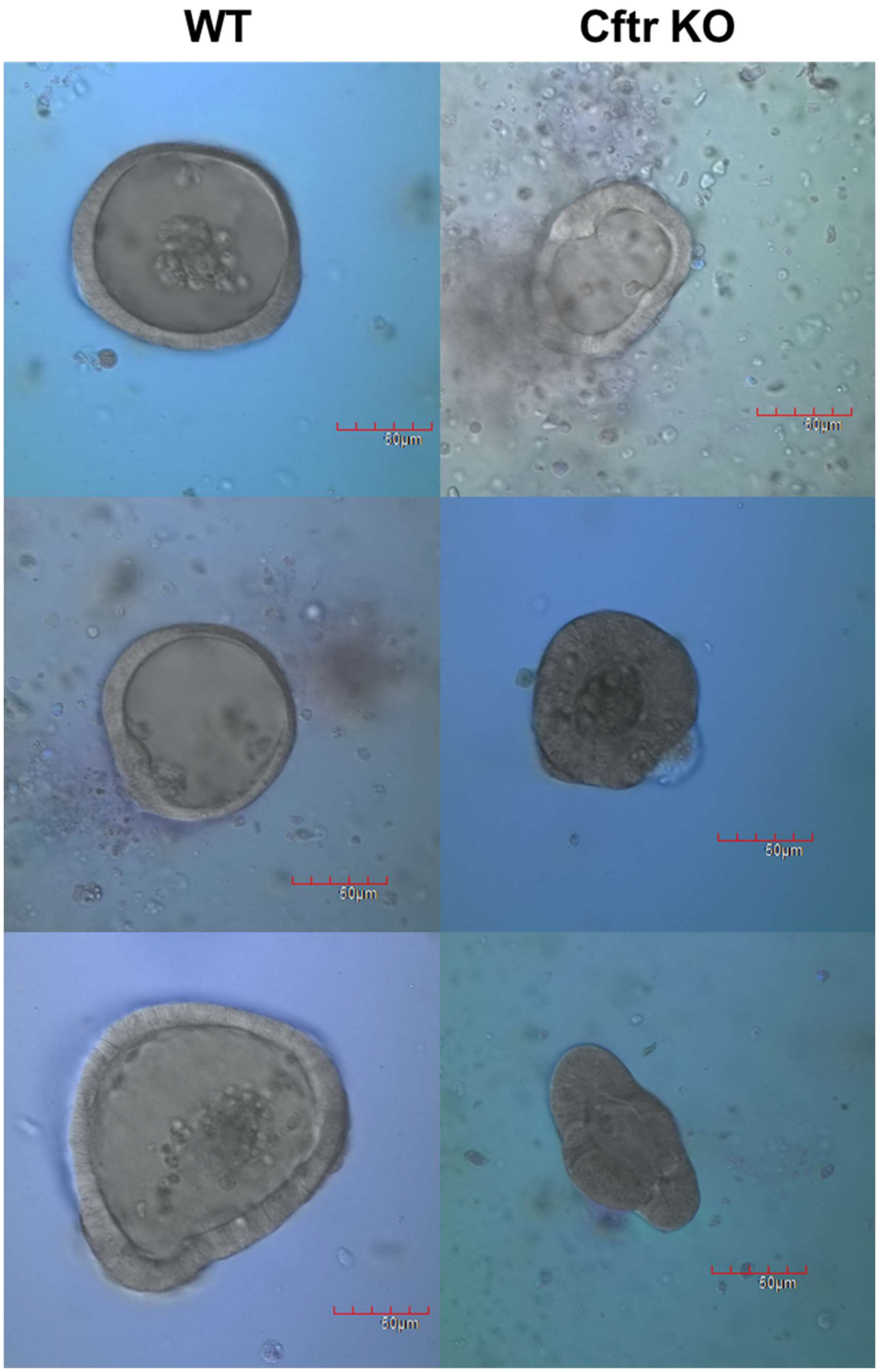
WT
Cftr KO
50µm
50µm
50µm
50µm
50µm
50µm

Figure 4.1. Limitations of the enteroid permeability assay in WT and *Cftr* KO enteroids. Representative images of several WT (left) and *Cftr* KO (right) enteroids 2-3 days post-plating used for measuring luminal entry of 3kD Cascade Blue dextran.

Caco-2 Monolayer Transwell Permeability Assay

Caco-2 cell monolayers have been used extensively as a model to study drug absorption in the human intestine and the effects of compounds on intestinal epithelial barrier function[133,135]. Contrary to the findings of other studies showing increased leak permeability in CF epithelium[53,54], *CFTR* KO Caco-2 cells did not show a significant difference in the apical-to-basal flux of a tight junction-permeant dextran probe when compared to WT. However, a study by Molenda et al. found that apical-to-basal flux of fluorescein-dextran was not significantly different in 16HBE14o– (WT) and CFBE41o– (*CFTR* KO) human bronchial epithelial cell lines under control conditions[56]. They noted important differences in the structure and morphology of cell-cell contacts, in which immunostaining of ZO-1 in 16HBE14o– and CFBE41o– monolayers showed that 16HBE14o– monolayers had significantly smaller cells and longer cell-cell contacts when compared to CFBE41o- monolayers. Further, they found that the microstructure of 16HBE14o– cell-cell contacts was characterized by numerous wrinkles and ruffles, increasing the area of cell-cell contacts. When the length of cell-cell contacts was used to normalized dextran flux values, CFBE41o- monolayer fluorescein-dextran flux was significantly greater than 16HBE14o– monolayers. In our studies of WT and *CFTR* KO Caco-2 cells, we are working with six different Caco-2 cell line subclones (three *CFTR* KO, three WT), which may have individual permeability characteristics. This finding is reflected in the variability of flux values that we found in *CFTR* KO and WT Caco-2 monolayers (figure 3.1A, right). Therefore, full characterization of the permeability characteristics of *CFTR*

KO and WT Caco-2 monolayers may require analysis of cell size and the length of cell-cell contacts.

Future studies

In this study, we provide evidence for increased noncanonical Wnt signaling and Cdc42 Rho GTPase activity in the CF intestinal epithelium, which influences epithelial permeability and migration. However, despite the similarities shared between the *Cftr* KO mouse intestinal epithelium and *CFTR* KO Caco-2 cells, these two models showed very different permeability characteristics. Therefore, further studies are needed to determine which model more accurately represents CF intestinal epithelium *in vivo*.

Determine the epithelial barrier characteristics of intestinal organoids from human induced pluripotent stem cells

Induced pluripotent stem cells (iPSCs) are generated from somatic cells taken directly from human patients[186]. This technique involves the introduction of *Myc*, *Oct3/4*, *Sox2*, and *Klf4* genes into human somatic cells, converting them into pluripotent stem cells[187]. Human iPSCs are self-renewing pluripotent cells that can produce cells from any of the three germ layers (endoderm, ectoderm, and mesoderm)[186,188]. Human iPSCs can be differentiated down the intestinal epithelial lineage and used to grow human intestinal organoids (HIOs)[189], which

have been used extensively to study IBD[190,191], host-microbe interactions[189,192], and, more recently, as a method to develop CFTR modulator therapies[193].

Recently, we have been very fortunate to gaining access to iPSC-derived HIOs from pwCF and healthy individuals from clinical trials through the Cystic Fibrosis Foundation Biorepository. Samples from pwCF retain the specific *CFTR* mutation as well as recapitulating the morphological and biochemical characteristics of intestinal epithelium *in vitro*[193,194]. We have successfully cultured HIOs from individuals homozygous for ΔF508, the most common CF-causing mutation[1], and we are in the process of attaining HIOs from healthy individuals for culture. Given the discrepancy of permeability characteristics between *Cftr* KO mouse intestine and *CFTR* KO Caco-2 monolayers, it is our goal to use HIOs from pwCF and healthy individuals to study the effects of CFTR dysfunction on epithelial barrier characteristics. Previous studies have demonstrated techniques for culturing monolayers from HIOs for the measurement of paracellular flux and TER[195]. By using this technique, our goal is to evaluate the pore and leak pathways of permeability in a more directly applicable model of CF intestinal epithelium.

Complete wound healing assays in CFTR KO and WT Caco-2 monolayers and pursue mechanisms of increased Cdc42 activity

Our preliminary data in Caco-2 cell monolayers indicates that migration rate is significantly increased in *CFTR* KO cells compared to WT, which

recapitulates the findings from Gallagher and Gottlieb, in which intestinal epithelial migration rate was increased in the crypt epithelium of *Cftr* KO mice *in vivo*[88]. The involvement of Cdc42 is also indicated in these preliminary findings, as treatment with the Cdc42 inhibitor ML141 significantly decreased migration rate. Our findings in both *Cftr* KO mouse enteroids and in *CFTR* KO Caco-2 cells point to an important role for Cdc42 in CF intestinal epithelium. However, we have yet to discover the mechanism by which CFTR dysfunction leads to increased Cdc42 activity, while the other primary Rho GTPases, RhoA and Rac1 are not significantly different. Upon completion of the wound healing assay experiments, our next step is to explore several possible mechanisms of Cdc42 activation.

As detailed in the discussion section of Chapter 2, we put forth several possible mechanisms of increased Cdc42 activity in CF. The association of Dishevelled (Dvl) and adenomatous polyposis coli (APC) is of particular interest given that we found increased Dvl apical membrane association throughout the crypt domain in CF epithelium. Dvl-APC association has been noted at the migration front of MDCK and HeLa epithelial cell lines[112], and it may facilitate Cdc42 localization to the tight junctions through the association of APC with the Cdc42-specific activator APC-Stimulated Guanine Nucleotide Exchange Factor (Asef)[124,125]. We had originally planned experiments measuring Cdc42 activity in Caco-2 cells treated with MAIT 203, a specific inhibitor of APC-Asef association. Unfortunately, this compound is no longer commercially available, but we plan on exploring this mechanism using siRNA-mediated knockdown of Asef. Another

possible mechanism is increased Cdc42 activity through the guanine nucleotide exchange factor (GEF) DBS (Dbl's Big Sister)[118,126]. DBS (also known as MCF.2 Cell Line Derived Transforming Sequence Like, or MCF2L) is a pH-sensitive Rho GTPase GEF that is involved in directed cell migration[127] and it is expressed in a variety of cell types, including Caco-2 cells[196]. Given that DBS is liberated from the Golgi membrane with increased pH_i, it is conceivable that it is involved in increased Cdc42 activity in CF[67,118]. There are no specific inhibitors of DBS-Cdc42 interaction, but this mechanism could be explored by looking at the effect of siRNA-mediated DBS knockdown on Cdc42 activity, or the measurement of Dbs-Cdc42 association via coimmunoprecipitation.

Aberrantly increased Cdc42 activity is associated with increased GI cancer invasion and metastasis, and Cdc42 has gained interest as a target in cancer treatment[73,197]. This highlights the importance of determining the mechanisms of increased Cdc42 activity in CF, especially as pwCF are at an increased risk of developing GI cancer[18].

Measure proliferation, ZO-1 protein expression and ZONAB nuclear localization in CFTR KO Caco-2 cells transfected with WT CFTR or CFTR without the C-terminal PDZ-binding domain (CFTRΔTRL)

CFTR interacts with the tight junction scaffolding protein ZO-1 through its C-terminal PDZ-binding domain (TLR)[57,119]. ZO-1 connects tight junction transmembrane proteins with the actin cytoskeleton via protein-protein

interactions through its three PDZ domains[24,111]. ZO-1 also sequesters the transcription factor ZONAB at the tight junctions of polarized epithelium[182]. Ruan et al. showed that siRNA-mediated knockdown of *Cftr* in murine epididymal epithelium resulted in reduced ZO-1 protein and the nuclear translocation of ZONAB, resulting in an increased proliferation rate[57], suggesting an important role for CFTR in the regulation of tight junction formation and cell differentiation. It is not known if CFTR plays an important role in the regulation of the ZO-1/ZONAB pathway in intestinal epithelium. Our previous findings of reduced ZO-1 in *Cftr* KO enteroids and the findings of Ruan et al. in murine epididymal epithelium suggest that *CFTR* KO Caco-2 cells will demonstrate decreased ZO-1 protein expression and increased nuclear ZONAB compared to WT Caco-2 cells. We have acquired constructs of 3HA-tagged and 3FLAG-tagged variants of WT *CFTR* and of *CFTR*ΔTRL, which lacks the C-terminal PDZ-binding motif (a kind gift from Dr. Peter M. Haggie, University of California, San Francisco). With transfection of *CFTR* KO Caco-2 cells with *CFTR*ΔTRL or WT *CFTR*, we would expect to find reduced ZO-1 and increased nuclear ZONAB to be corrected by WT *CFTR*, but not by *CFTR*ΔTRL. Given that *CFTR*ΔTRL is able to reach the plasma membrane and its channel function is unaffected[198], we anticipate that it will normalize pH_i, and reduce the proliferation rate of transfected *CFTR* KO Caco-2 cells. These constructs could also be used to study the effects of WT *CFTR* or *CFTR*ΔTRL on Cdc42 activity of transfected *CFTR* KO Caco-2 cells. The signaling proteins sequestered at the tight junctions include numerous Rho GTPase GEFs[24], so this experiment would provide further information regarding

the mechanism of increased Cdc42 activity in the CF intestine. If *CFTR*ΔTRL transfection of *CFTR* KO Caco-2 cells is sufficient to normalize Cdc42 activity, it would suggest that the mechanism is a result of pH_i dysregulation. However, if Cdc42 activity is still aberrantly increased with successful *CFTR*ΔTRL transfection, it would indicate that the association of CFTR with tight junction proteins plays a role in Cdc42 regulation.

REFERENCES

1. Cystic Fibrosis Foundation. Cystic Fibrosis Foundation Patient Registry 2020 Annual Data Report. (2021).
2. Miller, A. C. *et al.* Cystic fibrosis carriers are at increased risk for a wide range of cystic fibrosis-related conditions. *Proc Natl Acad Sci U S A* **117**, 1621–1627 (2020).
3. Gelfond, D. & Borowitz, D. Gastrointestinal Complications of Cystic Fibrosis. *Clinical Gastroenterology and Hepatology* **11**, 333–342 (2013).
4. De Lisle, R. C. & Borowitz, D. The Cystic Fibrosis Intestine. *Cold Spring Harbor Perspectives in Medicine* **3**, a009753–a009753 (2013).
5. Bourke, S. J. & Quibell, R. Cystic Fibrosis. in *Integrated Palliative Care of Respiratory Disease* (eds. Bourke, S. J. & Peel, T.) 159–172 (Springer International Publishing, 2019). doi:10.1007/978-3-030-18944-0_10.
6. Gentzsch, M. & Mall, M. A. Ion Channel Modulators in Cystic Fibrosis. *Chest* **154**, 383–393 (2018).
7. Davies, J. C. *et al.* VX-659–Tezacaftor–Ivacaftor in Patients with Cystic Fibrosis and One or Two Phe508del Alleles. *N Engl J Med* **379**, 1599–1611 (2018).
8. Adriaanse, M. P. M. *et al.* Evidence for a Cystic Fibrosis Enteropathy. *PLOS ONE* **10**, e0138062 (2015).
9. Strong, T. V., Boehm, K. & Collins, F. S. Localization of cystic fibrosis transmembrane conductance regulator mRNA in the human gastrointestinal

tract by in situ hybridization. *Journal of Clinical Investigation* **93**, 347–354 (1994).

10. Sathe, M. N. & Freeman, A. J. Gastrointestinal, Pancreatic, and Hepatobiliary Manifestations of Cystic Fibrosis. *Pediatric Clinics of North America* **63**, 679–698 (2016).
11. Sabharwal, S. Gastrointestinal Manifestations of Cystic Fibrosis. *Gastroenterol Hepatol (N Y)* **12**, 43–47 (2016).
12. Kastl, A. J., Terry, N. A., Wu, G. D. & Albenberg, L. G. The Structure and Function of the Human Small Intestinal Microbiota: Current Understanding and Future Directions. *Cellular and Molecular Gastroenterology and Hepatology* **9**, 33–45 (2020).
13. Lewindon, P. J., Robb, T. A., Moore, D. J., Davidson, G. P. & Martin, A. J. Bowel dysfunction in cystic fibrosis: importance of breath testing. *J Paediatr Child Health* **34**, 79–82 (1998).
14. Fridge, J. L., Conrad, C., Gerson, L., Castillo, R. O. & Cox, K. Risk Factors for Small Bowel Bacterial Overgrowth in Cystic Fibrosis. *Journal of Pediatric Gastroenterology and Nutrition* **44**, (2007).
15. Dorsey, J. & Gonska, T. Bacterial overgrowth, dysbiosis, inflammation, and dysmotility in the Cystic Fibrosis intestine. *Journal of Cystic Fibrosis* **16**, S14–S23 (2017).
16. Raia, V. *et al.* Evidence of Chronic Inflammation in Morphologically Normal Small Intestine of Cystic Fibrosis Patients. *Pediatr Res* **47**, 344–350 (2000).

17. Flass, T. *et al.* Intestinal lesions are associated with altered intestinal microbiome and are more frequent in children and young adults with cystic fibrosis and cirrhosis. *PLoS One* **10**, e0116967 (2015).
18. Bhattacharya, R., Blankenheim, Z., Scott, P. M. & Cormier, R. T. CFTR and Gastrointestinal Cancers: An Update. *JPM* **12**, 868 (2022).
19. Neglia, J. P. *et al.* The risk of cancer among patients with cystic fibrosis. *New England Journal of Medicine* **332**, 494–499 (1995).
20. Ooi, C. Y. *et al.* Impact of CFTR modulation with Ivacaftor on Gut Microbiota and Intestinal Inflammation. *Scientific Reports* **8**, (2018).
21. Bruzzese, E. *et al.* Disrupted intestinal microbiota and intestinal inflammation in children with cystic fibrosis and its restoration with Lactobacillus GG: a randomised clinical trial. *PLoS One* **9**, e87796 (2014).
22. Henker, R. *et al.* Severe ileocecal inflammatory syndrome in adult patients with cystic fibrosis. *Z Gastroenterol* **57**, 312–316 (2019).
23. Buckley, A. & Turner, J. R. Cell Biology of Tight Junction Barrier Regulation and Mucosal Disease. *Cold Spring Harb Perspect Biol* **10**, (2018).
24. Zihni, C., Mills, C., Matter, K. & Balda, M. S. Tight junctions: from simple barriers to multifunctional molecular gates. *Nature Reviews Molecular Cell Biology* **17**, 564–580 (2016).
25. Ulluwishewa, D. *et al.* Regulation of tight junction permeability by intestinal bacteria and dietary components. *J Nutr* **141**, 769–776 (2011).

26. Sakisaka, S. *et al.* Alterations in tight junctions differ between primary biliary cirrhosis and primary sclerosing cholangitis. *Hepatology* **33**, 1460–1468 (2001).
27. Bischoff, S. C. *et al.* Intestinal permeability – a new target for disease prevention and therapy. *BMC Gastroenterology* **14**, (2014).
28. Balda, M. S. & Matter, K. Tight junctions and the regulation of gene expression. *Biochimica et Biophysica Acta (BBA) - Biomembranes* **1788**, 761–767 (2009).
29. Volksdorf, T. & Brandner, J. M. Tight Junctions and Cutaneous Wound Healing. in *Wound Healing* 31–42 (John Wiley & Sons, Ltd, 2018). doi:10.1002/9781119282518.ch3.
30. Volksdorf, T. *et al.* Tight Junction Proteins Claudin-1 and Occludin Are Important for Cutaneous Wound Healing. *Am J Pathol* **187**, 1301–1312 (2017).
31. Leclercq-Foucart, J., Forget, P. P. & Van Cutsem, J. L. Lactulose-rhamnose intestinal permeability in children with cystic fibrosis. *J Pediatr Gastroenterol Nutr* **6**, 66–70 (1987).
32. del Campo, R. *et al.* Translocated LPS Might Cause Endotoxin Tolerance in Circulating Monocytes of Cystic Fibrosis Patients. *PLoS ONE* **6**, e29577 (2011).
33. Dalzell, A. M., Freestone, N. S., Billington, D. & Heaf, D. P. Small intestinal permeability and orocaecal transit time in cystic fibrosis. *Arch Dis Child* **65**, 585 (1990).

34. Munck, A. Cystic fibrosis: Evidence for gut inflammation. *The International Journal of Biochemistry & Cell Biology* **52**, 180–183 (2014).
35. De Lisle, R. C., Roach, E. & Jansson, K. Effects of laxative and *N* -acetylcysteine on mucus accumulation, bacterial load, transit, and inflammation in the cystic fibrosis mouse small intestine. *American Journal of Physiology-Gastrointestinal and Liver Physiology* **293**, G577–G584 (2007).
36. Colledge, W. H. *et al.* Generation and characterization of a [Delta]F508 cystic fibrosis mouse model. *Nat Genet* **10**, 445–452 (1995).
37. De Lisle, R. C., Mueller, R. & Boyd, M. Impaired Mucosal Barrier Function in the Small Intestine of the Cystic Fibrosis Mouse: *Journal of Pediatric Gastroenterology and Nutrition* **53**, 371–379 (2011).
38. Walkowiak, J. *et al.* Cystic fibrosis is a risk factor for celiac disease. *Acta Biochim Pol* **57**, 115–118 (2010).
39. Lloyd-Still, J. D. Crohn's disease and cystic fibrosis. *Digestive Diseases and Sciences* **39**, 880–885 (1994).
40. de Waal, G. M., de Villiers, W. J. S., Forgan, T., Roberts, T. & Pretorius, E. Colorectal cancer is associated with increased circulating lipopolysaccharide, inflammation and hypercoagulability. *Sci Rep* **10**, 8777 (2020).
41. Fukui, H. Increased Intestinal Permeability and Decreased Barrier Function: Does It Really Influence the Risk of Inflammation? *Inflamm Intest Dis* **1**, 135–145 (2016).

42. Price, C. E. & O'Toole, G. A. The Gut-Lung Axis in Cystic Fibrosis. *J Bacteriol* **203**, (2021).
43. Gillen, J. *et al.* LPS Tolerance Inhibits Cellular Respiration and Induces Global Changes in the Macrophage Secretome. *Biomolecules* **11**, (2021).
44. Magnusson, M., Magnusson, K. E., Sundqvist, T. & Denneberg, T. Impaired intestinal barrier function measured by differently sized polyethylene glycols in patients with chronic renal failure. *Gut* **32**, 754–759 (1991).
45. Vivinus-Nébot, M. *et al.* Functional bowel symptoms in quiescent inflammatory bowel diseases: role of epithelial barrier disruption and low-grade inflammation. *Gut* **63**, 744–752 (2014).
46. Sprooten, R. T. M. *et al.* Increased Small Intestinal Permeability during Severe Acute Exacerbations of COPD. *Respiration* **95**, 334–342 (2018).
47. Kowalski, K. & Mulak, A. Brain-Gut-Microbiota Axis in Alzheimer's Disease. *J Neurogastroenterol Motil* **25**, 48–60 (2019).
48. Salinas, E. *et al.* Bioactive Compounds in Food as a Current Therapeutic Approach to Maintain a Healthy Intestinal Epithelium. *Microorganisms* **9**, (2021).
49. Odenwald, M. A. & Turner, J. R. The intestinal epithelial barrier: a therapeutic target? *Nat Rev Gastroenterol Hepatol* **14**, 9–21 (2017).
50. Xu, P., Elizalde, M., Masclee, A., Pierik, M. & Jonkers, D. Corticosteroid enhances epithelial barrier function in intestinal organoids derived from patients with Crohn's disease. *J Mol Med* **99**, 805–815 (2021).

51. Bardenbacher, M. *et al.* Permeability analyses and three dimensional imaging of interferon gamma-induced barrier disintegration in intestinal organoids. *Stem Cell Research* **35**, 101383 (2019).
52. Brice, D. P. *et al.* Interleukin-27 Regulates the Function of the Gastrointestinal Epithelial Barrier in a Human Tissue-Derived Organoid Model. *Biology (Basel)* **11**, (2022).
53. Weiser, N. *et al.* Paracellular Permeability of Bronchial Epithelium is Controlled by CFTR. *Cellular Physiology and Biochemistry* **28**, 289–296 (2011).
54. Castellani, S. *et al.* NHERF1 and CFTR restore tight junction organisation and function in cystic fibrosis airway epithelial cells: role of ezrin and the RhoA/ROCK pathway. *Lab Invest* **92**, 1527–1540 (2012).
55. Gróf, I. *et al.* The Effect of Sodium Bicarbonate, a Beneficial Adjuvant Molecule in Cystic Fibrosis, on Bronchial Epithelial Cells Expressing a Wild-Type or Mutant CFTR Channel. *IJMS* **21**, 4024 (2020).
56. Molenda, N. *et al.* Paracellular transport through healthy and cystic fibrosis bronchial epithelial cell lines--do we have a proper model? *PLoS One* **9**, e100621 (2014).
57. Ruan, Y. C. *et al.* CFTR interacts with ZO-1 to regulate tight junction assembly and epithelial differentiation through the ZONAB pathway. *Journal of Cell Science* **127**, 4396–4408 (2014).

58. Fiorotto, R. *et al.* The cystic fibrosis transmembrane conductance regulator controls biliary epithelial inflammation and permeability by regulating Src tyrosine kinase activity: Fiorotto et al. *Hepatology* **64**, 2118–2134 (2016).
59. Sato, T. *et al.* Single Lgr5 stem cells build crypt villus structures in vitro without a mesenchymal niche. *Nature* **459**, 262–265 (2009).
60. Liu, J., Walker, N. M., Cook, M. T., Ootani, A. & Clarke, L. L. Functional Cftr in crypt epithelium of organotypic enteroid cultures from murine small intestine. *AJP: Cell Physiology* **302**, C1492–C1503 (2012).
61. Walker, N. M. *et al.* Cellular chloride and bicarbonate retention alters intracellular pH regulation in Cftr KO crypt epithelium. *American Journal of Physiology - Gastrointestinal and Liver Physiology* **310**, G70–G80 (2016).
62. Bernstein, B. W. *et al.* Intracellular pH modulation of ADF/cofilin proteins. *Cell Motility and the Cytoskeleton* **47**, 319–336 (2000).
63. Damaghi, M., Wojtkowiak, J. W. & Gillies, R. J. pH sensing and regulation in cancer. *Frontiers in Physiology* **4**, (2013).
64. Kruse, C. R. *et al.* The effect of pH on cell viability, cell migration, cell proliferation, wound closure, and wound reepithelialization: In vitro and in vivo study: Effect of pH on wound healing. *Wound Repair and Regeneration* **25**, 260–269 (2017).
65. Flinck, M., Kramer, S. H. & Pedersen, S. F. Roles of pH in control of cell proliferation. *Acta Physiologica* **223**, e13068 (2018).

66. Tarbashevich, K., Reichman-Fried, M., Grimaldi, C. & Raz, E. Chemokine-Dependent pH Elevation at the Cell Front Sustains Polarity in Directionally Migrating Zebrafish Germ Cells. *Current Biology* **25**, 1096–1103 (2015).

67. White, K. A., Grillo-Hill, B. K. & Barber, D. L. Cancer cell behaviors mediated by dysregulated pH dynamics at a glance. *Journal of Cell Science* **130**, 663–669 (2017).

68. Clevers, H. Wnt/β-Catenin Signaling in Development and Disease. *Cell* **127**, 469–480 (2006).

69. Gao, C. & Chen, Y.-G. Dishevelled: The hub of Wnt signaling. *Cellular Signalling* **22**, 717–727 (2010).

70. Simons, M. *et al.* Electrochemical cues regulate assembly of the Frizzled/Dishevelled complex at the plasma membrane during planar epithelial polarization. *Nature Cell Biology* **11**, 286–294 (2009).

71. Strubberg, A. M. *et al.* Cftr Modulates Wnt/beta-Catenin Signaling and Stem Cell Proliferation in Murine Intestine. *Cell Mol Gastroenterol Hepatol* **5**, 253–271 (2018).

72. Citi, S., Guerrera, D., Spadaro, D. & Shah, J. Epithelial junctions and Rho family GTPases: the zonular signalosome. *Small GTPases* **5**, e973760 (2014).

73. Pradhan, R., Ngo, P. A., Martínez-Sánchez, L. d. C., Neurath, M. F. & López-Posadas, R. Rho GTPases as Key Molecular Players within Intestinal Mucosa and GI Diseases. *Cells* **10**, 66 (2021).

74. Mezzacappa, C., Komiya, Y. & Habas, R. Activation and Function of Small GTPases Rho, Rac, and Cdc42 During Gastrulation. in *Planar Cell Polarity* (ed. Turksen, K.) vol. 839 119–131 (Springer New York, 2012).
75. Bishop, A. L. & Hall, A. Rho GTPases and their effector proteins. 15 (2000).
76. Etienne-Manneville, S. & Hall, A. Rho GTPases in cell biology. *Nature* **420**, 629–635 (2002).
77. Terry, S., Nie, M., Matter, K. & Balda, M. S. Rho signaling and tight junction functions. *Physiology (Bethesda)* **25**, 16–26 (2010).
78. Melendez, J. *et al.* Cdc42 Coordinates Proliferation, Polarity, Migration, and Differentiation of Small Intestinal Epithelial Cells in Mice. *Gastroenterology* **145**, 808–819 (2013).
79. Liu, M. *et al.* RHOA GTPase Controls YAP-Mediated EREG Signaling in Small Intestinal Stem Cell Maintenance. *Stem Cell Reports* **9**, 1961–1975 (2017).
80. Sumigray, K. D., Terwilliger, M. & Lechler, T. Morphogenesis and Compartmentalization of the Intestinal Crypt. *Dev Cell* **45**, 183-197.e5 (2018).
81. Segain, J.-P. *et al.* Rho kinase blockade prevents inflammation via nuclear factor κB inhibition: evidence in Crohn's disease and experimental colitis. *Gastroenterology* **124**, 1180–1187 (2003).
82. Martínez-Sánchez, L. del C. *et al.* Epithelial RAC1-dependent cytoskeleton dynamics controls cell mechanics, cell shedding and barrier integrity in

intestinal inflammation. *Gut* gutjnl-2021-325520 (2022) doi:10.1136/gutjnl-2021-325520.

83. Tang, W.-J. *et al.* MicroRNA-15a - cell division cycle 42 signaling pathway in pathogenesis of pediatric inflammatory bowel disease. *WJG* **24**, 5234–5245 (2018).
84. Zhou, K. *et al.* RAC1-GTP promotes epithelial-mesenchymal transition and invasion of colorectal cancer by activation of STAT3. *Laboratory Investigation* **98**, 989–998 (2018).
85. Jeong, D. *et al.* RhoA is associated with invasion and poor prognosis in colorectal cancer. *Int J Oncol* **48**, 714–722 (2016).
86. Gómez Del Pulgar, T. *et al.* Cdc42 is highly expressed in colorectal adenocarcinoma and downregulates ID4 through an epigenetic mechanism. *Int J Oncol* **33**, 185–193 (2008).
87. Koch, S. & Nusrat, A. Dynamic Regulation of Epithelial Cell Fate and Barrier Function by Intercellular Junctions. *Annals of the New York Academy of Sciences* **1165**, 220–227 (2009).
88. Gallagher, A. M. & Gottlieb, R. A. Proliferation, not apoptosis, alters epithelial cell migration in small intestine of CFTR null mice. *American Journal of Physiology-Gastrointestinal and Liver Physiology* **281**, G681–G687 (2001).
89. Hao, S. CF intestinal pathology involves both a disease milieu and absence of CFTR from epithelial cells. (Case Western Reserve University School of Graduate Studies, 2019).

90. Schuijers, J. & Clevers, H. Adult mammalian stem cells: the role of Wnt, Lgr5 and R-spondins: The role of Wnt, Lgr5 and R-spondins. *The EMBO Journal* **31**, 2685–2696 (2012).

91. Schlessinger, K., Hall, A. & Tolwinski, N. Wnt signaling pathways meet Rho GTPases. *Genes & Development* **23**, 265–277 (2009).

92. Nilsson, H. E., Dragomir, A., Lazorova, L., Johannesson, M. & Roomans, G. M. CFTR and tight junctions in cultured bronchial epithelial cells. *Experimental and Molecular Pathology* **88**, 118–127 (2010).

93. Schlessinger, K., Hall, A. & Tolwinski, N. Wnt signaling pathways meet Rho GTPases. *Genes & Development* **23**, 265–277 (2009).

94. Hao, S. *et al.* Inactivation of CFTR by CRISPR/Cas9 alters transcriptional regulation of inflammatory pathways and other networks. *J Cyst Fibros* **19**, 34–39 (2020).

95. Etheridge, S. L. *et al.* Murine dishevelled 3 functions in redundant pathways with dishevelled 1 and 2 in normal cardiac outflow tract, cochlea, and neural tube development. *PLoS Genet* **4**, e1000259 (2008).

96. Clarke, L. L., Gawenis, L. R., Franklin, C. L. & Harline, M. C. Increased survival of CFTR knockout mice with an oral osmotic laxative. *Lab Anim Sci* **46**, 612–618 (1996).

97. Wang, J. *et al.* Dishevelled genes mediate a conserved mammalian PCP pathway to regulate convergent extension during neurulation. *Development* **133**, 1767–1778 (2006).

98. Livak, K. J. & Schmittgen, T. D. Analysis of relative gene expression data using real-time quantitative PCR and the 2(-Delta Delta C(T)) Method. *Methods* **25**, 402–408 (2001).

99. Simpson, J. E., Gawenis, L. R., Walker, N. M., Boyle, K. T. & Clarke, L. L. Chloride conductance of CFTR facilitates basal Cl^-/HCO_3^- exchange in the villous epithelium of intact murine duodenum. *American Journal of Physiology-Gastrointestinal and Liver Physiology* **288**, G1241–G1251 (2005).

100. De Lisle, R. C. Disrupted tight junctions in the small intestine of cystic fibrosis mice. *Cell and Tissue Research* **355**, 131–142 (2014).

101. Hallberg, K., Grzegorczyk, A., Larson, G. & Strandvik, B. Intestinal Permeability in Cystic Fibrosis in Relation to Genotype. *Journal of Pediatric Gastroenterology and Nutrition* **25**, (1997).

102. Gawenis, L. R. *et al.* cAMP inhibition of murine intestinal Na+/H+ exchange requires CFTR-mediated cell shrinkage of villus epithelium1. *Gastroenterology* **125**, 1148–1163 (2003).

103. Liu, J., Walker, N. M., Cook, M. T., Ootani, A. & Clarke, L. L. Functional Cftr in crypt epithelium of organotypic enteroid cultures from murine small intestine. *American Journal of Physiology-Cell Physiology* **302**, C1492–C1503 (2012).

104. Umar, S. Intestinal stem cells. *Curr Gastroenterol Rep* **12**, 340–348 (2010).

105. Luettig, J., Rosenthal, R., Barmeyer, C. & Schulzke, J. D. Claudin-2 as a mediator of leaky gut barrier during intestinal inflammation. *Tissue Barriers* **3**, e977176–e977176 (2015).

106. van Noort, M., Meeldijk, J., van der Zee, R., Destree, O. & Clevers, H. Wnt Signaling Controls the Phosphorylation Status of β-Catenin. *Journal of Biological Chemistry* **277**, 17901–17905 (2002).

107. Bruewer, M. RhoA, Rac1, and Cdc42 exert distinct effects on epithelial barrier via selective structural and biochemical modulation of junctional proteins and F-actin. *AJP: Cell Physiology* **287**, C327–C335 (2004).

108. Fihn, B., Sjöqvist, A. & Jodal, M. Permeability of the rat small intestinal epithelium along the villus-crypt axis: Effects of glucose transport. *Gastroenterology* **119**, 1029–1036 (2000).

109. Fuller, M. K. *et al.* Intestinal crypts reproducibly expand in culture. *Journal of Surgical Research* **178**, 48–54 (2012).

110. Gregorieff, A. *et al.* Expression Pattern of Wnt Signaling Components in the Adult Intestine. *Gastroenterology* **129**, 626–638 (2005).

111. Citi, S., Guerrera, D., Spadaro, D. & Shah, J. Epithelial junctions and Rho family GTPases: the zonular signalosome. *Small GTPases* **5**, e973760 (2014).

112. Matsumoto, S., Fumoto, K., Okamoto, T., Kaibuchi, K. & Kikuchi, A. Binding of APC and dishevelled mediates Wnt5a-regulated focal adhesion dynamics in migrating cells. *EMBO J* **29**, 1192–1204 (2010).

113. Martin, T. A. & Jiang, W. G. Loss of tight junction barrier function and its role in cancer metastasis. *Biochimica et Biophysica Acta (BBA) - Biomembranes* **1788**, 872–891 (2009).

114. Takehara, M., Nishimura, T., Mima, S., Hoshino, T. & Mizushima, T. Effect of Claudin Expression on Paracellular Permeability, Migration and Invasion of Colonic Cancer Cells. *Biological & Pharmaceutical Bulletin* **32**, 825–831 (2009).

115. Rojas, R., Ruiz, W. G., Leung, S.-M., Jou, T.-S. & Apodaca, G. Cdc42-dependent Modulation of Tight Junctions and Membrane Protein Traffic in Polarized Madin-Darby Canine Kidney Cells. *MBoC* **12**, 2257–2274 (2001).

116. Stamatovic, S. M., Johnson, A. M., Sladojevic, N., Keep, R. F. & Andjelkovic, A. V. Endocytosis of tight junction proteins and the regulation of degradation and recycling: Endocytic sorting of tight junction proteins. *Annals of the New York Academy of Sciences* **1397**, 54–65 (2017).

117. Frantz, C. *et al.* Cofilin is a pH sensor for actin free barbed end formation: role of phosphoinositide binding. *The Journal of Cell Biology* **183**, 865–879 (2008).

118. Frantz, C., Karydis, A., Nalbant, P., Hahn, K. M. & Barber, D. L. Positive feedback between Cdc42 activity and H^+ efflux by the Na-H exchanger NHE1 for polarity of migrating cells. *The Journal of Cell Biology* **179**, 403–410 (2007).

119. Pankonien, I., Quaresma, M. C., Rodrigues, C. S. & Amaral, M. D. CFTR, Cell Junctions and the Cytoskeleton. *IJMS* **23**, 2688 (2022).

120. Watson, M. J. *et al.* The Cystic Fibrosis Transmembrane Conductance Regulator (CFTR) Uses its C-Terminus to Regulate the A2B Adenosine Receptor. *Sci Rep* **6**, 27390–27390 (2016).
121. Corvol, H. *et al.* FAM13A is a modifier gene of cystic fibrosis lung phenotype regulating rhoa activity, actin cytoskeleton dynamics and epithelial-mesenchymal transition. *Journal of Cystic Fibrosis* **17**, 190–203 (2018).
122. Fanen, P., Wohlhuter-Haddad, A. & Hinzpeter, A. Genetics of cystic fibrosis: CFTR mutation classifications toward genotype-based CF therapies. *The International Journal of Biochemistry & Cell Biology* **52**, 94–102 (2014).
123. Carothers, A. M., Melstrom, K. A., Mueller, J. D., Weyant, M. J. & Bertagnolli, M. M. Progressive Changes in Adherens Junction Structure during Intestinal Adenoma Formation in Apc Mutant Mice. *Journal of Biological Chemistry* **276**, 39094–39102 (2001).
124. Jiang, H. *et al.* Peptidomimetic inhibitors of APC–Asef interaction block colorectal cancer migration. *Nat Chem Biol* **13**, 994–1001 (2017).
125. Kawasaki, Y., Sato, R. & Akiyama, T. Mutated APC and Asef are involved in the migration of colorectal tumour cells. *Nat Cell Biol* **5**, 211–215 (2003).
126. Liu, Z., Adams, H. C. & Whitehead, I. P. The Rho-specific Guanine Nucleotide Exchange Factor Dbs Regulates Breast Cancer Cell Migration. *Journal of Biological Chemistry* **284**, 15771–15780 (2009).
127. Rodriguez, O. C. *et al.* Conserved microtubule–actin interactions in cell movement and morphogenesis. *Nature Cell Biology* **5**, 599–609 (2003).

128. Fitzpatrick, E. R., Hu, T., Ciccarelli, B. T. & Whitehead, I. P. Regulation of vesicle transport and cell motility by Golgi-localized Dbs. *Small GTPases* **5**, e972860 (2014).

129. Crites, K. S.-M. *et al.* CFTR Knockdown induces proinflammatory changes in intestinal epithelial cells. *Journal of Inflammation* **12**, (2015).

130. Cystic Fibrosis Foundation, B., Maryland. 2021 Cystic Fibrosis Foundation Patient Registry Highlights. (2022).

131. Shen, L., Weber, C. R., Raleigh, D. R., Yu, D. & Turner, J. R. Tight Junction Pore and Leak Pathways: A Dynamic Duo. *Annual Review of Physiology* **73**, 283–309 (2011).

132. Guimbellot, J. S. *et al.* Role of Oxygen Availability in CFTR Expression and Function. *Am J Respir Cell Mol Biol* **39**, 514–521 (2008).

133. Verhoeckx, K., Cotter, P., & European Cooperation in the Field of Scientific and Technical Research (Organization). *The impact of food bioactives on gut health: in vitro and ex vivo models*. (2015).

134. Hidalgo, I. J., Raub, T. J. & Borchardt, R. T. Characterization of the Human Colon Carcinoma Cell Line (Caco-2) as a Model System for Intestinal Epithelial Permeability. *Gastroenterology* **96**, 736–749 (1989).

135. Duizer, E., Koeman, J. H., Bladeren, P. J. van & Groten, J. P. *Permeability and modulation of the intestinal epithelial barrier in vitro*. (1999).

136. Srinivasan, B. *et al.* TEER Measurement Techniques for In Vitro Barrier Model Systems. *Journal of Laboratory Automation* **20**, 107–126 (2015).

137. Noren, N. K., Niessen, C. M., Gumbiner, B. M. & Burridge, K. Cadherin Engagement Regulates Rho family GTPases*. *Journal of Biological Chemistry* **276**, 33305–33308 (2001).

138. D'Souza, R. S. *et al.* Calcium-stimulated disassembly of focal adhesions mediated by an ORP3/IQSec1 complex. *eLife* **9**, e54113 (2020).

139. Nobes, C. D. & Hall, A. Rho, rac, and cdc42 GTPases regulate the assembly of multimolecular focal complexes associated with actin stress fibers, lamellipodia, and filopodia. *Cell* **81**, 53–62 (1995).

140. Ridley, A. J. Rho GTPase signalling in cell migration. *Curr Opin Cell Biol* **36**, 103–112 (2015).

141. Li, L., He, Y., Zhao, M. & Jiang, J. Collective cell migration: Implications for wound healing and cancer invasion. *Burns Trauma* **1**, 21–26 (2013).

142. Pinto, M. Enterocyte-like differentiation and polarization of the human colon carcinoma cell line Caco-2 in culture. *Biology of the Cell* **47**, 323–330 (1983).

143. Sood, R. *et al.* Regulation of CFTR expression and function during differentiation of intestinal epithelial cells. *EMBO J* **11**, 2487–2494 (1992).

144. Scott, P., Anderson, K., Singhania, M. & Cormier, R. Cystic Fibrosis, CFTR, and Colorectal Cancer. *IJMS* **21**, 2891 (2020).

145. Massip-Copiz, M., Clauzure, M., Valdivieso, Á. G. & Santa-Coloma, T. A. Epiregulin (EREG) is upregulated through an IL-1β autocrine loop in Caco-2 epithelial cells with reduced CFTR function. *J Cell Biochem* **119**, 2911–2922 (2018).

146. Escobar, H. *et al.* Intestinal permeability to 51Cr-EDTA and orocecal transit time in cystic fibrosis. *J Pediatr Gastroenterol Nutr* **14**, 204–207 (1992).
147. Bhat, A. A. *et al.* Tight Junction Proteins and Signaling Pathways in Cancer and Inflammation: A Functional Crosstalk. *Front. Physiol.* **9**, 1942 (2019).
148. Hartsock, A. & Nelson, W. J. Adherens and tight junctions: Structure, function and connections to the actin cytoskeleton. *Biochimica et Biophysica Acta (BBA) - Biomembranes* **1778**, 660–669 (2008).
149. Rajasekaran, A. K. & Rajasekaran, S. A. Role of Na-K-ATPase in the assembly of tight junctions. *Am J Physiol Renal Physiol* **285**, F388-396 (2003).
150. Gopal, S., Multhaupt, H. A. B. & Couchman, J. R. Calcium in Cell-Extracellular Matrix Interactions. in *Calcium Signaling* (ed. Islam, Md. S.) 1079–1102 (Springer International Publishing, 2020). doi:10.1007/978-3-030-12457-1_43.
151. Elbediwy, A. *et al.* Epithelial junction formation requires confinement of Cdc42 activity by a novel SH3BP1 complex. *J Cell Biol* **198**, 677 (2012).
152. Sakamori, R. *et al.* CDC42 Inhibition Suppresses Progression of Incipient Intestinal Tumors. *Cancer Research* **74**, 5480–5492 (2014).
153. Trinh, N. T. N. *et al.* Improvement of defective cystic fibrosis airway epithelial wound repair after CFTR rescue. *Eur Respir J* **40**, 1390–1400 (2012).
154. Xu, J. *et al.* High level of CFTR expression is associated with tumor aggression and knockdown of CFTR suppresses proliferation of ovarian cancer in vitro and in vivo. *Oncology Reports* **33**, 2227–2234 (2015).

155. Wu, Z., Li, J., Zhang, Y., Hu, L. & Peng, X. CFTR Regulates the Proliferation, Migration and Invasion of Cervical Cancer Cells by Inhibiting the NF-κB Signalling Pathway. *Cancer Manag Res* **12**, 4685–4697 (2020).
156. Dong, J. *et al.* Dynamically Regulated CFTR Expression and Its Functional Role in Cutaneous Wound Healing. *Journal of Cellular Physiology* **230**, 2049–2058 (2015).
157. Thomas Hess, C. Checklist for Factors Affecting Wound Healing. *Advances in Skin & Wound Care* **24**, (2011).
158. Gehart, H. & Clevers, H. Tales from the crypt: new insights into intestinal stem cells. *Nat Rev Gastroenterol Hepatol* **16**, 19–34 (2019).
159. Pearce, S. C. *et al.* Marked differences in tight junction composition and macromolecular permeability among different intestinal cell types. *BMC Biology* **16**, (2018).
160. Sun, H., Chow, E. C., Liu, S., Du, Y. & Pang, K. S. The Caco-2 cell monolayer: usefulness and limitations. *Expert Opinion on Drug Metabolism & Toxicology* **4**, 395–411 (2008).
161. Ohura, K., Nishiyama, H., Saco, S., Kurokawa, K. & Imai, T. Establishment and Characterization of a Novel Caco-2 Subclone with a Similar Low Expression Level of Human Carboxylesterase 1 to Human Small Intestine. *Drug Metab Dispos* **44**, 1890–1898 (2016).
162. Dang, A. T. & Marsland, B. J. Microbes, metabolites, and the gut-lung axis. *Mucosal Immunol* **12**, 843–850 (2019).

163. Uko, V., Thangada, S. & Radhakrishnan, K. Liver disorders in inflammatory bowel disease. *Gastroenterol Res Pract* **2012**, 642923 (2012).
164. Albillos, A., de Gottardi, A. & Rescigno, M. The gut-liver axis in liver disease: Pathophysiological basis for therapy. *Journal of Hepatology* **72**, 558–577 (2020).
165. Vanuytsel, T., Tack, J. & Farre, R. The Role of Intestinal Permeability in Gastrointestinal Disorders and Current Methods of Evaluation. *Front. Nutr.* **8**, 717925 (2021).
166. Bjarnason, I., MacPherson, A. & Hollander, D. Intestinal permeability: an overview. *Gastroenterology* **108**, 1566–1581 (1995).
167. Hollander, D. & Kaunitz, J. D. The 'Leaky Gut': Tight Junctions but Loose Associations? *Dig Dis Sci* **65**, 1277–1287 (2020).
168. Yasuda, M. *et al.* Pseudomonas aeruginosa serA Gene Is Required for Bacterial Translocation through Caco-2 Cell Monolayers. *PLoS One* **12**, e0169367 (2017).
169. Wang, B. *et al.* Lactobacillus plantarum L9 but not Lactobacillus acidophilus LA reduces tumour necrosis factor induced bacterial translocation in Caco-2 cells. *Benef Microbes* **8**, 497–505 (2017).
170. Backert, S., Boehm, M., Wessler, S. & Tegtmeyer, N. Transmigration route of Campylobacter jejuni across polarized intestinal epithelial cells: paracellular, transcellular or both? *Cell Commun Signal* **11**, 72 (2013).

171. Opal, S. M. *et al.* Relationship between plasma levels of lipopolysaccharide (LPS) and LPS-binding protein in patients with severe sepsis and septic shock. *J Infect Dis* **180**, 1584–1589 (1999).

172. Connan, C. & Popoff, M. R. Uptake of Clostridial Neurotoxins into Cells and Dissemination. *Curr Top Microbiol Immunol* **406**, 39–78 (2017).

173. Nagpal, R. & Yadav, H. Bacterial Translocation from the Gut to the Distant Organs: An Overview. *Ann Nutr Metab* **71 Suppl 1**, 11–16 (2017).

174. Landy, J. *et al.* Tight junctions in inflammatory bowel diseases and inflammatory bowel disease associated colorectal cancer. *World Journal of Gastroenterology* **22**, 3117 (2016).

175. Werlin, S. L. *et al.* Evidence of Intestinal Inflammation in Patients With Cystic Fibrosis: *Journal of Pediatric Gastroenterology and Nutrition* 1 (2010) doi:10.1097/MPG.0b013e3181d1b013.

176. Maisonneuve, P., Marshall, B. C., Knapp, E. A. & Lowenfels, A. B. Cancer Risk in Cystic Fibrosis: A 20-Year Nationwide Study From the United States. *JNCI Journal of the National Cancer Institute* **105**, 122–129 (2013).

177. Matter, K. & Balda, M. S. SnapShot: Epithelial Tight Junctions. *Cell* **157**, 992-992.e1 (2014).

178. Balda, M. S. & Matter, K. Tight junctions and the regulation of gene expression. *Biochimica et Biophysica Acta (BBA) - Biomembranes* **1788**, 761–767 (2009).

179. Harder, J. L. & Margolis, B. SnapShot: Tight and Adherens Junction Signaling. *Cell* **133**, 1118-1118.e2 (2008).

180. Matter, K., Aijaz, S., Tsapara, A. & Balda, M. S. Mammalian tight junctions in the regulation of epithelial differentiation and proliferation. *Current Opinion in Cell Biology* **17**, 453–458 (2005).

181. Matter, K. & Balda, M. S. Signalling to and from tight junctions. *Nature Reviews Molecular Cell Biology* **4**, 225–237 (2003).

182. Balda, M. S., Garrett, M. D. & Matter, K. The ZO-1–associated Y-box factor ZONAB regulates epithelial cell proliferation and cell density. *The Journal of Cell Biology* **160**, 423–432 (2003).

183. Strubberg, A. M. Hyperproliferation and altered WNT signaling in the Cystic fibrosis mouse intestine. (University of Missouri--Columbia, 2016). doi:10.32469/10355/57414.

184. Chelakkot, C., Ghim, J. & Ryu, S. H. Mechanisms regulating intestinal barrier integrity and its pathological implications. *Experimental & Molecular Medicine* **50**, 1–9 (2018).

185. Altay, G. *et al.* Self-organized intestinal epithelial monolayers in crypt and villus-like domains show effective barrier function. *Sci Rep* **9**, 10140 (2019).

186. Singh, V. K., Kalsan, M., Kumar, N., Saini, A. & Chandra, R. Induced pluripotent stem cells: applications in regenerative medicine, disease modeling, and drug discovery. *Front Cell Dev Biol* **3**, 2 (2015).

187. Takahashi, K. & Yamanaka, S. Induction of Pluripotent Stem Cells from Mouse Embryonic and Adult Fibroblast Cultures by Defined Factors. *Cell* **126**, 663–676 (2006).

188. Karagiannis, P. *et al.* Induced Pluripotent Stem Cells and Their Use in Human Models of Disease and Development. *Physiological Reviews* **99**, 79–114 (2019).

189. Forbester, J. L., Hannan, N., Vallier, L. & Dougan, G. Derivation of Intestinal Organoids from Human Induced Pluripotent Stem Cells for Use as an Infection System. in *Organoids: Stem Cells, Structure, and Function* (ed. Turksen, K.) 157–169 (Springer New York, 2019). doi:10.1007/7651_2016_7.

190. Sarvestani, S. K. *et al.* Induced organoids derived from patients with ulcerative colitis recapitulate colitic reactivity. *Nature Communications* **12**, 262 (2021).

191. Estrada, H. Q. *et al.* Development of a Personalized Intestinal Fibrosis Model Using Human Intestinal Organoids Derived From Induced Pluripotent Stem Cells. *Inflammatory Bowel Diseases* **28**, 667–679 (2022).

192. AU - Lees, E. A. *et al.* Using Human Induced Pluripotent Stem Cell-derived Intestinal Organoids to Study and Modify Epithelial Cell Protection Against Salmonella and Other Pathogens. *JoVE* e59478 (2019) doi:10.3791/59478.

193. de Poel, E., Lefferts, J. W. & Beekman, J. M. Intestinal organoids for Cystic Fibrosis research. *Journal of Cystic Fibrosis* **19**, S60–S64 (2020).

194. Mahe, M. M. *et al.* Establishment of Gastrointestinal Epithelial Organoids. *Curr Protoc Mouse Biol* **3**, 217–240 (2013).

195. Kozuka, K. *et al.* Development and Characterization of a Human and Mouse Intestinal Epithelial Cell Monolayer Platform. *Stem Cell Reports* **9**, 1976–1990 (2017).
196. Crudele, A. *et al.* Hydroxytyrosol Recovers SARS-CoV-2-PLpro-Dependent Impairment of Interferon Related Genes in Polarized Human Airway, Intestinal and Liver Epithelial Cells. *Antioxidants* **11**, (2022).
197. Sakamori, R. *et al.* CDC42 Inhibition Suppresses Progression of Incipient Intestinal Tumors. *Cancer Research* **74**, 5480–5492 (2014).
198. Haggie, P. M., Stanton, B. A. & Verkman, A. S. Increased Diffusional Mobility of CFTR at the Plasma Membrane after Deletion of Its C-terminal PDZ Binding Motif *. *Journal of Biological Chemistry* **279**, 5494–5500 (2004).

VITA

Rowena Aba Mbrobah Opal Woode was born in St. Louis, Missouri on January 27th, 1988 to John and Belinda Woode. She was raised in Barnhart, Missouri with her two brothers, Leonard and Franklin Woode. Rowena earned her Bachelor of Science degree in Animal Science from Missouri State University in Springfield, Missouri. Rowena graduated from the University of Missouri College of Veterinary Medicine in 2016 with honors. After earning her DVM, she decided to pursue a career in biomedical research as a PhD student in the Department of Biomedical Sciences at MU. Rowena joined Dr. Lane L. Clarke's laboratory in the spring of 2017 where she performed her dissertation research. Rowena has accepted a postdoctoral position in Dr. Clarke's laboratory and plans on staying in Columbia, MO for the time being. Rowena currently lives happily in Columbia, MO with her three Pomeranians, Maximus, Milky Joe, and Button.